Universität Rostock

JOINT MASS SPECTROMETRY CENTRE

Toward Understanding the Chemical Composition of Carbonaceous Aerosols Emitted by Solid Fuel Burning

Cumulative dissertation
for the attainment of the academic degree
doctor rerum naturalium (Dr. rer. nat.)
from the Faculty of Mathematics and Natural Sciences
of the University of Rostock

submitted by
Patrick Martens,
born August 24, 1995

in Waren (Müritz), Mecklenburg-West Pomerania, Germany

The work for this dissertation was carried out from October, 2019 to September 2023 at the Institute of Chemistry of the University of Rostock at the chair of Technical and Analytical Chemistry under the supervision of Prof. Dr. Ralf Zimmermann.

Year of submission: 2023
Year of defense: 2023

1. Referee:
  Prof. Dr. Ralf Zimmermann
  University of Rostock
  Rostock, Germany
2. Referee
  Alexandre Albinet, Ph. D., HDR
  Institut National Environnement industriel et Risques (INERIS)
  Verneuil-en-Halatte, France

Danksagung – Acknowledgement

Table of Contents

Abstract (English–Englisch)

Air pollution by combustion aerosols are frequently identified as a major contributor to climate change and the health burden. Solid fuel burning was found to be the most impactful combustion source on a global scale, even outrivaling emissions from the transport sector. Particularly in South and Southeast Asia, solid fuel burning is a leading contributor to the health burden due to high emissions from rather unguided combustion processes, such as various forms of open biomass burning. In Europe, solid fuel burning, e.g., coal and wood, is mainly carried out in combustion appliances that are specifically designed for high combustion quality and high thermal efficiency and thus emitting comparatively few pollutants compared to open burning. Nevertheless, solid fuel burning in these appliances is still one of the major contributors to poor air quality, particularly in Eastern Europe where coal burning still has not phased out.

In order to reduce adverse effects on the climate and humans, the European Union released new emission thresholds, which came into effect in all European member states in January 2022, setting new threshold for these appliances installed in all member state, among others. Despite being a non-renewable source of energy and a big contributor to air pollution, the use of coal in residential heating appliances has not been limited or banned, and therefore coal burning remains a viable option for residential heating despite its non-renewable nature. While wood combustion in state-of-the-art appliances is a field of research that is already comparatively well studied, information on the combustion of coal in state-of-the-art heating appliances equipped is scarce. In order to better estimate the impact of these emissions on humans, a comprehensive understanding of physical properties of emitted aerosol as well as its chemical composition is needed.

Combustion processes are highly complex, particularly for solid fuels, and involve a series of sub-processes, e.g., the pyrolysis and partial oxidation of the fuel's condensed and gas phase, a mass transfer via buoyancy diffusion of gases and the flux of energy via emission of electromagnetic radiation. Each of these processes depends on a multitude of different factors, e.g., thermal properties of the surrounding gas and its chemical composition as well as physical and thermal properties of the fuel and its chemical composition, among others. Moreover, every process has feedback on all others, making the fuel progression through the combustion process and the evolution of emission highly dynamic. This leaves a gap for applied research to investigate properties of these emissions and build an association between these factors and toxic responses.

Within the thesis, the chemical composition and physical properties of emissions from solid fuel burning were investigated in order to advance the current understanding of their potential impact on humans. Increasing combustion quality in modern heating appliances was found emit organic compounds that are characterized by a high degree of graphitization and a loss of functional groups vice versa. Moreover, emissions from brown coal briquette burning in a modern heating appliances were found to exert higher toxicity in toxicological tests in cell models than emissions that were burned in the same device, which might be due to the elevated water solubility of functionalized aromatic compounds in comparison to their parent and alkylated species. To study chemical sub-fractions of organic aerosol emitted from solid fuel pyrolysis, organic compounds from biomass pyrolysis, were subdivided into a water-soluble and aqueous soluble fraction, and toxicological testing revealed that both fractions may trigger different pathways in the response of cells to their exposure.

Abstract (German–Deutsch)

Die Luftverschmutzung durch Aerosole aus Verbrennungsprozessen belastet das Klima und die Gesundheit von Menschen. Auf globaler Ebene haben Emissionen aus der Verbrennung von festen Brennstoffen eine hohe Relevanz bezüglich ihrer Auswirkungen auf den Menschen und übertreffen selbst die Relevanz von Emissionen aus dem Transportsektor. Insbesondere in Ost- und Südostasien ist die Reduzierung der Lebenserwartung durch diese Luftschadstoffe hoch, da das Verbrennen von häuslichen Abfällen in Verbrennungsanlagen und Feuerstellen mit schlechter Verbrennungsführung und das unkontrollierte Verbrennen von Ernteabfällen auf Ackern gängige Praktiken sind. Auch in Europe trägt die Verbrennung von festen Brennstoffen zur lokalen Gesundheitsbelastung bei, jedoch findet die Verbrennung hier hauptsächlich modernen Öfen und Boiler mit guter Verbrennungsführung statt, welches zu einer hohen thermischen Effizienz und auch niedrigen Schadstoffemissionen führt. Dennoch gehören Emissionen aus diesen Prozessen immer noch zu den Hauptursachen für schlechte Luftqualität, insbesondere in Osteuropa, wo die Verbrennung von Kohle immer noch gängige Praxis ist.

Um negative Auswirkungen von Aerosolen aus Verbrennungsprozessen zu reduzieren, hat die Europäische Union ein Gesetzespaket, EcoDesign2022, erlassen, welches im Januar 2022 in Kraft trat und unter anderem neue Emissionsgrenzwerte für diese Geräte in allen Mitgliedstatten definiert. Die Verwendung von Kohle, als fossiler, und potenziell stark luftverschmutzender Brennstoff, wurde nicht eingeschränkt oder verboten, weshalb dessen Nutzung immer noch eine kosteneffizient Möglichkeit zum Heizen von Wohngebäuden ist. Die Luftschadstoffe aus der häuslichen Verbrennung von Kohle in modernen Kleinfeuerungsanlagen sind im Vergleich zu den Schadstoffen aus der Holzverbrennung schlecht erforscht. Um die Auswirkungen dieser Emissionen auf den Menschen besser abschätzen zu können, ist eine umfangreiche Charakterisierung der physikalischen Eigenschaften der emittierten Aerosole sowie Kenntnisse über dessen chemischen Zusammensetzung notwendig.

Verbrennungsprozesse im Allgemeinen und insbesondere von festen Brennstoffen sind äußerst komplex und kann als das Resultat einer Reihe von Teilprozesse angesehen werden. Prozesse die stattfinden sind, unter anderem, die Pyrolyse und unvollständige Oxidation der kondensierten und gasförmigen Phase, den Stofftransport durch Auftrieb und Diffusion von Gasen und den Fluss von Energie durch das Aussenden von elektromagnetischer Strahlung. Jeder dieser Prozesse hängt dabei von einer Vielzahl an Faktoren ab, unter anderen von den thermischen Eigenschaften der Umgebung und dessen chemische Zusammensetzung sowie physikalische und thermische Eigenschaften des Brennstoffs sowie dessen Zusammensatzung. Darüber hinaus koppelt jeder Prozess alle anderen zurück, was des Verlaufs von Verbrennung, die nicht im modellmaßstab stattfinden, sowie die daraus resultierenden Emissionen hoch dynamisch macht. Dies hinterlässt eine Nische für angewandte Forschung, die sich mit der Aufklärung von Eigenschaften eben dieser Emissionen auseinandersetzt und eine Verbindung zwischen ihnen Emissionen und toxikologischen Reaktionen aufbaut.

Im Rahmen der Arbeit wurden die chemische Zusammensetzung und physikalischen Eigenschaften von Emissionen aus der Verbrennung von Festbrennstoffen untersucht, um das aktuelle Verständnis ihrer potenziellen Auswirkungen auf den Menschen zu vertiefen. Eine erhöhte Verbrennungsqualität in modernen Heizgeräten führte zu einem zunehmenden Grad der Graphitisierung und umgekehrt zum Verlust von funktionellen Gruppen in emittieren organischen Bestandteilen. Die Emissionen aus der Verbrennung von Braunkohlebriketts in modernen Heizgeräten zeigten in Zellmodellen eine höhere Toxizität als Emissionen aus Verbrennung von Holz, was auf die erhöhte Wasserlöslichkeit von funktionalisierten aromatischen Verbindungen zurückzuführen sein könnte. Die getrennte Analyse von Verbindungen mit erhöhter Löslichkeit in Wasser bzw. organischen Lösungsmittel, welche aus der Biomassepyrolyse stammten, half dabei potentielle Mechanismen in der toxikologischen Wirkung

aufzudecken.

1.   A Brief Introduction to Air Pollution

The Earth's atmosphere is primarily composed of molecular nitrogen and oxygen, and argon with average mixing ratios of about 78, 21, and 1%, respectively. Water vapor is the next most abundant constituent, found primarily in the lower atmosphere, where it can locally reach concentrations as high as 3%.[1] Other constituents, i.e., gases, vapors and airborne particulate matter (droplets and solid particles suspended in air), are present in trace amounts but play a fundamental role in the atmosphere's chemical properties and radiative budget. Some may be harmful to humans and the environment, that is, ecosystems, buildings and vegetation, and these are then referred to as air pollutants. Some may even not be harmful when they are present in the air, but they may become harmful upon transfer to other environmental media, upon possible chemical and physical transformation and/or bioaccumulation in these media. The presence of these air pollutants at sufficiently high levels over sufficiently long time spans is referred to as air pollution.[2]

Air pollution is a phenomenon that occurs mostly in the troposphere, and it may impact humans and the environment in different ways depending on the type of pollutant and place of occurrence within the troposphere.[3] In the winter of 1952 in London, smoke emitted from residential coal burning mixed with fog to create 'smog', which dwelled in the greater London area for a few days due to inverted temperature conditions of the atmosphere that prevented a flux of pollutants to higher altitudes, reduced the visibility to locally less than a meter and caused elevated mortality and hospitalization rates. A different type of air pollution is known to occur as a result of chemical reactions of volatile organic species, nitrous oxides, and ozone induced by ultraviolet radiation. The smog that arises under these conditions is characterized by elevated levels of pollutants that have been formed within the atmosphere, and it is typically referred to as photochemical smog. Air pollution is a rather broad term for a multi-facetted problem, and the consequences of air pollution for humans and the environment may vary depending on pollution sources and meteorological conditions.

1.1.   Sources and Sinks of Aerosols

Aerosols, that is, the mixture of airborne particulate matter as well as the gases and vapors that particles are suspended in,[2] may be emitted into the troposphere from both natural and biogenic as well as anthropogenic sources, and they may be classified accordingly. Typical natural sources involve erosion, e.g., suspension of dust (e.g., sandstorms) and seawater (e.g., sea spray aerosol) at the air-land and air-sea interface, and suspension of organic material from organisms, like debris, pollen and spores, hair from plants, fungi, and animals, and microorganisms (bacteria, viruses).[4] Moreover, low-temperature phenomena, such as evaporation of volatile plant constituents (e.g., terpenoids) or organic compounds dissolved in seawater and formed by marine bacteria, as well as high-temperature processes, such as combustion and
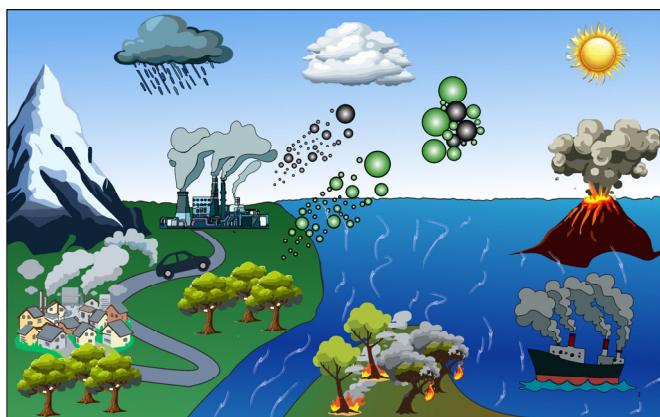
Figure 1-1 Illustration of sources and sinks of atmospheric aerosols.

pyrolysis (e.g., eruption of volcanoes and wildfires), can also be considered natural. Anthropogenic sources are those that involve human activity, such as large-scale industrial sources (coke ovens, smelters in steel industry), agriculture (evaporation of ammonia from fertilized farmland and erosion of dust from cultivated farmland), traffic (break and tire wear, fossil fuel combustion in engines of cars, ships, and aircraft) and small-scale, domestic combustion for heating and cooking activity.

In terms of mass of atmospheric aerosols, sea salt and mineral dust account for the largest portion of globally.[5] Nevertheless, anthropogenic sources, particularly those originating from combustion processes, are of great relevance for humans due to their comparatively high prevalence in metropolitan areas.[6]

All of the aforementioned processes refer to primary sources that emit pollutants directly into the troposphere. Yet, once emitted, pollutants may undergo chemical changes upon exposure to airborne reactive oxygen species ($OH^{-\cdot}$, $NO_3^{\cdot}$, O_3, etc.) and sun light,[7–9] and they may be subject to physical processes, such as gas-particle phase transitioning and coagulation, making research on atmospheric aerosols a multi-phase problem.[10–12] All of these processes are collectively referred to as aging of aerosols. Generally, homogeneous reactions among gaseous molecules and reactive oxygen species occur on much higher rate than reactions in the condensed aqueous phase.[8,11] Moreover, surface-mediated reactions at the air-liquid and air-solid interface of gaseous pollutants and airborne particles (e.g., rain droplets, ice cores, soot and mineral dust particles) may offer yet another pathway for airborne pollutants to be chemically transformed with yet another set of kinetic constants, which not only depend on temperature, pressure and concentration levels of pollutants, but also add the interfacial layer with its vastly changing density, viscosity over a range of few angstrom as a variable to the equation.[13] Regardless which route airborne pollutants follow, they are then said to be secondary pollutants.

The life time of these pollutants in the atmosphere is limited and may span ranges from several minutes to up to a several weeks.[14] The removal of particles may occur in two different pathways, which is dry and wet deposition. Dry deposition refers to the transport of gaseous species and airborne aerosols to the Earth's surface in the absence of precipitation, whereas wet deposition refers to the same process but under the presence of precipitation.[1] The former strongly depends on wind speed and turbulence, particularly in the near-surface layers of the troposphere, the terrain and the type of the surface (continental, snow, or ocean), season and temperature. Moreover, dry deposition of gaseous species depends strongly on the water solubility, chemical reactivity and physical properties of the depositing species, which governs the phase state of the molecules. Wet deposition involves both in-cloud scavenging and below-cloud scavenging and is even more complex than dry deposition as not only are there multiple phases involved, but particularly, the aqueous phase exhibits distinct particle size distributions for each of its forms, e.g., cloud water, rain, fog, snow, ice crystals, sleet, hail, etc.). Moreover, some processes, e.g., scavenging of particles, dissolution of gases in droplets, gas-particle phase transition of airborne organic matter, are reversible, making these processes even more complex.

1.2. Climate Change and Burden of Disease as Drivers of Research on Air Pollution

1.2.1 Aerosols and Climate Change

Anthropogenic emissions of air pollutants have increased substantially since the preindustrial age,[15] and this poses two major challenges for mankind, which are the effects of aerosols on the climate and on humans themselves. As for the former, the ability of gases and particles to interact with incoming solar radiation leads to a significant and long-lasting change in the Earth's radiative budget, which manifests in an increase of the atmosphere's temperature and changing weather patterns.[14] In that context, air pollutants and greenhouse gases are often classified based on their atmospheric life times into long-lived and short-lived climate forcers.[16] The atmospheric lifetime describes how well a chemical species can accumulate and how well they are mixed in the atmosphere. Climate forcers such as carbon dioxide are characterized by long atmospheric lifetimes of more than a year,[17] which leads to a good mixing within the atmosphere. Aerosols and other air pollutants generally have rather short atmospheric lifetimes and are therefore poorly mixed within the atmosphere. This leads to rather high temporal and spatial variability in potential climate effects of these species.

Due to their short atmospheric life times, the average global abundance of short-lived climate forcers in

the total atmosphere is rather low when compared to the concentration levels of long-lived ones. Therefore, the direct forcing effect of short-lived climate forcers, that is, a net warming or cooling effect through scattering of radiation via particles and absorption of incoming radiation by gases and particles, is also comparatively low with an average of -0.25 W m^{-2} in comparison to long-lived climate forcers like carbon dioxide and methane with averages of 2.16 and 0.54 W m^2, respectively.[18] The negative sign implies a net redirection of incoming radiation back to space. More important are indirect effects that refer to the effects other components within a climate system, e.g., modifications of microphysical properties of clouds, which modify lifetimes of clouds and their albedo as well as albedo modifications of surface albedo by oceans and snow. Particularly, the interaction of aerosols with clouds is thought to be a major contributor to the effective radiative forcing with an average of -0.84 W m^{-2}.[18] Overall, aerosols are thought to lead to a net cooling effect of the atmosphere, and the interaction of aerosols with clouds is likely the governing factor for this effect.

1.2.2   The Burden of Aerosols on Public Health

Increasing emissions over the last century do not solely affect the climate, but they are also recognized for their potential effects on public health. The first milestone in research focusing on toxicity of aerosol was a study by Wilkens[19] who suggested a relationship between elevated concentrations of air pollutants in outdoor air with elevated local mortality rates in the Greater London Area during the severe London Smog period in 1952. Decades later, Bell and Davis[20] analyzed mortality rates in the months that followed this extreme event and suggested persisting adverse effects and not only an immediate response of mortality response to outdoor air quality, leading to an increase from initially assumed 4000 to 12000 deaths that were attributed to only one extreme event. The second landmark in the history of air pollution research is the "Harvard Six Cities Study", which established an association between levels of fine particulate matter and mortality rates.[21] Many other studies have followed in North America[22–24], Europe[25–27] and Asia[28,29], which substantiated the relationship. These cohort studies are often limited to populations living in a certain location over rather short time scales, and in order to receive a more comprehensive picture on the net global effect of aerosols, the health burden is modeled by considering the contribution of various risk factors, such as environmental pollutants (e.g., particulate matter) and behaviors (e.g., first-hand smoking and diet), among others, to overall mortality.[30]

Exposure to fine particulate matter (PM) is often found as a major contributor to mortality,[31–33] with ambient air pollution by residential solid fuel combustion ranking as the second most impactful

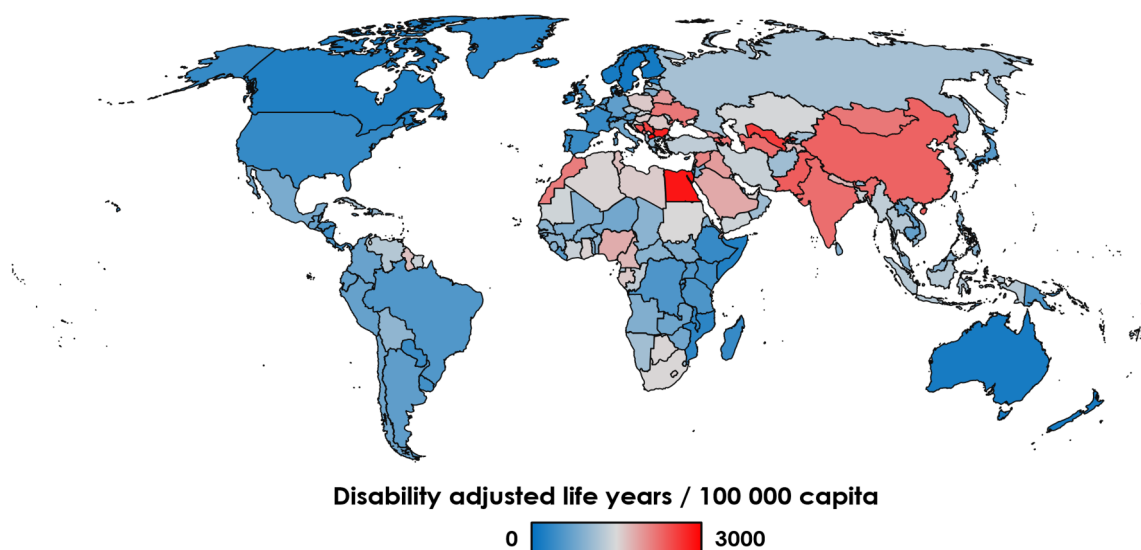**Disability adjusted life years / 100 000 capita**

0 ▭ 3000

Figure 1-2 Effect of ambient particulate matter on human health, expressed as disability adjusted life-years, around the globe. The map was created using data from the Global Burden of Disease Collaborative Network. 2020. Global Burden of Disease Study 2019 (GBD 2019) Results[35].

environmental risk in terms premature mortality and a reduction of disability-adjusted life-years.[34] Reasons for the great global importance of solid fuel combustion are the high prevalence of solid fuel burning alongside high population levels and densities as well as overall low air quality in South and South-East Asia. For Europe, the European Topic Centre on Human Health and the Environment attributed roughly 238 000 deaths to the exposure to fine particulate matter in all 27 member states of the European Union in 2020. On a per capita basis, the greatest health burden was found in Eastern European member states (Figure 1-2),[35] where a reduction of anthropogenic emissions from the residential and commercial sector was found as a major contributor to overall mortality, only being rivalled by emissions from the land transport sector.[36] In this regions, domestic coal burning is often identified as a major source of ambient fine particulate matter in urban areas.[37–42] The health burden that is associated with fine particulate matter from combustion aerosols is the main motivation for research aiming to unravel the chemical complexity of these types of aerosols.

1.3.   Properties of Aerosols

As already noted, aerosols are mixtures of PM and their surrounding gases and vapors, and thus aerosols from different sources may be parametrized according to the proportions the individual constituents. Gases are those compounds that are incondensable within the range of environmentally reasonable conditions of pressure and temperature; their boiling point is generally far below tropospheric temperatures. The term vapor refers to the gas phase of those compounds that are in a state of equilibrium or distorted equilibrium with the same substance deposited on particulate matter; vapors have a boiling point that make phase changes from gaseous to liquid generally feasible within the expected range of pressure and temperature within the troposphere. PM, as noted earlier, refers to both solid and liquid particles suspended in air and is a poorly characterized bulk substance without discrete properties. Thus, the following chapter aim to present various concepts for describing particulate matter.

1.3.1   Particle Size Metrics and their Relevance for Toxicology

The interaction of airborne particles with humans and the environment depends on the concentration levels and further on the sizes of particles. The geometric size of a particle refers to its physical dimensions, and it is a fundamental parameter that influences all other size related metrics, that is, surface area, volume, and mass. The term size typically refers to the diameter, which implies a somewhat spherical shape, an assumption that does not necessarily hold for all particles. The aerodynamic diameter is related to the geometric size of particles, but instead of describing physical dimensions, the parameter is measure of the mobility of a given particle in a fluid by also considering the particle's mass, shape and density. It equates the mobility of a particle to the mobility of a true spherical particle.[43] The aerodynamic diameter governs the inhalation of particles by humans and their deposition in the different regions of the respiratory tract (Figure 1-3 top panel).[44] Particularly, ultrafine particles with diameters of less than 100 nm can deeply penetrate the lung and reach the alveoli. Thus, the properties and effects of these particles have experienced a growing interest in the recent past.[45–47]
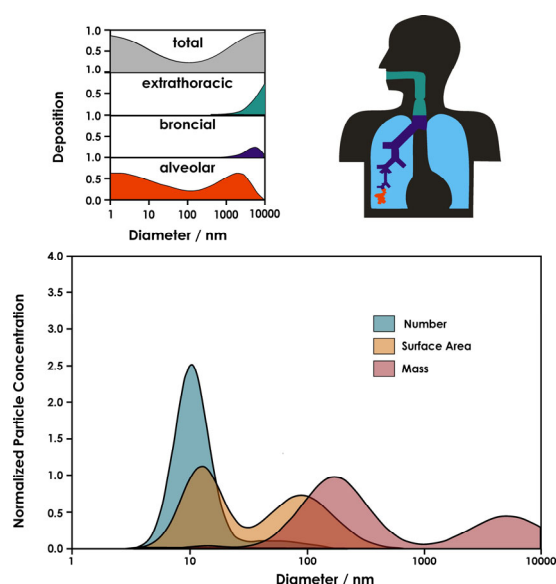

Figure 1-3 Size-dependent deposition of particles in the human respiratory tract, taken from Heyder[44], and the relationship between different particle size metrics for an idealized ambient aerosol by size distribution of particle number, surface area and mass adapted from

Once particles are deposited, the deposited dose as a toxicologically relevant metric may be defined in a variety of different ways (Figure 1-3 bottom panel).[48] For soluble particle constituents, traditional mass-based approaches may be most adequate since soluble toxins may dissolve into bodily fluids and react with native compounds or biological tissue and disrupt the cell homeostasis. The surface area may be an appropriate metric for insoluble nanoparticles.[49] Insoluble, non-toxic particles may act as carrier of other toxins, and the surface area may be an indicator for the amount of toxins a particle may carry. For insoluble toxic particles, a particle's surface area may also be the governing metric as the surface is the interface for reaction with bodily substances, such as proteins and lipids, or tissue.[49] Number emissions may be more relevant for larger, bio persistent particles and fibers, which are too big to be eliminated by natural defense/clearance mechanisms and lead to toxic responses via so-called frustrated phagocytosis of macrophages, e.g., as shown for asbestos and carbon nanotubes.[50,51]

Current European standards on ambient air quality generally do not involve measurements of particle metrics other than mass concentration of particulate matter with diameters below 10 μm (PM_{10}) and 2.5 μm ($PM_{2.5}$).[52] Adding new size metrics to air quality standards may shift the focus onto different classes of particles. For example, particle mass concentrations are dominated by rather few particles that are comparatively large and heavy, and including other relevant size metrics, such as number emissions, in monitoring stations of ambient air quality would help to shift the focus onto ultra-fine particles and shed more light into their effects.

1.3.2   The Nature of Carbonaceous Aerosols

Once deposited in the human respiratory tract, particles may cause substantially different effects depending on their chemical composition. Being exposed to sea spray aerosol, mainly comprised of sodium chloride, may have significantly different consequences for humans than the exposure to aerosols emitted from combustion processes. The composition of ambient particulate matter, which humans are exposed to, is highly variable, depending on factors, such as location of the sampling site, season and weather, among others. Typical constituents are ionic species (NH_4^+, NO_3^-, SO_4^{2-}, Na^+, Cl^-), metals (Al, Fe), particle-bound water, and carbonaceous material.[16,53] If the latter is emitted by incomplete combustion processes, the carbonaceous material is commonly referred to as soot.

Soot is not a unique but a bulk substance class with indiscrete structure and/or chemical composition. Early approaches to characterize soot used to inventory macroscopic properties.[54,55] For example, soot that was sampled on filters can be classified into a non-refractory fraction of organic matter, whose carbonaceous portion is referred to as organic carbon (OC), and a refractory, near-elemental carbon fraction (EC).[56] Both of these fractions are typically further subdivided based on their volatility, thermal stability and refractoriness.

Figure 1-4 Thermo-optical classification of carbonaceous particulate matter. The figure was adapted from Pöschl et al.[56].

EC refers to the inorganic portion of soot, typically characterized by large graphite-like structures (Figure 1-4), and it is equivalent to another frequently used term, black carbon (BC).[57] BC aims for the same structures of soot but targets the chemical composition by their optical properties, and it is particularly important for studies focusing for modeling studies to estimate the soot portion of PM using satellite-based approaches.[58–60] Optical techniques however cannot, or only in a very limited way, account for the variable chemical composition of organic matter that is co-emitted during incomplete combustion processes and deposited on BC, leaving a gap for thermal approaches that are able to parametrize the organic matter.[61]
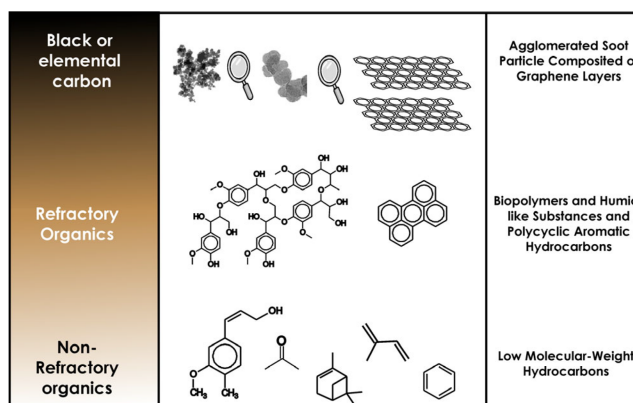
OC refers to rather small, particle-bound constituents that are able to desorb thermally or pyrolyze below a certain temperature in an inert atmosphere. Beyond the bulk parametrization of volatility and thermal stability, modern analytical equipment, such as gas chromatography (GC) mass spectrometry (MS),[62,63] allows for describing the molecular composition of OC, which may provide further insights into the toxic effects of carbonaceous aerosols.[64]

1.4. Coping with Chemical Complexity to Refine Air Quality Management Strategies

Due to the variable nature of ambient aerosols, especially particulate matter, current efforts that aim to quantitatively assess their global burden on public health are subject to uncertainty and biases. These analyses assume that the relative risk that is associated with the exposure of humans to ambient air pollutants, such as ambient particulate matter, is uniform for all types of (combustion) sources,[65] which is partly due to the exposure assessment being carried out via satellite-based, remote-sensing approaches[66] that provide the spatial coverage needed for a global risk assessment but cannot account for the variable chemical composition and physical properties and thus variable toxicity of these sources. While these studies are essential in providing an overall magnitude of the public health burden and illustrating air pollution hot spots, the remote-sensing strategies that these modeling rely on fall short in providing the detailed information that is necessary if one wants to develop a mechanistic understanding of the health. With the aim of providing such a mechanistic understanding, individual sources of air pollution are frequently tested for their toxic potential, which reveals differences among particulate matter emitted from different combustion sources,[67] among different scales of combustion appliances (residential vs district solid fuel heating appliances[68]), among different small-scale heating systems (oil vs wood[69] and wood stove vs pellet boiler[70]), and among different fuels in the same system[71–73] as well as for individual fuel types used in marine engines[74], among others.

These differences in the toxicological potency imply that there it may be more cost-effective to restrict specific sources rather than to restrict bulk pollutants, as it is currently the case in many developed countries by means of restricting the ambient concentration of different size fractions of particulate matter. Gaining a mechanistic understanding on health effects of aerosols in the laboratory, identifying sources with the most toxicological potency and restricting the contribution of these emission sources to ambient air may be much more cost-effective than the shotgun approach of a restriction of particulate matter as a whole. Although this approach is not carried out in routine monitoring of air quality, these source-oriented approaches are frequently carried out by many research groups across the globe.[75], and it is referred to as receptor modelling.[76]

Two receptor modelling algorithms have gained much popularity over the past decades. The chemical mass balance approach refers to a supervised matrix factorization approach were a matrix storing information of m samples and p properties is reproduced by the linear combination of a loadings matrix that contains source profiles (chemical fingerprints) of a number of sources and a score matrix that stores information on how to scale these individual factors for any sample.[77] While the information stored in the loadings matrix is provided by the user, the score matrix is optimized to minimize the difference between the linear combination of loadings and scores and true sample matrix.[76,78] This approach typically requires that information on the source profile is available *a priori*, implying pre-experiments with combustion sources,[79–83] and consequently estimates are sensitive to the choice of source profiles, leading to uncertainty in the estimations.[84,85] Moreover, this approach does not account for the chemical transformation of factor profiles during their stay in the atmosphere, which is another contributor to overall uncertainty that is associated with estimates provided from these methods.

Positive matrix factorization or non-negative matrix factorization on the other hand refer to a unsupervised strategies where a matrix of m samples and p properties are decomposed in two matrices,

with one containing a source profile and the other containing their scores.[86,87] In these approaches, not only the matrix storing the scores is variable but also the matrix storing the chemical fingerprint, which may account for chemical reactions and physical processes that pollutants are subjected to in the environment. The positive matrix factorization relies on the comparison of model results with these profile *a postiori,* implying that some kind of knowledge must be present for interpretation of the output source profiles yet not mandatory. A common problem that goes along with these approach is that sources that have similar seasonal and/or diurnal time profiles may occur as a mixed factor, as described by Leonie et al.[38] for residential biomass and coal combustion in the Moravian-Silesian border region. Thus, constrained algorithms that require source profiles *a priori* yet allow these factors to be adjustable in user-defined ranges have also been used.[88]

A particular challenge that comes with these estimations is that the information that these algorithms use as input information needs to be as simple as possible in order for the results to be easily interpretable and cost-efficient yet as descriptive as possible in order to avoid large ambiguity in the apportionment of sources. Moreover, these approaches are not limited to chemical data sets but can be applied to any kind of multivariate information, e.g., size distributions of sub-micrometer particles,[38,39,89] Nevertheless, molecular based approaches are still highly desired since this knowledge on molecular markers is beneficial to rationalize the results.[88] The question arises in how much detail the chemical composition needs to be understood to for monitoring purposes to create cost-effective air quality management strategies, and a variety of definition emerged for the various levels of molecular identification, from a rather unspecific level of identification for the purpose of creating inventories to quasi molecular identification for problems that have never been faced before.[90] The development of instruments for monitoring purposes typically do not require a full characterization of the molecular composition but rely on the characterization of compounds in the laboratory in order to create reference library for comparison *a postiori*. For this, a broad range of instruments have been developed to characterize emissions on a semi-molecular level, such as aerosol mass spectrometer that reduce the chemical complexity of aerosols by means electron ionization to rather few and rather unspecific chemical moieties,[91,92] mass spectrometers that gain insights on the composition of particle-bound constituents on a single-particle level,[93,94] as well as filter-based approaches that make use of existing analytical platforms, such as thermal-optical carbon analysis.[95] Regardless of the type of instrument, source libraries need to be created in order to use these instruments as tools in air quality management, and due to fact that many of these approaches operate on semi-molecular level, chemical knowledge on the nature of the emission source and what pollutants are to be expected is needed. Hence, the following chapter will focus the evolution of carbonaceous emissions from combustion processes.

1.5. Evolution of Carbonaceous Emissions in Combustion Processes

1.5.1 A General Description of a Fire

Given the importance of emissions from solid fuel burning for the global public health burden, the next section aims to provide a comprehensive understanding of the processes that lead to the evolution of emissions.[34] Fires from solid fuel burning are highly-complex, and several sub processes and their feedback on one another have to be considered to describe the phenomenon. Fires are often perceived in two different modes, that is, the high-temperature flaming combustion and the low-temperature, flameless smoldering combustion (Figure 1-5 right panel). The differences between both types is the phase of the matter that is oxidized during the combustion. In a flaming combustion, the homogeneous oxidation of gas-phase constituents is dominant, whereas oxidation occurs mostly at the surface of the condensed fuel in a smoldering combustion.[96]

Regardless of the type, the start of the combustion of a solid is initiated with a so-called pilot ignition.[97] The flames of the pilot radiate energy, which leads to a flux of energy from the pilot to the surrounding fuel, causing the fuel to dry out and eventually initiating pyrolysis reactions (Figure 1-5 left panel).[98] Fuel pyrolysis

releases combustible gases and vapors that may ignite when concentrations of combustible gases are high enough and mixing with oxidants is sufficient, that is, the fire exceeds the flammability limit.[99] Not meeting these criteria may not necessarily cause the fire to extinguish since pyrolysis reactions may be exothermic causing the fuel to heat up to temperatures that allow for heterogeneous oxidation at the surface of the fuel, and by doing so, these reactions sustain a smoldering combustion.[100] If these criteria are met, and pyrolysis gas ignites, the combustion proceeds in a flaming combustion.[101] Either way, the fire spreads from the pilot to the surrounding area and consumes the fuel. The fire proceeds until the energy flux to the fuel in the proximity of the flame is too small to initiate further pyrolysis reactions and surface oxidation at a sufficient rate in order to sustain a flaming or smoldering combustion, respectively.

The sub-processes involved in fires are the pyrolysis of the macromolecular network leading to the evolution of combustible gases, oxidation at the surface of the condensed material, diffusion and convection of combustible gases and oxidants, chemical
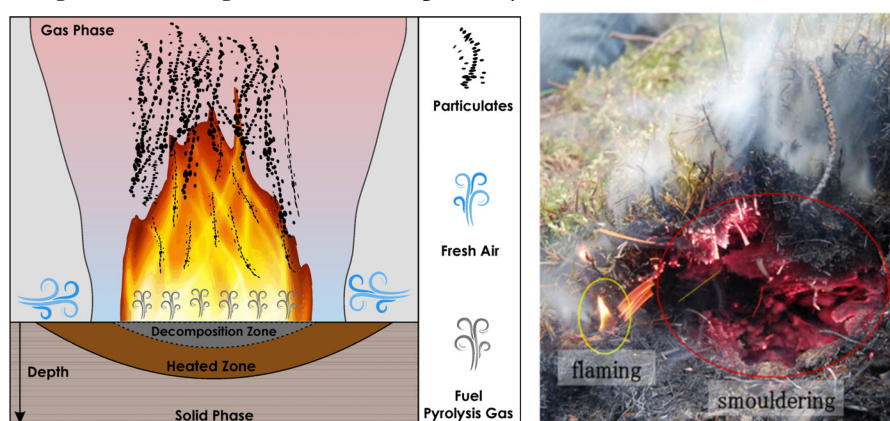
Figure 1-5 Illustration of Macroscopic Processes Upon Solid Fuel Burning, adapted from Rogaume[66] (left), and a photograph illustrating the two different types of fires, taken from Rein[64].

reactions in the gas phase (partial oxidation and pyrolysis), and radiative processes that lead to a flux of energy from the flame to its surrounding.[97] These reactions may occur simultaneously in different proportions at different location of the fire (Figure 1-5 left panel). The kinetics of these processes are influenced by the location, size and orientation of the pilot, influencing the energy flux and fluid dynamics of gases (buoyancy), properties of the surrounding gas (temperature, pressure, oxygen concentrations and flow velocity and direction), the sample's geometry, thickness, surface area, porosity and permeability for gases as well as its chemical composition and thermal conductivity, permeability and capacity.[102] Moreover, these factors change over the progression of the combustion as the chemical composition and physical appearance of the fuel changes due to the exposure to high temperatures.

1.5.2   The Chemical Composition of Common Solid Fuels

Before going deeper into the reactions that lead to the evolution of combustible gases, the fuel's composition needs to be discussed since properties of the unburned fuel define the starting point for each combustion process and may influence the pathway the process may take. What type of reactions may occur depends on the chemical composition, that is, the elementary composition (C, H, N, O, and S) and the type of chemical bonds that connect these elements in the fuel (C-C, C=C, C-O, C=O, etc.). This section evolves around the chemical composition of biomass and coal because they are the most common fuels in both intended fires, as found in modern residential wood and coal stoves, and unintended fires, like wildfires as well as natural peat and coal fires.

The composition of biomass is highly complex and varies from species to species and even for different organs of the same plant (e.g., root, stem, leaves, petals, fruit bearing organs, etc.). In all land-based plants, cellulose, hemicellulose and lignin are primary plant constituents and make up for a large fraction of biomass.[103] The rigidity that these structures provide to the plants initially allowed the plants to transition from the ocean to the Earth's surface. Moreover, there is a great variety of secondary plant constituents, which may also be present in large amounts in plants, but the overall concentration and composition may

vary substantially among different species and even different organs of the same species.[104] Plants produce secondary constituents as a defense strategy against pests and predators as well as a reproduction strategy by attracting pollinators or fruit-dispersing animals. These substances are of great importance since they may be produced in larger amounts in comparison to some other secondary constituents that regulate the metabolism.[104,105]

Table 1 Major constituents of biomass.

Cellulose

Monomer

β-D-glucopyranose (Glu)

Polymer

→4)Glu β (1→4) Glu β (1

Hemicellulose

Monomer

β-D-glucopyranose (Glu)   α-D-xylopyranose (Xyl)

Polymer - xyloglucan

Xyl
λ
1
↓
6
→4)Glu β (1→4) Glu β (1→4) Glu β (1→4) Glu β (1→4) Glu β (1→4) Glu β (1
6
↑
1
λ
Xyl

Lignin

Monomer:

p-coumaryl alcohol:
R₁ = R₂ = H

coniferyl alcohol:
R₁ = OMe, R₂= H

sinapyl alcohol:
R₁ = R₂ = OMe

Polymer – characteristic features of linkages marked red

beta-O-4   resinol

biphenyl   diaryl ether

Secondary plant constituents

Abietic acid   Betulinic acid

The composition of biomass is highly complex and varies from species to species and even for different organs of the same plant (e.g., root, stem, leaves, petals, fruit bearing organs, etc.). In all land-based plants, cellulose, hemicellulose and lignin are primary plant constituents and make up for a large fraction of biomass.[103] The rigidity that these structures provide to the plants initially allowed the plants to transition

from the ocean to the Earth's surface. Moreover, there is a great variety of secondary plant constituents, which may also be present in large amounts in plants, but the overall concentration and composition may vary substantially among different species and even different organs of the same species.[104] Plants produce secondary constituents as a defense strategy against pests and predators as well as a reproduction strategy by attracting pollinators or fruit-dispersing animals. These substances are of great importance since they may be produced in larger amounts in comparison to some other secondary constituents that regulate the metabolism.[104,105]

Cellulose and hemicellulose are both primary plant constituents and are made of polysaccharides. Cellulose is formed from a single monomer, that is, β-D-glucopyranose, and it comprises thousands of individual monomers that are connected via β (1→4) glycosidic linkages (Table 1).[103] Hemicellulose on the other hand is a rather undefined polymer class that can be formed from various monosaccharides. The most representative of hemicellulose is xyloglucan, which is made of a main chain of glucose with a side chains of xylose attached to it.

Lignin typically consists of units of p-cumaryl alcohol, coniferyl alcohol and sinapyl alcohol. Lignin from gymnosperms typically has higher proportions of coniferyl alcohol, while p-cumaryl alcohol and sinyapyl alcohol are only minor constituents, whereas angiosperms comprise approximately similar amounts of sinapyl and coniferyl alcohol and only minor amounts of sinapyl alcohol.[106] The way that these monomers are not uniquely linked, yet the most abundant feature in many biomass types is the β-O-4 linkage, which is formed via the enzymatic oxidation of the hydroxy group at position 4 leading to the formation of a radical that attacks the C- atom at position β of another monomer with subsequent hydrogenation of the radical that forms at the C-atom at position α.[106] These type of linkages in lignin make up large fractions (>45%) of the total lignin in all types of biomass and in grasses even up 80%, while other types of linkages, such as the resinol-type, biphenylic, and diaryl ether linkages, etc., are less abundant.[106]

Secondary plant constituents are highly diverse in terms of their chemical nature and can be separated into many compound classes.[104] The most important of them are terpenoid, which are characterized by the common feature of isoprene as a building block. Members of this compound classes can be subdivided based on how many isoprene units are present within the molecule; monoterpenes, sesquiterpenes, diterpenes, sesterterpenes, triterpenes vary from two to six isoprene units, respectively. Many of these terpenoids can be found in high concentrations in outer organs and tissue of plants, e.g., bark and leaves, where these compounds are produced for protection against predators or attraction of pollinators or fruit dispersing animals.[104] Yet, the most relevant organ in terms of overall mass are plant epithelial cells surrounding resin ducts, which produce oleoresin, which is a complex mixture of various terpenoids and can be further separated into turpentine (monoterpene olefins) and rosin (diterpene resin acids). Some of these resin acid terpenoids may be highly specific; for example, betulin is a triterpenoid that is found in birch wood, whereas abietan is highly specific for gymnosperms, such as spruce.[79] Other secondary plant constituents, such as phytosterols, may also be relevant, yet their occurrence is not nearly as high as resin acids and their function is less well understood.

A second major feedstock for combustion processes is coal. Coal is a complex carbonaceous sedimentary rock, largely composed of plant debris that was buried over tens to hundreds of million years below the Earth's surface. Due to the exposure to elevated temperatures and pressure, the organic material underwent physical and chemical alterations, that is, diagenesis and metamorphosis.[107] Diagenesis refers to the physical compaction of loose material to solid rocks, the elimination of excess water and air from loose material, and the subsequent squeezing of the buried material leading to the production of an organic liquid, which can distribute comparatively freely within the entirety of the buried material. Metamorphisms on the other hand refers to the chemical and physical alterations of the buried material upon exposure to elevated temperatures and pressures after diagenesis. Coal is typically classified based on the extent diagenesis and metamorphosis as well as the nature of the organic material and the nature and amount of sediments that 'contaminated'

the organic matter. The organic composition is typically reflected by the type of coal, the amount of inorganics is reflected by the grade, and the extent of diagenesis and metamorphism is reflected by the rank. Coal types are said to be either humic, that is, the organic material origins from largely woody sources, or sapropelic, that is, the organic material origins from largely non-woody sources.[108] Grade is determined based on the ash content and may vary for different coal seams. The rank is a measure for the maximum pressure and temperature that the coal was exposed to, and according to O'Keefe et al.[108] this indirectly reflects the depth of burial and the geothermal gradient.

As the organic matter progresses through the individual ranks of coal, the organic material undergoes chemical changes, which have been summarized by O'Keefe et al.[108] for wood to the rank of bituminous coal. In the early stages, cellulose and hemicellulose are eliminated, and the transformation of lignin to lignite is initiated by the dissociation of aryl-ether bonds, including the β-O-4 bond connecting individual monomeric units as well as dissociation of methoxy groups, leading to the formation of catechol units and increased crosslinking between individual monomers via alkylation reactions. The subsequent transition from lignite to sub-bituminous coal is marked by the loss of all methoxy groups and the loss of hydroxy groups from catecholic structures leading to phenolic structures with few substituents. Subsequently, the aromatic rings begin to fuse to larger polycyclic aromatic hydrocarbons (PAHs), which marks the transition from sub-bituminous to bituminous coal.

1.5.3 Pyrolysis in the Condensed Phase

Due to the high structural complexity of both biomass and coal, pyrolysis reactions are manifold. Moreover, the energy released by these reactions influences the chemical composition of the pyrolysate vapor and gas-phase reactions have a feedback on pyrolysis reaction in the fuel via a radiative transfer of energy, as well. Due to the sheer number of potential reactions, it is common to lump them into three principal mechanisms: (i) fragmentation, (ii) depolymerization, and (iii) char formation, which have been reviewed by Collard and Blin[109] in the context of biomass pyrolysis (Figure 1-6).

Fragmentation refers to the type of reactions that lead to the dissociation of chemical bonds within one monomeric unit of the macromolecular network, regardless whether it is cellulose or lignin or their coalified analogues. Possible fragmentation within a molecule of coniferyl alcohol, as an example, are the dissociation of the C_3 chain (dissociations between members of the chain), hydroxy groups and methoxy groups. These types of reactions are thought to yield a variety of smaller incondensable gases as well as condensable yet volatile short-chain hydrocarbons.
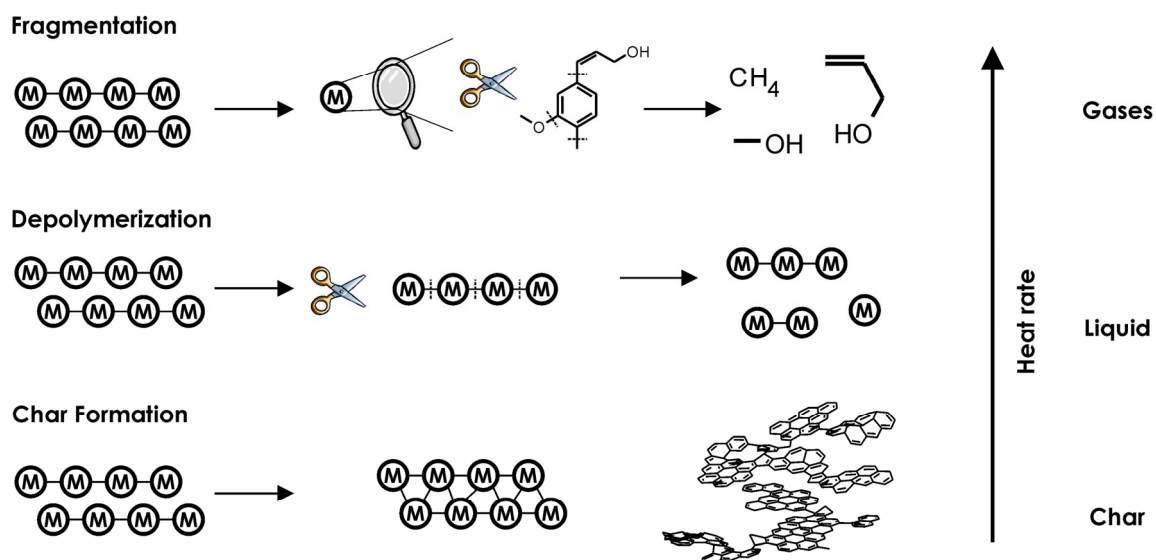

Figure 1-6 Principal pyrolysis mechanisms in the condensed phase of the fuel, adapted from Collard and Blin.[74]

Depolymerization reactions refer to a series of reactions that lead to the dissociation of bonds between individual monomeric units of the macromolecular network followed by reactions that stabilize the new chain ends after each dissociation. They occur until the products becomes volatile enough to be transferred to the gaseous phase. These reactions typically yield a product mix that is condensable at room temperature. Although being referred to as depolymerization, the dissociation of monomeric units does not have to retain the integrity of each individual monomer, but instead these reactions retain characteristic features of a monomeric unit, that is, the feature of benzene rings with side chains that may vary in length still attached to them in case of the example coniferyl alcohol.

Char formation refers to the networking-building reactions in the condensed phase of the material. It is characterized by a high degree of inter- and intramolecular rearrangement and ring fusion reactions that lead to the formation of larger aromatic structures. Char formation occur mostly in the condensed phase

All of these reactions occur simultaneously, but the proportion of their occurrences may vary depending on the heat rate and progress during a pyrolytic process, which may affect the composition of bulk pyrolysis products (gases-condensable vapors-solids).[109] Under low heating rates, fragmentation reactions occur only in the most labile bonds, which is followed by series of inter and intra-molecular rearrangement and recombination reactions forming a more thermally stabile char matrix. Many of the more stable bonds will still be intact and incorporated into the char matrix via aromatization/graphitization, which makes them less susceptible for pyrolysis reactions at higher temperatures. Thus, lower heat rates favor the formation of char. At higher heat rates, there is not enough time for these rearrangement reactions to occur at a significant rate, and the cleavage occurs even within more stable bonds, which favors the pathways of depolymerization and fragmentation reactions that yield higher proportions of liquid and gaseous compounds in the pyrolysate. The char content is reduced in comparison to low heating rates.

1.5.4   Decomposition Reactions of Organic Molecules in the Gas-Phase

Primary pyrolysis leads to the release of combustible gases and vapors, which may undergo further reactions at high temperatures in the gas phase. Once more, all reactions occur simultaneously and compete with one another, and different processes dominate in different areas of the flame depending on the availability of oxygen, mixing ratio of combustible gases as well as the molecular composition. Mechanistic studies under the absence of oxygen may resemble the fuel-rich and oxygen-scarce area of the flame only millimeters above the fuels surface, which is characteristic for diffusive flames that are characterized by a mixing pyrolysis gases and oxidants within the flame. When combustible gases and oxidants are already mixed before the combustion, these flames are referred to as premixed flames. Solid fuel burning like most other real-world fire scenarios are diffusive flames.[97]

Reaction kinetics and reaction mechanisms for the gas-phase cracking and oxidation are typically studied in shock tubes, and these experiments can provide kinetics for the initial steps of the reaction but not for the complete process as the mechanisms involve hundreds of reactions for a single species due to the vast number of different types of reactions, i.e., hydrogen abstraction, isomerization, rearrangement reactions, carbon-carbon dissociation, among others.[110] Shock tube experiments have been conducted for a variety of different proxies, e.g., smaller aliphatic hydrocarbons[111–115], various linearly alkylated benzenes, [112,115–118] anisole,[119,120] indane- and indene,[121,122], anisole,[119,120] naphthalene[123,124] and furan derivatives.[125,126] Furan derivatives and benzene/phenol derivatives can be seen as proxies for cellulose pyrolysis products and lignin pyrolysis products, respectively.
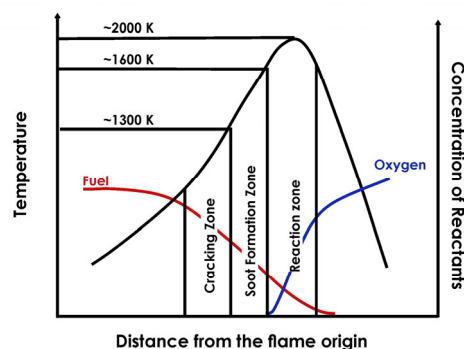

Figure 1-7 Combustion zone, temperatures and concentrations of reactants in diffusive flames, adapted from Rangwala[65] .

Of particular importance is the pathway that leads to ring-opening reactions for aromatic molecules as this pathway allows further degradation to even smaller species, such as acetylene. For furan derivatives, these reactions have been found as a major pathway in the initial degradation of the furan-type precursor regardless of the type of the substituent,[125] whereas ring-opening in alkylated benzenes occurs only at high temperatures well above 2000 K, when all other bond have already been stripped from the aromatic benzene core.[127,128] Anisole as a proxy for the phenolic structures in lignin does not follow the typical decomposition path to unsubstituted benzene like the alkylated benzenes. In the early stages of pyrolysis, anisole loses the methyl group from the methoxy group, which is followed by the ejection of CO from the phenoxy- radical and the formation of cyclopentadiene.[119,120] Subsequently, cyclopentadiene react with methyl radicals to form methylcyclopentadiene and eventually rearrange to benzene.[120] These reaction mechanisms become even more complex when the interaction of pyrolysis products from more than one precursor is considered.[115] Product yields of individual molecules from shock tube experiments cannot accurately resemble the mechanisms that govern the cracking and partial oxidation in flames, but it allows for isolation of reaction constants that are difficult to access in pre-mixed and diffusive flames.

1.5.5   Soot Formation

Pyrolysis is not only a process that leads to the decomposition of chemical compounds in the gas phase of flames, but it also can lead to the formation of larger organic molecules, i.e., PAHs,[129] and soot.[130,131] Soot formation is often described by four principal processes, that is, (i) the formation of larger molecular PAHs, (ii) the inception of particles from precursors, (iii) surface growth and coagulation of particles and (iv) agglomeration of particles.

For the formation of larger PAHs, the rate-limiting step is thought to be the formation of the first aromatic ring, that is, benzene. One route that is frequently acknowledged to be dominating in terms of benzene production is the addition of acetylene to vinylacetylene or butadiene, with subsequent elimination of hydrogen in case of the latter. This was initially proposed by Frenklach et al.[132], and it is now widely accepted as one of the major pathways. Yet, as discussed earlier, there are also other pathways that lead to the formation of the first benzene ring via pyrolysis of aromatic structures, such as furans, alkylated benzenes and phenols. Once the first aromatic has formed, Frenklach et al.[132] proposed the hydrogen abstraction C_2-absorbtion mechanisms (HACA) for the growth of smaller aromatic rings to larger polycyclic aromatic structures, which is still recognized as the major pathways for growth.[129] However, in the last decades, other pathways have been proposed evolving around the addition and, if necessary, subsequent rearrangement and cyclization reactions of either methyl-, vinylacetylene-, phenyl-, resonantly-stabilized radicals (propargyl-, cyclopentadiene, and indenyl-radicals).[129,133–135] Particularly, resonantly-stabilized radicals have been in the center of attention as they may be highly relevant in the inception of particles.

Particle inception refers to the point where larger PAHs form clusters of PAHs and mark the transition from the gaseous to the condensed phase. Three possible pathways for the inception of soot particles are currently discussed in the scientific community: (i) the formation of larger, three-dimensional PAHs, (ii) the stacking of moderately sized PAHs into clusters/layers via Van der Waals forces, and (iii) and the formation of larger PAH cluster via covalent cross-linking reactions.[136] The latter two came up due to the fact that the HACA mechanism cannot form three dimensional structures via the first pathway at a rate that is observed for soot formation in flames and the fact that the first pathway is not able to explain the bimodal size distribution of particle numbers.[136] Mechanisms for stacking of PAHs were already incorporated in the early numerical simulations of soot formation and growth by Frenklach and Wang[137], but the models have failed to accurately predict the observed bimodal size distributions of very small nascent soot particles.[138] Recently, Johansson et al.[139] proposed a mechanism that involved resonantly-stabilized radicals (indenyl-type radicals) in the inception of particles and advocated for the role of covalently cross-linked PAHs in particle inception. Noteworthy, they have shown that crosslinking reactions at indenyl-type radical sites lets PAH grow quickly

without depleting the radical pool, which is needed to explain soot particle growth in later stages of the flame. The subsequent ejection of the H atom at the indenyl attack site has a very low kinetic barrier, which allows high reaction rates.

Once soot particles have nucleated, they can grow in mass and surface via HACA-type reactions in the periphery of the particle as well as through condensation of PAHs onto the particles' surfaces.[130] Moreover, particles may coagulate, which refers to a collision of soot particle that leads to the formation of a bigger spherical soot particle, implying a somewhat liquid nature of nascent soot particles. At later stages of the flame, particles collide with one another to form larger fractal particles. The growth can be separated into a coalescent growth, where spherical nascent particles collide with one another to form a larger, spherical soot particle, and into agglomeration, where spherical particles collide with one another to form a larger soot particle of fractal appearance.
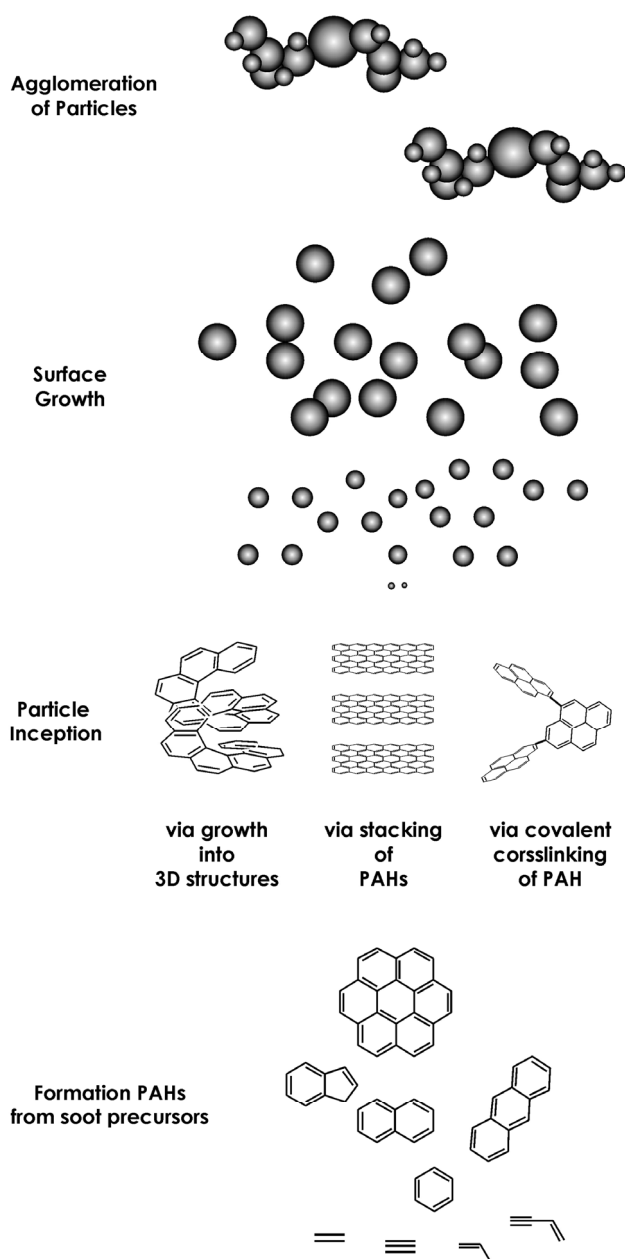

Figure 1-8 Principal steps in soot formation adapted from Wang[104] and Richter and Howard[100]

2. Scope of this Thesis: Coal Burning in Modern Combustion Appliances

In January 2022, new emission standards for residential heating appliances using solid fuels (among others) came into force under EU Directive 2009/125/EC.[140] Manufacturers of these appliances will have to comply with new emission thresholds for bulk air pollutants (CO, nitrogen oxides NO and NO_2 as NO_x, PM, organic gaseous carbon) and thermal efficiency in order to reduce local air pollution and greenhouse gas emissions. Some countries, such as Germany, have already adopted these emission limits before, but beginning January 1, 2022 these standards will apply to all 27 member states of the European Union. Although these regulations aim to limit greenhouse gas emissions, they do not limit the use of fossil fuels such as coal, which is a non-renewable solid fuel, or set any fuel-specific limits, and thus coal is still a viable fuel in areas where coal is still mined and thus remains inexpensive.

Due to the complexity of fire and pyrolysis phenomena, it is still difficult to predict the chemical composition of emissions from real-world combustion units with numerical simulations, which leaves a gap for hands-on research on emissions from these appliances. Most of the information on emissions from coal-fired domestic heating appliances, beyond the policy-relevant bulk pollutants, is limited to automatically fueled domestic hot water boilers.[141–144] or on cooking stoves[145–154], which are not commonly found in Europe but in China. Detailed chemical information on emissions from manually fueled stoves that meet latest European emission limits is lacking, and the existing information on modern boilers does not represent these appliances well due to their differences in operation modes. Boilers have a continuous operation principle where only a small amount of fuel is fed into the process in comparatively short intervals. Stoves on the other hand operate discontinuously, that is, a large amount of fuel is added in rather large intervals. Consequently, stoves usually pass through distinct combustion phases, which are characterized by variations of chemical fingerprints in the time domain.[155] Overall, many researchers have found these appliances to emit higher levels of pollutants than equivalent hot water boilers.[83,141–143]

Emissions from burning coal and logwood in a modern single-room heater were investigated in a field campaign carried out by Helmholtz Virtual Institute of Complex Molecular Systems in Environmental Health (HICE) consortium, whose main goals were the elucidation of the molecular mechanisms and agents in combustion aerosols relevant for the observed health effects, the identification of biomarkers for exposure and health effects, and the evaluation of the relative toxicological potential of different anthropogenic aerosol sources. Toxicity of PM was hypothesized to depend strongly on the chemical composition of the respective aerosol sources, aside from the total deposition of particles. Thus the main research questions were:

(1) How do emission profiles of the evolving chemical constituents differ between coal and wood, and are there factors that influence the chemical composition of emissions in real-world solid fuel combustion?

(2) Are there differences to other forms of solid fuel burning in terms of the chemical composition and toxicity?

(3) Is it possible to identify markers for coal and wood burning to improve their identification in source apportionment and help policy-makers in doing informed decisions?

3.   Methodology

3.1.   Infrared Spectroscopy as a Tool for Analysis of Gases

3.1.1   Theory of Molecular Vibrations

Infrared spectroscopy (IR) is an essential tool for research on combustion processes, and it may offer information on emission of various incondensable gases that can be found in bulk in combustion aerosols. The working principle of every form of spectroscopy is the interaction of electromagnetic radiation and matter, with IR spectroscopy aiming for molecular vibrations.[156] Vibrations of molecules may be fairly simple, such as a coupled motion of two atoms, but become more complex with increasing number of atoms N within a molecule. Each of these atoms has three degrees of freedom for its motion, and three modes of the molecule represent a translational motion into a specific direction and three represent the rotational motion of the molecule, respectively, generally leaving $3N - 6$ modes for the vibration of a molecule. Each of these modes can be described by Hooke's law (Figure 3-1), which linearly relates the displacement of the atoms from their equilibrium position to a restoring force. The first few energy states V_{iv} can be described rather well by (3.1), where h is Planck's constant, v_i is the fundamental frequency of the respective mode, and v_i is the vibrational quantum number of the ith mode. The energy difference between individual states is approximately the same.

$$V_{iv} = hv_i \left(v_i + \frac{1}{2} \right)$$

(3.1)

For higher vibrational modes, Hooke's law cannot account for the decreasing attraction and increasing repulsion at the extreme points, and therefore the model of an anharmonic oscillator is applied to describe the behavior for transition between energy states (3.2), where x_i is the anharmonicity constant.

$$V_{iv} = hv_i \left(v_i + \frac{1}{2} \right) + hv_i x_i \left(v_i + \frac{1}{2} \right)^2$$

(3.2)

While the vibrational motion of a diatomic molecule is fairly simply with exactly one stretching vibration, molecules with more than one atom generally exhibit more vibrational modes. These can either be categorized as stretching (symmetrical or asymmetrical), bending in plane (rocking and scissoring), or bending out of plane (twisting and wagging). In order to use these vibrations for analytical purposes, it needs to be considered that the absorption of radiation is only possible when transitions between vibrational states undergo a change in dipole moment μ. Thus, depending on the molecules symmetry, some vibrations cannot be observed in IR spectroscopy. Moreover, many molecules have only few vibrations with large displacements, while the rest of the molecule appears almost stationary. These vibrations are often associated with functional

Figure 3-1 Potential energy models for the vibration of molecules

groups of a molecule, and their characteristic frequencies are only affected by the nature of other atoms within the molecule to a lesser degree. The absence of certain vibrations in IR spectra and the presence of characteristic vibrations due to functional groups allow for the creation of spectral libraries that aid in the interpretation of mass spectra.

3.1.2   Interferometers and Fourier- transform for Infrared Spectroscopy

IR spectrometers may come in different set-ups, and the difference lies in the way these instruments split light into different wavelengths or frequencies. In Fourier-Transform infrared (FTIR) spectroscopy, the radiation from a broad-banded light source is split by an interferometer. In the center of the interferometer,

there is a half-transparent mirror that is able to let a portion of radiation partially pass directly through to a fixed mirror while also partially reflecting light toward a moving mirror. Both beams are reflected from the fixed and moving mirror back to the semi-transparent mirror and are partially passed through or are reflected by the semi-transparent mirror toward the detector. Constructive interference for a given wavelength occurs when the beams are in phase, that is, the movable mirror is either at the position of zero path difference or when the path difference is an integer multiple of the wavelength. On the contrary, fully destructive interference occurs when the optical path difference is equal to one-half wavelength added to an integer multiple of the wavelength. The term retardation δ refers to the phase delay or phase difference between the two

Figure 3-2 Experimental set-up of a two-beam Michelson interferometer.

beams caused by the optical path difference. At a given wavenumber $\tilde{\nu}$, this relationship is described by (3.3), where, I_0 is the intensity of the incoming radiation, I is the intensity of the outgoing radiation upon interference at a retardation δ.
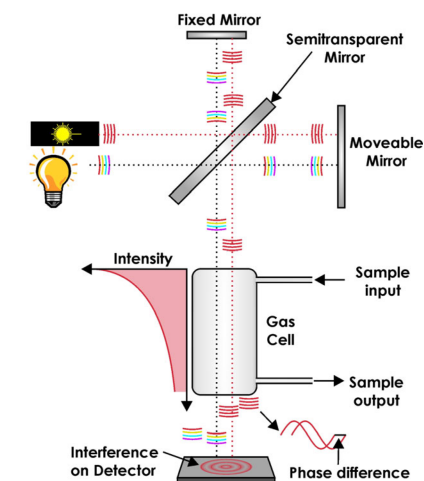
$$I(\delta) = I_0(1 + \cos(2\pi\tilde{\nu}\delta))$$ (3.3)

Commercial FTIR spectrometers typically move the mirror at a constant velocity V in cm s^{-1}, which allows the substitution of $\delta = 2\,V\,t$, with t being the time, transferring the equation into the time domain. For a polychromatic source, the detector signal is the result of the sum of the intensities at all wavenumbers $\tilde{\nu}$, and the recorded signal is referred to as an interferogram. Subsequently, Fourier transform is applied to convert the information stored in the interferogram from the time to the frequency or wavenumber domain, yielding a spectrum. Lastly, Beer's law is applied to quantify the wavenumber-dependent absorbance A for the sample, which is related to the transmittance according to (3.4), where α is the wavenumber-dependent absorption coefficient, and d is the thickness of the sample.

$$A(\tilde{\nu}) = \log_{10}\frac{1}{T(\tilde{\nu})} = \frac{1}{\ln 10}\,\alpha(\tilde{\nu})\cdot d$$ (3.4)

3.2.   Mass Spectrometry as a Tool for Analysis of Organic Compounds

While FTIRs perform well for bulk gases, the fact that characteristic vibrations of functional groups in organic molecules are often overlapping is disadvantageous for analysis of complex mixtures of organic molecules, where similar functional groups can be found in a variety of different molecules. Thus, this chapter introduces MS as a tool for more advanced analysis of organic compounds from combustion processes. The fundamental principle of MS is to generate ions, to separate these ions by their mass-to-charge ratios m/z, and ultimately to detect them qualitatively by their respective m/z and quantitatively by their abundance. Mass spectrometers can be differentiated by the ionization technique and operation principle of the mass analyzer. There is a great variety of different technique for both segments, and those techniques that are relevant for this work will be presented in more detail below. The choice of the ionization technique and mass analyzer is affected by the nature of the problem, i.e., whether the analyte is already present in a gaseous form or whether it is present in condensed form and has to be transferred to the gaseous phase.

3.2.1   Ionization Techniques

In order for a neutral to be ionized, the energy transferred to it has to be equal to or exceed its ionization energy (IE), which is defined as the minimum amount of energy that needs to be absorbed by a neutral in its electronic and vibrational ground states in order to form an ion that is also in its ground states by ejection of an electron. Electrons can formally be removed from either σ- or π-bonds, or lone electron pairs, with IEs from molecules with a π-bond generally being lower than from molecules that only possess σ-bonds. The lower limit of the IE is described by molecules that both have a condensed π-system and heteroatoms. IEs typically range between 7-15 eV.[157]

The speed that ions are removed from the shell of a neutral is extremely fast, and due to the great mass difference between electrons and the nucleus, the motion of electrons can be considered independent of the motion of the nuclei (Born-Oppenheimer approximation), which simplifies quantum mechanical consideration of molecules and solid bodies.[157] Consequently, the nuclei do not move to their new equilibrium position during transition between electronic states upon ionization, which is referred to as the Franck-Condon principle. In an energy-bond length diagram, these transitions are said to be vertical transition, and the probability of a transition is described by its Franck-Condon factor.[157] The factors approach a maximum for the case when the electronic wave functions of both ground and excited state have the greatest overlap. For the ground state, this is at the equilibrium position, whereas wave functions of higher vibrational states have their maxima at the turning points of the motion. As a result, ionization is also accompanied by vibrational excitation of a molecule, and the greater the difference between equilibrium distances in the ground and excited state the greater is the chance for the molecule's dissociation. The process of dissociation is referred to as fragmentation, which depends on the amount of excess energy. The excess energy is dependent on the type of ionization that is used and can be both desired and undesired. Ionization techniques that use a lot of excess energy are typically regarded as 'hard' techniques, while those that try to use as little as possible are considered 'soft'.

An example for the former is electron ionization (EI). Here, a sample is introduced into the ion source of a mass spectrometer, usually in the form of a gas, and subsequently exposed to a beam of electrons. The beam is created by a tungsten filament that is placed within an electric field, which guides the electrons to the sample inlet and increases their kinetic energy to approximately 70 eV, which is much larger than the IE of organic molecules with 7-15 eV. These high-energy electrons collide with molecules, causing the removal of one or more electrons from the analyte, resulting in the formation of positively charged molecular ions. Due to the concurrent vibrational excitation that occurs alongside electronic excitation and ionization and the large amount of excess energy, chemical bonds dissociate, and this process results in intense formation of fragment ions that are highly reproducible. If there has been any form of compound separation prior to the analysis within a mass spectrometer, as for example by GC, these patterns may aid structure identification, yet, when this is not the case, using EI is not feasible

Figure 3-3 Ionization scheme of single-photon ionization

due to superposition of complex fragmentation patterns. Moreover, the ability to ionize all compounds, even common matrix gases, such as N_2 and O_2 in air but also carrier gases He and H_2 in chromatography applications, may limit the dynamic range of the instrument. Desired ions from organic species may collide with these matrix gas ions on their way to the detector, or these matrix gas ions may also be guided to the detector and contribute immensely to background noise. Both drawbacks make clear that EI is not a suitable method for all applications, and some problems require ionization techniques that do not lead to ionization of matrix gases and that do not produce lots of fragment ions.
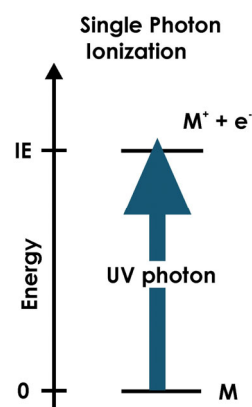
This gap may be filled by photoionization (PI). The energy that is used for ionization is much closer to the IE of common organic molecules of 7-15 eV, and, consequently, much less fragmentation is observed, and the signal of the molecular ion can be observed at much higher intensity compared to EI. Moreover, many light sources that are suitable for photoionization provide photons that do not possess enough energy to ionize matrix gases, leading to a smaller background noise. Light sources can be differentiated based on the energy and energy distribution of generated photons as well as their operation mode, that is, either pulsed or continuous operation. Depending on which light source is used, different ionization schemes are possible, that is, either single-photon ionization (SPI) or resonance enhanced multi-photon ionization (REMPI).

SPI relies on the absorption of a single photon for ionization of neutrals (Figure 3-3). The radiation that was used within thesis had an energy of 10.49 eV, equivalent to 118 nm radiation, and was generated by tripling the third harmonic of a commercially available laser (light amplification by stimulated emission of radiation) made of Nd^{3+}-doped yttrium aluminum garnet crystal $Y_3Al_5O_{12}$ (Nd:YAG) in a Xe gas cell (Figure 3-4). For generation of the fundamental radiation at 1064 nm, the laser medium is placed within an optical resonator set-up, typically a fully reflecting mirror and a Pockel cell, which is permeable for radiation with a certain polarization plane.[158] Without any voltage applied to the electrodes of a Pockel cell, the greatest portion of the radiation cannot leave the assembly as it does not match the polarization of the Pockel cell. This is needed to optically pump the laser medium with a pulsed xenon flash lamp. Electrons within the laser medium are excited from the ground state to rather broad, short-lived energy bands, and subsequently, the electrons fall relatively fast (30 ns) to a second meta-stable level

Figure 3-4 Schematic representation on the energy levels of a 4-level solid-state laser.

with elevated lifetime of approximately 230 µs via a non-radiative transition. Optical pumping creates a population inversion, that is, more electrons within the laser medium can be found in the excited state than in the ground state. Only when a population inversion is present within the system, stimulated emission may occur since emission rates overcome absorption rates, achieving a net optical amplification. The transition from the excited meta-stabile energy level to a third lower energy state is caused by stimulated emission. Ultimately, the remaining excess energy at the lowest energy level is released as heat to the crystal lattice.

The photon energy of the fundamental radiation that the laser provides however is insufficient to be used for ionization in SPI, and therefore the outgoing radiation needs to be energy-multiplied by factor nine via nonlinear optical effects, which is done in anisotropic crystals for the generation of the third harmonic and subsequently energy tripled again in a xenon gas cell.[159] Frequency multiplication is based on the fact that the polarization P of a medium cannot be described as linear response of the medium with its electric susceptibility χ to an incoming electric field E, and higher order terms need to be considered.[160] This is the case for intense electric fields, as emitted by lasers, where border conditions, such as that the polarization of a medium depends only on the instantaneous value of the electric field at a given time t and the polarization is lossless and without dispersion, that typically apply in linear optics do not hold anymore. This enables the incoming radiation to be frequency tripled and subsequently tripled in a xenon gas cell. With IEs of organic molecules ranging from 7-15 eV and most of them having an IE of less than 10 eV, SPI with the ninth harmonic of ND:YAG is rather universal, with the only limiting factor being the IE of the analyte. At the same time, photons of 10.49 eV transfer only minimal excess energy to the neutral analyte, leading to less-pronounced fragmentation compared to EI.
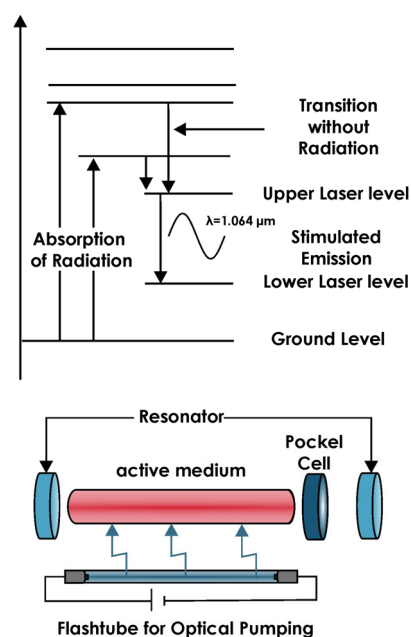
For applications that require more selectivity and sensitivity, REMPI has been shown to be an adequate tool.[161] REMPI requires at least two photons for ionization and combines both aspects of ultraviolet spectroscopy and MS (Figure 3-5). There are a variety of different REMPI schemes that rely on different colored photons or on more than two photons. However, the simplest case is [1+1] REMPI with two photons of identical energy, which was also used in this thesis. Here, a first photon is absorbed to transfer the analyte molecule into an excited, meta-stable electronic state, which is followed by the absorption of a second photon with the same energy. The broadness and lifetime of the meta-stable energy level depends on the structure of the analyte, and the absorption of a second photon may only occur if the meta-stable energy level is long-lived enough and the energy density for the incoming radiation is sufficiently high for a second absorption process to become likely with adequate

Figure 3-5 Transitions between energy levels in resonance-enhanced multi-photon ionization.

efficiency. Light sources for REMPI are typically lasers since the two photon absorption require high power densities.
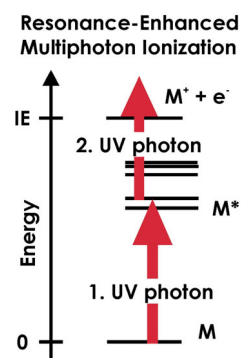
A KrF excimer laser, which emits radiation with a wavelength of 248 nm, was used. REMPI at 248 nm is selective for aromatic hydrocarbon and PAHs, with few exceptions. Excimer lasers are molecular gas lasers, and the most common lasers rely on mixtures of rare gases and halogen as a laser medium. The excited state of the active medium are typically excited dimers that are formed by the collision of excited rare gas atoms and halogen molecules, thus the name excimer. The excited rare gas atoms are provided by

optical pumping with a spark discharge in a gas chamber filled with an excimer gas premix. After the excited dimer has been formed upon collision of excited rare gas and neutral halogen molecules, it falls to a lower energy state after a few nanoseconds (Figure 3-6). The average lifetime of the excited dimer KrF is estimated to be 7 ns, while the ground state of the dimer is much more short-lived with approximately 1 ps. Pulse widths of a laser pulse depend on the geometry of the discharge unit and electrode set-up in the laser medium, the pressure within the gas chamber, and the lifetime of the excited dimer.
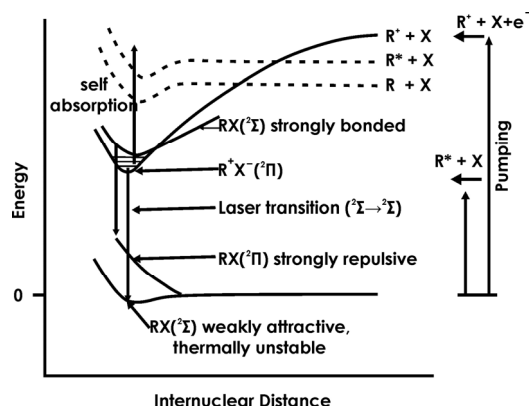
Figure 3-6 Energy diagram of an excimer laser.

3.2.2 Time-of-Flight Mass Analyzer

Once ions have been created, they need to be analyzed according to their m/z ratio. There is a great variety of different analyzers available, which differ in sensitivity, resolving power, and mass accuracy. Time-of-Flight (ToF) analyzers are one of the most common analyzers, particularly in untargeted analyses of complex organic mixtures as one of their main features is that they analyze a full spectrum with each extraction cycle. Consequently, these analyzers are the type of analyzer that inherently work well with naturally pulsed ionization techniques, where scanning mass analyzers lose lots of the generated ions.[162] Moreover, they provide high acquisition rates, which is useful when used alongside a separation technique, such as GC.

The fundamental principle of a ToF is the dispersion of an ion package along a field-free drift path of known length (Figure 3-7). For the simplest set-up of a ToF, i.e., a static, uniform electric field applied two plate electrodes and a linear drift region in the ToF, the motion of a charged ion with mass M in kg in an electric field and the field-free drift region is described by Newtonian physics, see (3.5),[163] and the total flight time of the ions is the sum of flight times in the ion source and the drift region, as described by (3.6). Briefly,

the electric field applies a force to ions causing them to be accelerated toward the detector, and the acceleration a can be retrieved by considering that $a = Eq\,M^{-1}$, with E being the electric field and q being the electric charge of the ion. For a uniform electric field, the strength of the field is $E = U \cdot d^{-1}$ with voltage U and plate distance d.

Figure 3-7 Schematic set-up a time-of-flight mass spectrometer.

The time the ions take to leave the field can be described by (3.7) by assuming that the starting point s_0 is in the center of the source, i.e., $d = 2 \cdot s_a$, and an initial velocity $v_0 = 0$ for simplicity. The drift time t_d in the field-free ToF analyzer can be described by equating the electric work applied to the ions after they left the so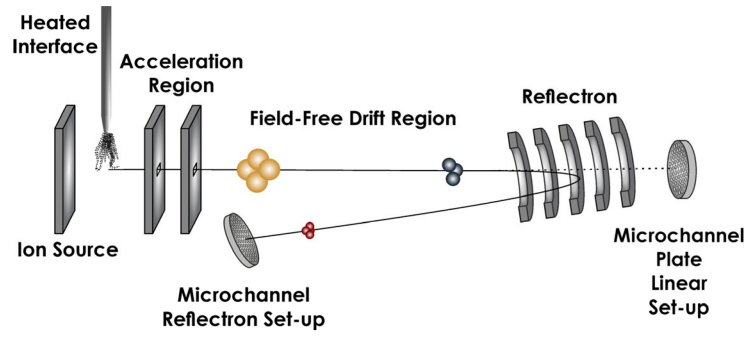urce and the translational energy of the ions, yielding (3.8). M and q may be converted to the artificial yet conventional m/z by considering that $m = M \cdot m_{1/12\,C}$ and $Q = z \cdot e$, where $m_{1/12\,C}$ is the 12th fraction of the mass of a carbon atom, e is the elementary charge, and z is the number of charges.

$$s(t) = s_0 + v_0 \cdot t + 0.5\,a \cdot t^2 \tag{3.5}$$

$$t_{\text{total}} = t_a + t_d \tag{3.6}$$

$$t_a = 2s_a \cdot \sqrt{\frac{M}{UQ}} \tag{3.7}$$

$$t_d = s_d \cdot \sqrt{\frac{M}{UQ}} \tag{3.8}$$

The resolving power of a linear ToF analyzers is limited by several factors.[162] The first limiting factor is the initial space distribution, i.e., ions with the same m/z have slightly different starting points within the ion source, and this causes a dispersion of translational energy for ions of the same m/z. The second factor is the initial time distribution, for example, caused by the finite pulse width of a laser shot or the rise time of the extraction pulse. Given the electric field is already present at the moment of ion generation, the molecules may be ionized at the beginning of a laser pulse or at the end, and consequently ions of the same m/z may arrive at different times at the detector. The third factor is the initial energy spread. When the sample is introduced into the ion source, some neutrals may naturally drift toward the detector, while others drift in the opposite direction. Once ionized, ions who already drift toward the detector arrive sooner at the detector than the ones that drifted in the other direction. It takes time for the ions to turn around and move to the detector. The problem of the initial space distribution leads to the fact that ions depending on their position acquire different amount of energies, and ions are located further away from the detector acquire higher translational energy and overtake slower ions initially formed closer to the detector. The point where all ions of the same m/z meet is referred to as the space focus, and for a single-field linear ToF, its location depends greatly on the dimensions of the ion source, which creates challenges for scaling up resolution of mass spectrometers.

To overcome the problem, adding a second electric field between the ion source and the mass analyzer removes adds more criteria, such as the field strength and dimensions of the first and second electric field, which makes instruments easier to adjust and improves the resolving power of the instrument.[164] The next landmark for ToFs was the development of the reflectron by Mamyrin,[165] which aims to compensate the remaining energy spread of the ions. A reflectron consists of a series of ring-shaped electrodes with increasing potential, which is placed within the formerly field-free drift region. Ions penetrate the reflectron to a depth that is equivalent to their kinetic energy and are then ejected via repulsion by the electric field. The ions generally leave the reflectron with the same kinetic energy they entered, but the path that the ions

take depends on the energy they possess before entering. The reflectron therefore achieves a correction in the time-of-flight, leading to an enhancement of resolution. The resolution enhancement of a reflectron is mainly attributed to reduction of the energy spread.

3.2.3 Detection of Ions

The fast separation of ions within a ToF analyzer also requires sophisticated detection methods, both in terms of data acquisition as well as amplification of the current that a single ion provides. At the heart of micro channel plate (MCP) technology lies an array (10^4–10^7) of tiny, closely packed channels, typically measuring only 10-100 µm in diameter.[166] These channels are created using advanced microfabrication techniques, such as lithography and etching, to form an open-faced plate structure made of semi-conducting lead glass, whose surface is covered with metallic coating to supply voltage to all channel. Each channel acts as an independent electron multiplier, allowing for the amplification of particle signals generated during the mass analysis process. When ions enter the channels, they collide with the inner walls of a channel, causing the release of electrons through secondary electron emission of the semi-conduction lead glass. These electrons are accelerated by the voltage applied to the faces of the MCP, causing them to collide with the channel walls again, leading to further electron emission. Each of the channels can be considered a continuous dynode acting as its own resistor chain. This cascading effect results in a significant amplification of the original signal. Channels are often biased at a slight angle to enhance this cascading effect. Wiza[166] reported a multiplication of signal intensity by 10^5–10^7 for their Chevron plate, which is a double-stacked MCP, whose bias angles are in opposing directions. MCPs offer excellent spatial resolution, which is only limited by the spacing's of the channels, and temporal resolution (<100 ps), making them ideal for ToF MS. The narrow channel dimensions ensure that ion packets passing through the MCP experience minimal spread, preserving the mass resolution of the instrument.

3.3. Mobility Particle Size Spectrometry for the Analysis of Particle Size Distributions

Common optical particle spectrometers or counters rely on the ability of particles to scatter light, which particularly ultra-fine particles are not able to do sufficiently due to the wavelength dependency of the scattering cross section. Given this thesis scope on combustion and the particle size range of well below 1 µm that combustion processes are already known for, mobility particle size spectrometry was used as a tool to get information on particle size distributions. These instruments rely on the ability of particles to carry charges, and they consist of three fundamental parts, which are a neutralizer, a differential mobility analyzer (DMA) and condensation particle counter.

3.3.1 Separation of Particles by Electrical Mobility

At the heart of the instrument is the DMA, which separates the particles based on their electrical mobility Z_p. Generally, the mobility is described by the ratio of the velocity v_E of the charged particles in an electric field and the electric field strength E, which is described in (3.9).[167] The velocity of a particle can be obtained by equating the electrostatic force to the Stokes drag force. The electric mobility is further related to the particle diameter D_P, the number n of elementary charges e that a particle carries, and the viscosity of the gas η that carries the particle. Moreover, the mobility of a particle needs to be corrected for a slip flow effect that leads to gas molecules slipping past the particle's surface due to differences in their velocities, which changes the effective drag experienced by the particle. This applies particularly to particles smaller than 100 nm, whose size is approaching or even under passing the mean free path of the surrounding gas molecules. $C(D_p)$ is the Cunningham-Slip-correction Factor that accounts for that behavior

$$Z_p = \frac{v_E}{E} = \frac{n \cdot e \cdot C(D_p)}{3\pi \cdot \eta \cdot D_p} \tag{3.9}$$

DMAs are often cylindrical capacitors whose electric field removes a fraction of particle with known electric mobility from a polydisperse particle population (Figure 3-8). It consists of one cylindrical, inner and one cylindrical, outer electrodes. During operation, the instrument is flushed with clean, particle-free air that acts as a carrier for a particle-laden sample air flow. The latter is introduced into the DMA through an annular slit near the outer electrode and merged with a particle-free sheath air flow V_S. Applying a DC voltage to the electrodes, charged particles are forced to migrate to either one of the electrode, which these particles collide with. At the bottom the instrument is another annular orifice, which operates as an outlet. Only particles that exhibit a certain electric mobility can reach this outlet under known conditions, e.g., sheath air flow V_S and DC voltage U, and geometry of the instrument, i.e. the effective length L and the radii of the inner and outer electrodes r_i and r_a, and this can be calculated (3.10). The monodisperse particle fraction that meets this specific electric is subsequently passed to a condensation particle counter for optical detection.
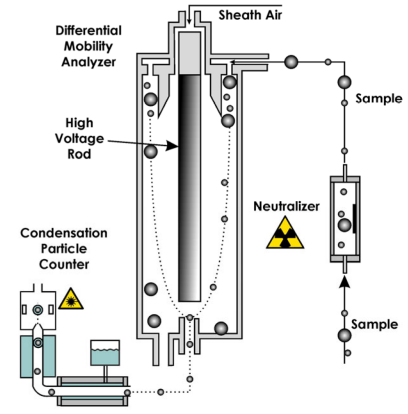

Figure 3-8 Set-up of a mobility particle size spectrometer.

$$Z_p^* = \frac{V_S \cdot \ln\left(\frac{r_a}{r_i}\right)}{2\pi \cdot U \cdot L} \tag{3.10}$$

3.4. Instrumentation

3.4.1 Experimental Set-up

The samples that were used for the main scope of this thesis were generated during a field campaign at the University of Eastern Finland. The combustion tests were performed with a modern, non-heat-retaining, single-room heating appliance (Aduro 9.3, Aduro A/S, Denmark, energy efficiency class: A+) approved for installation in the European Union and Norway. The wood stove used for testing is treated as a proxy for modern European Appliances equipped with modern emission reduction technology, e.g., air staging.[168] Information on how well the stoves currently installed in Europe are maintained or how old they are is generally very scarce or largely not available in English and hence not accessible to the international audience. The stove is equipped with three dampers that regulate the combustion air. The primary air supply is opened only for a few minutes when the fuel is ignited, the secondary air supply is used to regulate the energy output, and the tertiary air supply is used to reduce flue gas emissions.

Spruce logs (Picea abies) and Lusatian brown coal briquettes (Rekord, Lausitz Energie Bergbau AG, Germany) were tested as fuels for residential heating. Both fuels were analyzed for their calorific properties, water content, and elemental composition by an external laboratory based upon international standards. The result of which can be found in the study presented by Martens et al.[169].

The combustion tests were designed to cover a period of 4 h to fit provide emissions for concurrent *in-vitro* and *in-vivo* experiments. Due to inherent differences, the ease of ignition and combustion rate, the mass of fuel, and the number of batches that were burned varied between both fuels. For SL experiments, one experiment comprised five consecutive batches of fuel with a weight of ca. 2 kg each, and each experiment started with the appliance conditioned to room temperature. For experiments with BCBs, the combustion procedure comprised three batches with ca. 1.7 kg each. Because of the poor ease of ignition, the manufacturers from both the briquettes and stove recommend to burn at least one batch of wood prior to coal. In the present study, at least two batches of SLs were burned prior to BCBs to provide a sufficient bed of glowing ember for proper ignition of the BCBs. No emission samples were collected during these preparatory batches. The experiments were repeated four times with SLs and ten times for BCBs, of which

4 experiments were not considered in on-line analysis of volatile organics due to problems with the custom sampling unit for volatile organics.
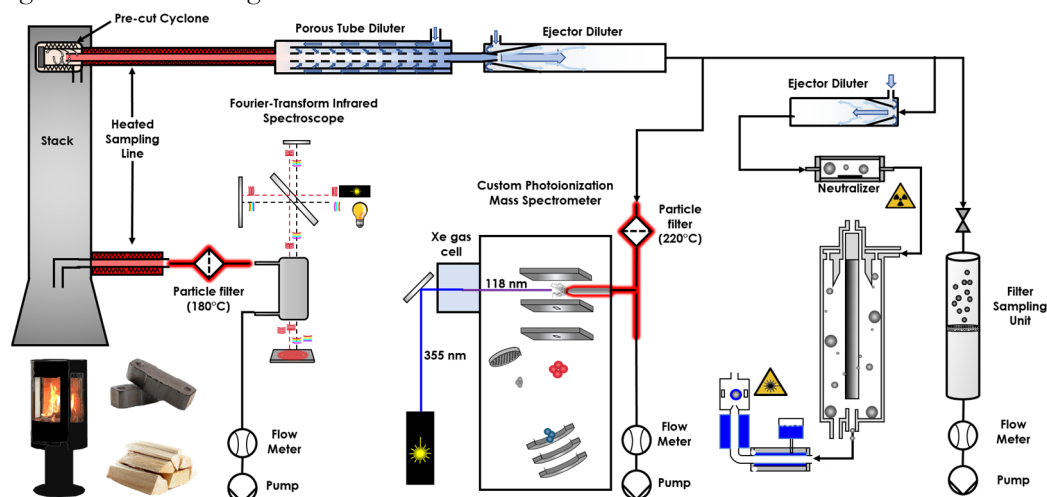

Figure 3-9 Sampling set-up for on-line analysis of the combustion process and filter sampling.

The evolving emissions were monitored by a commercial FTIR spectroscope (Gasmet Technologies Oy, Finland) for bulk gaseous components directly through the stack (Figure 3-9). To avoid interference with emitted particles, the spectroscope is equipped with a heated particle filter. Moreover, emissions were sampled with a diluting aerosol sampler (Venacontra Oy, Finland), comprising a pre-cut cyclone and a porous tube diluter ejector diluter sampling system with anticipated dilution ratios of 30 during experiments with SLs and 60 and 30 for the intitial 10 and remaining 230 min during experiments with BCBs. Filter sampling of volatile organics was carried out with 10 L min^{-1} from this dilution stage with a modified filter sampler (Partisol 2300, Rupprecht & Patashnick, USA). For the analysis of volatile organic compounds, as custom sampling unit was used, which is described in more detail below. Lastly, particle size distributions were sampled after a second ejector diluter with a constant dilution ratio of 10 with a scanning mobility particle sizer (SMPS, TSI GmbH, Germany), which was operated according to standard operating procedures.

3.4.2   Sampling of Volatile Organic Compounds with a Custom Set-up

In the sampling unit, the internal standard (toluene methyl-D3, 98% purity; mass-to-charge ratio m/z = 95; Cambridge Isotope Laboratories, Inc.) was constantly added at levels of 300 to 600 ppbv to the diluted flue gas. After each experiment, exact concentrations of the internal standard were determined by replacing the sample aerosol with a calibration gas (benzene 0.96 ppm, toluene 1.01 ppm, p-xylene 0.72 ppm, 1,2,4-trimethyl benzene 1.39 ppm, in: N_2, Linde AG, Germany) and comparing the signal intensity of the internal standard $C_7H_5D_3$ to that of regular toluene C_7H_8 (m/z = 92). A glass fiber filter (F-0,1GF, M&C Tech Group, Germany) heated to 220 °C was used to remove particles and evaporate semi-volatile organic compounds. All gaseous compounds were transported from the hot sampling unit to the ion source of the mass spectrometer via a 3 m stainless steel capillary (ID 280 µm, MXT Guard column) in heated stages of 235 °C/240 °C/245 °C to prevent back-condensation. Organic gaseous compounds were analyzed by a time-of-flight mass spectrometer (ToF-MS; Compact Reflectron Time-of-Flight Spectrometer II, Kaesdorf Geräte für Forschung and Industrie, Germany) using single-photon ionization (SPI) at 118 nm (10.49 eV). The vacuum ultraviolet radiation used for ionization was produced by frequency tripling of the third harmonic of a pulsed Nd:YAG laser (Spitlight 400, Innolas GmbH, Krailling, Germany; 40 mJ at 355 nm, pulse duration: 5−7 ns, 20 Hz) in a gas cell filled with 4 mbar of xenon. Ions were subsequently extracted by a delayed electric field, transported to the mass analyzer, and detected at a micro channel plate (MCP, Chevron plate, Burle Electro-Optics Inc.).

3.4.3 Analysis of Particle-bound Organics

Particle-bound organic species were analyzed by means of in situ derivatization (ID) thermal desorption (TD) gas chromatography (GC) time-of-flight (TOF) mass spectrometry (MS) with electron ionization to gain quantitative information on semi-volatile organic species. Briefly, a filter aliquot was placed into the liner and rapidly heated to 300 °C to desorb organic species. At the same time, N-methyl-N-trimethyl silyl-trifluoroacetamide was constantly added to the injector for derivatization of polar compounds in order to prevent thermal decomposition of fragile oxygen containing components. Identification and quantification were made based on retention time, similarity of mass spectra to NIST library entries as well as native and isotope-labeled standards of same or similar compounds. A variety of different polycyclic aromatic compounds (PACs), including 28 unsubstituted PAHs, 6 alkylated PAHs, 13 Oxy-PAHs, 3 aromatic O-heterocycles, as well as 3 resin acid derivatives, 3 anhydrous sugars, and 2 tetraphenyls.
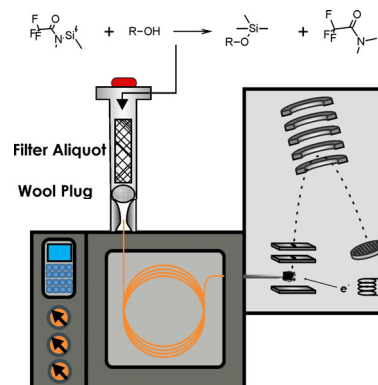

Figure 3-10 Instrumental setup of the in-situ derivatization thermal desorption gas chromatography mass spectrometry (IDTD GCMS) unit for targeted analysis of organic

The bulk carbonaceous particle fraction deposited on quartz fiber filters was analyzed by subjecting punches of 0.5 cm2 to a thermal-optical carbon analysis (DRI 2001a, Atmoslytic Inc., USA), following the IMPROVE_A protocol. Briefly, filter samples were stepwise heated in helium at temperatures of 140, 280, 480, and 580 °C and an oxidizing atmosphere of 98% helium and 2% oxygen at temperatures of 580, 740, and 840 °C. The optical correction was carried out by means of the reflectance signal of a 635 nm laser diode.

In addition to the targeted analysis of organic species, the carbon analyzer was coupled to a TOF-MS (Compact Reflectron Time-of-Flight Spectrometer II, Kaesdorf Geräte für Forschung and Industrie, Germany), and a fraction of the evolving gas portion was analyzed by means of resonance-enhanced multi-photon ionization (REMPI) and single-photon ionization (SPI) using 248 and 118 nm radiation, respectively. For REMPI, radiation from a KrF excimer laser (248 nm, 4.0 mJ/shot, shot frequency: 50 Hz, pulse duration: 5−15 ns, data acquisition rate 1 Hz, MLI-200, MLase AG, Germany) was used. For SPI, vacuum ultraviolet radiation of 118 nm was generated by tripling the third harmonic of a Nd:YAG solid-state laser (50 mJ/shot at third harmonic with 355 nm, shot frequency: 20 Hz, pulse

Figure 3-11 Analysis of carbonaceous particulate matter in a thermal-optical carbon analyzer. The untargeted analysis of organic compounds is carried out with photoionization mass spectrometry. The figure was taken from Diab et al.[162].

duration: 5−7 ns, data acquisition rate 1 Hz, Spitlight 400, Innolas GmbH, Germany) in a gas cell filled with 4 mbar of xenon. Instrument performance was checked at the end of each day of measurements with a pre-mixed calibration gas (benzene 0.96 ppm, toluene 1.01 ppm, p-xylene 0.72 ppm, 1,2,4-trimethyl benzene 1.39 ppm, in: N_2, Linde AG, Germany). The combined use of thermal-optical carbon analysis with photoionization mass spectrometry has a key advantage over other competitive techniques, such as gas and liquid chromatography, particularly to liquid chromatography. Methods that rely on these instruments typically require sample pretreatment prior to analysis, typically by extraction of compounds from filters with a solvent and possibly enrichment of the sample by evaporation of the solvent. These initial steps may influence the scope of the analysis, that is, not all compounds are necessarily soluble within a given solvation procedure (choice of solvent and extraction time). This may be particularly true for rather large molecules within the class of low-volatile organic compounds.
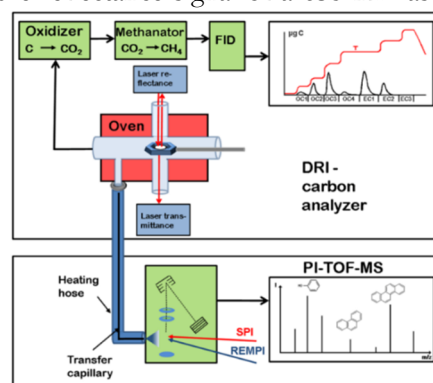
4. Results and Discussion

4.1. Studying the Nature of Combustion Aerosols

4.1.1 Dynamics in the Evolution of Solid Fuel Burning

Emissions of incondensable gases and volatile organic compounds (VOCs) are generally a major product of combustion outrivaling emissions of PM in terms of mass by far,[168,170,171]and thus the a major part of this thesis was dedicated to these emissions, which are presented Martens et al.[169]. FTIR spectroscopy and a custom SPI-ToF-MS based approach were used to analyze the emissions of small incondensable gases as well as organic emissions on-line. These approaches may be superior to traditional approaches in sampling container and bags, which may lose a fraction of the VOC mixtures due to wall losses and cannot describe dynamics in the combustion behavior, that is, at least not in a convenient way.[172] Wood combustion in small-scale heating appliances has been shown to pass through three distinct burning phases, the ignition, stable combustion and char burning phase, and each of these phases has identifiable chemical fingerprint, both in terms of VOC as well as PM emissions.[155,173] When fuel is added to the stove with discontinuous operation, the kindling or the existing ember cannot fully ignite the fuel immediately, so the combustion is incomplete. At first, more volatile or fragile fuel components are evaporated or pyrolyzed, and these components feed the flame in the stove. With increasing combustion temperatures, the combustion is more complete and more refractory components of the fuel are degraded and fuel the flame. The combustion is generally rather complete, leading to only few emissions of VOCs. At the end of each combustion cycle, the pyrolysis of fuel components leaves a very refractory residue, that is, char, which is oxidized without producing a flame. Fuel consumption and thus conversion of energy stored in chemical bonds to heat occurs at a low rate, causing the stove to become cooler, which further slows down oxidation. Eventually, the combustion to comes to an end if no further fuel is added. These phases can be readily identified by the
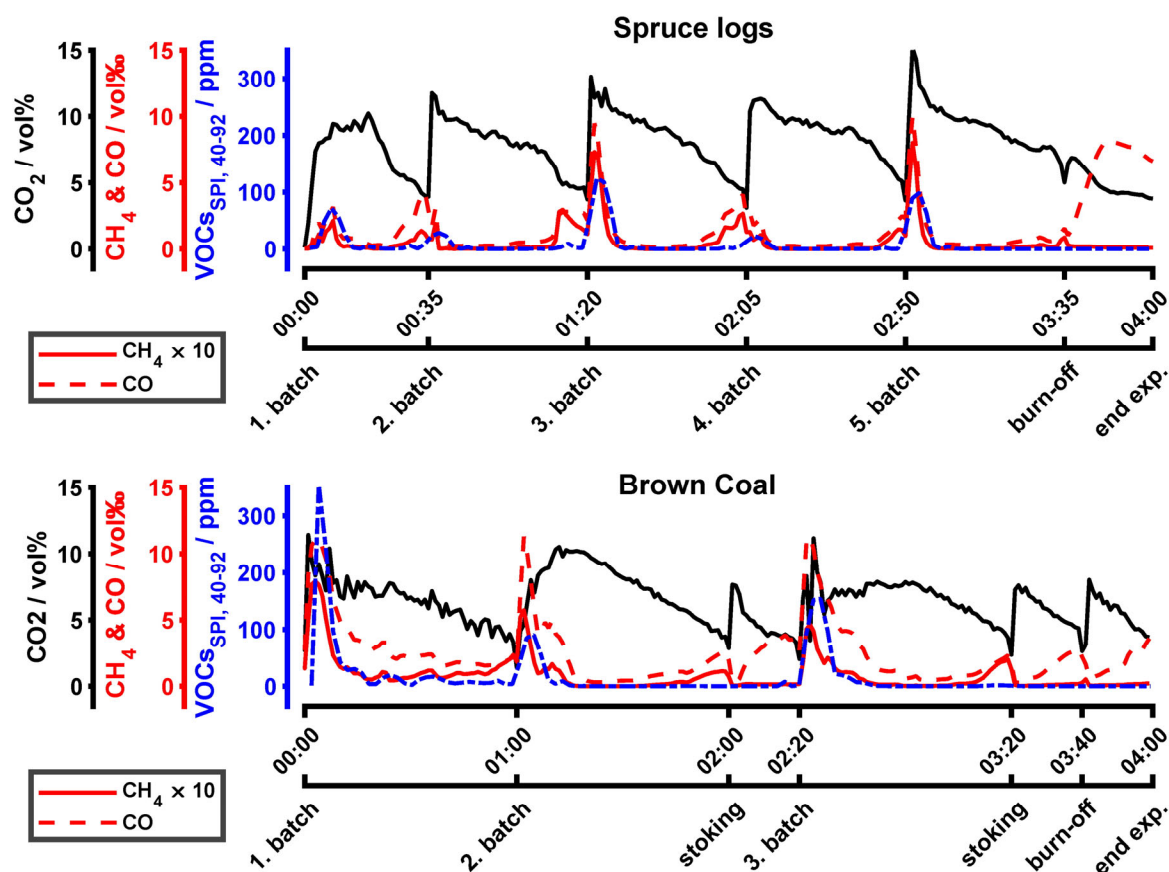

Figure 4-1 Evolution of carbonaceous gases during brown coal and spruce log combustion, taken from Martens et al.[141]

evolution of bulk carbonaceous species, such as CO_2, CO, and VOCs emissions. The ignition phase is characterized by rapidly increasing emissions of CO_2 and peaking emissions of incomplete combustion products (Figure 4-1), and it is of particular importance for VOCs.

4.1.2 Slower ignition Causes Elevated VOC Emissions

Emission of VOCs are predominantly released during the ignition of an individual batch and only to a lesser degree during the stable combustion and ember phase.[169] One goal of research is to provide information on optimal heating practices with lowest emission of pollutants, and one crucial parameter is the fuel choice, specifically, the composition and shape. Traditionally, solid fuels can be characterized by their content of volatile matter, fixed carbon, and ash content, with the former two parametrizing the thermal stability of the organic constituents. Volatile matter refers to the moieties of fuel that can easily be volatilized when burned or pyrolyzed, typically cellulose and hemicelluloses as well as non-aromatic moieties in lignin, and it accounts for 55% of the Lusatian lignite and typically 80% in biomass.[174,175] Fixed carbon on the other hand refers to the species that cannot easily be volatilized, typically the carbonaceous matter found in aromatic moieties of the fuel. Some researchers brought up the idea that fuels with low volatile matter content tend to produce fewer VOC emissions when used in Chinese rural cooking stoves,[176] while results from others indicate the opposite.[177] Volatile matter is typically seen as one of the major advantages of biomass over coal mechanistic studies since solid fuels with higher volatile matter content have lower ignition temperatures leading to overall faster ignition, implying lower VOC emissions.[174,178,179] Most of these studies focusing on real-world heating appliances however were performed with small-scale cooking stoves common in China,

Figure 4-2 Ease of ignition and its correlation to the amount of emitted volatile organic compounds, taken from Martens et al.[141]

which do are not equipped with air staging technology such as European appliances,[168,170] and no information was available on state-of-the-art appliances compliant with latest emission standards in Europe.

$$MCE = \frac{[CO_2]}{[CO_2] + [CO]} \qquad (4.1)$$

In order to find out about the optimal fuel choice, emissions were related to the time that it takes for the fuel to ignite properly. The time needed for ignition was related to the modified combustion efficiency (MCE), which is an indicator for the efficiency of combustion that is calculated according to (4.1). Here, $[CO_2]$ refers to the concentration of CO_2 in the exhaust gas and $[CO_2] + [CO]$ refers to the sum of concentrations of CO_2 and CO. The ignition was defined as the time between the addition of a new batch and the point when proper combustion (MCE = 0.975) conditions after the global MCE minimum was reached (Figure 4-2, top). Generally, the time that it takes for the fuel to ignite was found to correlate for all batches of fuel(Figure 4-2, bottom). Ignition times of BCBs are found to be four times longer with an ignition time of ~16 min ± 9 min, and organic emissions of BCBs were estimated to be on average two times higher. For SL batches, the positive correlation is stronger than for all of our experiments since the majority of organic compounds was emitted directly upon adding of a batch. For experiments on BCBs

however, the correlation was weaker (r = 0.46) and not significant, which could be a result of higher emissions of VOC throughout an individual batch of BCBs. These results indicate that in order to reduce emissions from residential solid fuel burning, the chosen fuel should be optimizing for quickest ignition times.

4.1.3 Emissions of VOCs from Brown Coal Have Petrogenic Origin

Moreover, chemical composition of VOCs was investigated within the first publication.[169] In mass spectra from both fuels (Figure 4-3), intensities in the lower m/z range from 40 to 86 mostly appeared as groups of triplets or quartets with m/z intervals of 6 to 10 between each group. The limited resolution of the SPI-ToF-MS is not sufficient to resolve isobars with different sum formulae but by considering that the majority of the VOC is composed of the elements C, H, and O and limitation by the ionization method SPI shrinks the possible number of viable sum formulae for each signal to a reasonable level. Signals with the lowest m/z within each multiplet cannot contain oxygen, and thus these signals can only refer to polyunsaturated aliphatic hydrocarbons, e.g., propadiene/propyne (m/z 40), vinyl acetylene (m/z 52), and
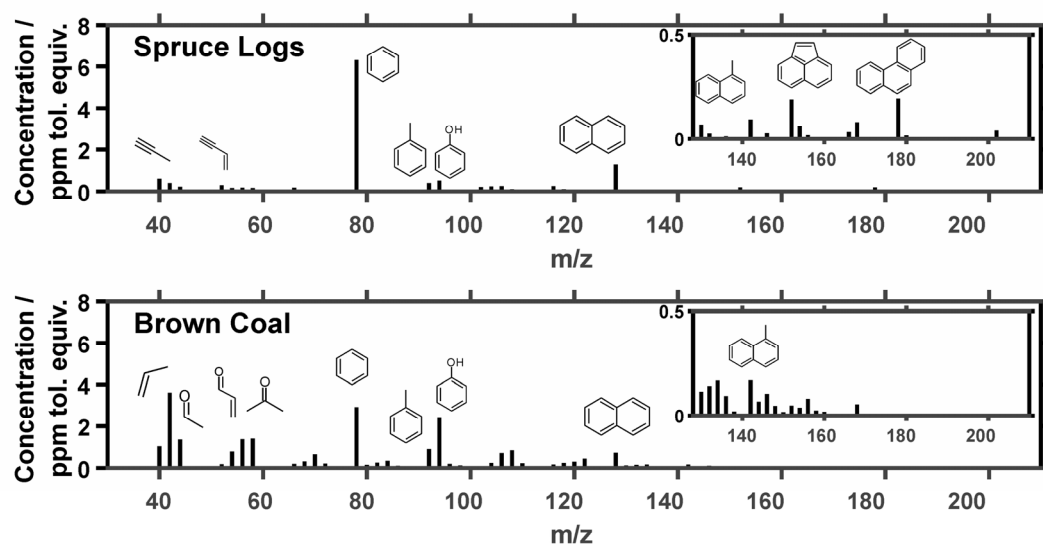
Figure 4-3 Exemplary chemical fingerprint of emissions of volatile organic compounds from brown coal briquette and spruce logwood burning, adapted from Martens et al.[141]

cyclopentadiene (m/z 66). On the other hand, signals with higher m/z within each multiplet can and likely contain oxygen, e.g., acetaldehyde (m/z 44), acrolein/butene (m/z 56), or acetone/ propanal (m/z 58).[150,180] Mono- and polycyclic aromatic species, such as benzene (m/z 78), toluene (m/z 92), styrene (m/z 104), xylene (m/z 106), and naphthalene (m/z 128) as well as phenolic species, e.g., phenol (m/z 94) and methyl phenol (m/ z 108), can be found in the higher m/z range

Emission factors of 5 bulk inorganic combustion gases (CO, NO_x, SO, NH_3, and HCN), CH_4, lumped organic emissions (unsaturated aliphatics, UA; alcohols; single-ring aromatic compounds, Arom; non-methane alkanes, NM-Alkanes) monitored with the FTIR and 10 selected VOCs monitored with SPI-ToF-MS were compared on a quantitative basis, by also considering the photoionization cross sections of individual VOCs in SPI.[181] Significant differences in means of emissions from BCB and SL burning were mainly found for species that were interpreted as petrogenic, whereas compounds with pyrogenic origin did not show significant differences.

In accordance with the different mechanisms that may lead to the evolution of emissions, as presented in section 1.5, it is common to classify emissions as either predominantly pyrogenic, that is, combustion-derived, or predominantly petrogenic, that is, predominantly fuel-derived, based on ratios of specific compounds. Compounds that are attributed to a pyrogenic nature are those that do not contain oxygen and

exhibit elevated number of unsaturated bonds, whereas petrogenic emissions are those that contain fuel-specific motifs. For the smaller aliphatic VOC emissions, oxygenated compounds can be interpreted to still have fuel-specific motifs as these compounds did not undergo secondary pyrolysis, which would lead to the elimination of oxygen via dehydrogenation or de-carbonylation reactions in flame and the formation of highly unsaturated compounds. For VOCs with higher molecular-weight, i.e., VOCs with a molecular weight of benzene and larger, compounds such as benzene and naphthalene, the pyrogenic motif can be interpreted by the presence of phenolic and substituted phenolic units, which refer to rather well preserved monomers of lignin, while their benzene and parent PAHs may be interpreted as pyrogenic fingerprints since these are only produced under a temperature regime that leads to pronounced cracking and recombination reactions in the gas phase. None of the compounds that had available photoionization cross sections was significantly higher in emissions from SLs, while many compounds with petrogenic origin, such as toluene and acetaldehyde, were found in significantly higher amounts in emissions from BCB burning. This was found to indicate that BCB burning refers to a petrogenic source, whereas emissions from SL burning were found to be pyrogenic.
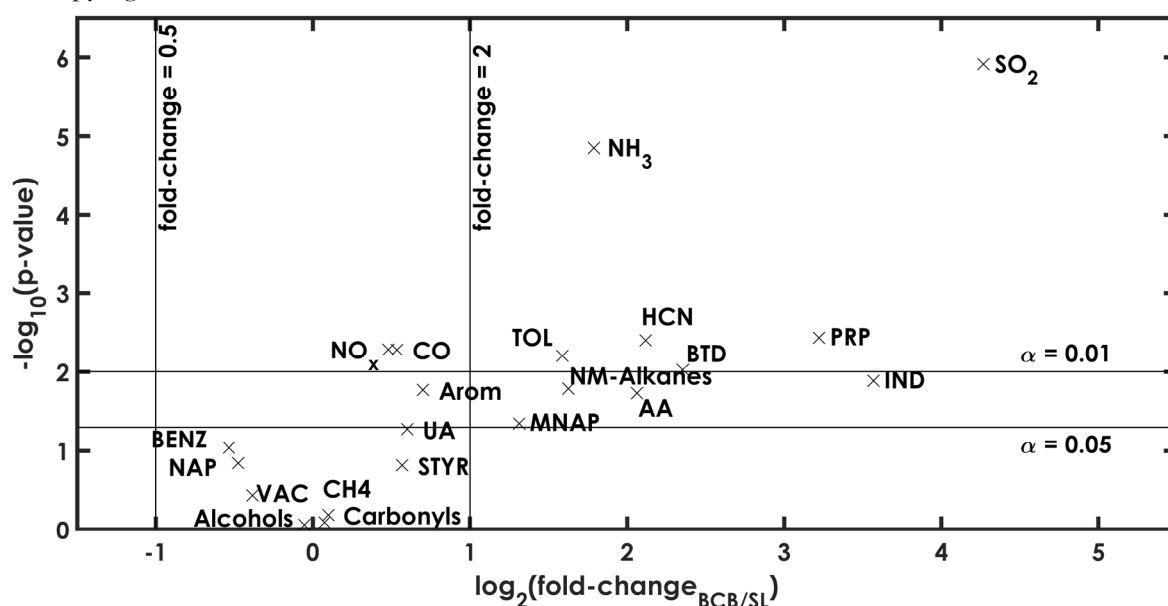
Figure 4-4 Volcano-plot of emission factors for various volatile organic compounds and major inorganic gases. The figure was taken from Martens et al.[141]

4.1.4   The Evolution of Particles and the Nature of Particulate Matter

The second publication as a first author shifted the focus toward emissions of particles and the chemical nature of particle-bound organics. The evolution of particles over the combustion cycle was monitored with an SMPS to gain information on overall particle number (PN) emissions and their size distribution. During the experiments, differences in particle formation were already visibly perceived. The flames during burning of BCBs were much smaller and the flameless oxidation of char accounted for larger fraction of each combustion cycle. During the burning of SLs on the other hand, flames were so large that they hit the inner casing of the stove leading to visible soot production. Particles emitted by SL burning emitted on average larger particles that are more perceptible to the human high by more efficient scattering of visible radiation (Figure 4-5, top), whereas particles emitted from BCB burning (Figure 4-5, bottom), were much smaller in diameter than particles emitted from SL burning. The evolution of particles emitted by SLs burning seemed to pass through three distinct phases, with each emitting particles of a distinctive size distribution. Upon the ignition of a batch of fuel, particles were rather small with particle diameter modes below 100 nm(Figure 4-5, top panel, batch 1); yet, this was not observed in every batch since some batches passed through the ignition so quickly that the SMPS scanning through the particle range of 10-600 nm with a duty cycle of 3 min was not able to capture this phase appropriately. Subsequently, the combustion transitioned to flaming
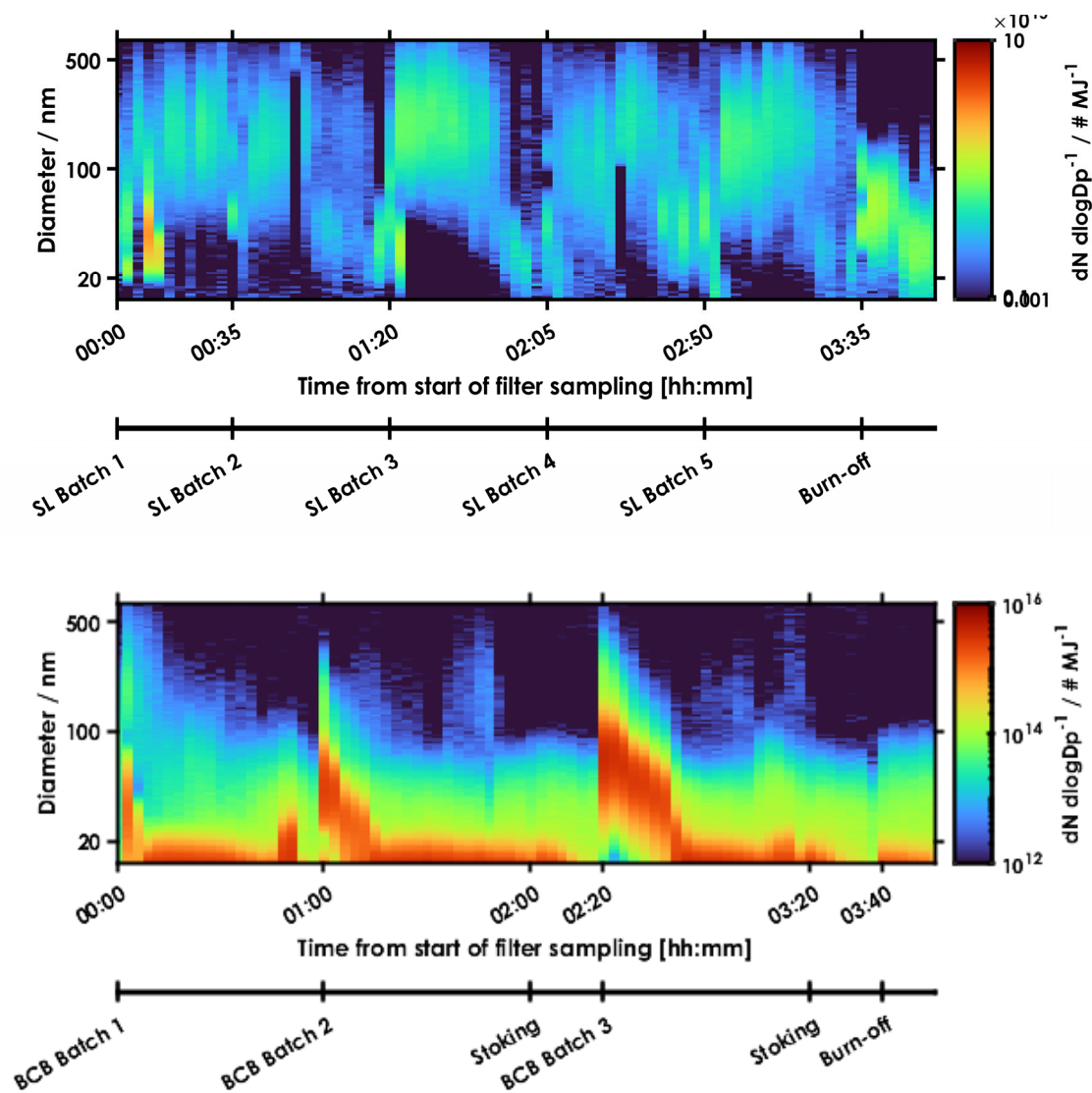
Figure 4-5 Evolution of particles during combustion of spruce logs and brown coal briquettes, taken from Martens et al.[159].

combustion with visible flames and soot production, and particles emitted during this phase had diameter modes of ca. 200 nm. Once the majority of the batch was consumed, the combustion transitioned to a flameless, heterogeneous oxidation of char, and particle modes during the char oxidation fell to below 100 nm. Particles emitted by BCB burning did not appear to pass through three distinctive phases. The ignition of the fuel was a distinctive phase, and particle number emissions were particularly higher in batches that ignited comparatively slow (Figure 4-5, bottom, batch 3). Particles that were emitted during this phase had mode in a range of 30-100 nm, and these modes quickly declined to even lower numbers close to the lower size range of the instrument upon transition to the flaming combustion. Flames during the flaming combustion were generally much smaller and did not get quenched by hitting the inner casing of the stove. The transition from flaming to char combustion however was not noticeable in particle number emissions, which remained small in diameter and similar in intensity compared to the flaming combustion.

As for the nature of these particles, thermal-optical carbon analysis of particulate matter sampled on filter provided more insights into the carbonaceous fraction. Emissions from BCB burning were characterized by OC/EC ratios above unity, i.e., from 1.09 to 3.65, whereas emissions from SL burning had rather low ratios ranging from 0.16 to 0.25 (Figure 4-6). OC/EC ratios in emissions from BCB burning appeared to be related with the combustion quality, as indicated by CO emissions averaged over the course of the entire combustion experiment. These observations are in alignment with those made in many previous studies, which predominantly reported high OC/EC for coal[146,148,182–185] and low ones for

wood[83,186–188] combustion. The thermal-optical carbon analyzer also allows for deeper insights into different volatility fractions of OC. Semi-volatile compounds are associated with the two low-temperature fractions of OC, that is, OC1 and OC2 (Figure 4-7), and their emissions seemed highly susceptible to the combustion quality, as indicated by CO emissions. OC3 and OC4, referring to low-volatile organic compounds, were less susceptible to the combustion quality.

The results suggest that high EC emissions in SL experiments appear to be emitted during flaming combustion with PN modes greater than 100 nm, indicating that the majority of the emitted particles do not qualify as ultrafine particles. Because of the high share of volatile matter, SLs ignite faster and burn at a higher rate leading to large flames that were quenched by the inner casing of the stove. Larger

Figure 4-6 The nature of carbonaceous emissions in brown coal briquette and spruce log combustion and their association to combustion quality, taken from Martens et al.[159].

flames suggest that the organic gases released from primary pyrolysis of the fuel is hold at elevated temperatures for longer time spans, which may have led to stronger decomposition in secondary pyrolysis mechanism in the gas phase. Due to the flames striking the inner casing of the stove, the oxidation of soot that has formed in fuel-rich zones of the flame may have been prematurely terminated leading to the incomplete oxidation of soot, vapors and gases. BCBs on the other hand ignite poorly and burn slowly because of the comparatively low content of volatile matter in the fuel macromolecular network. Due to the flames being smaller, the time the molecules are hold at elevated temperatures in the fuel-rich zone of the flame may have been shorter, which may have caused the compounds to undergo fewer secondary pyrolysis reactions. These reactions might have led to fewer production of EC precursor species and thus fewer production of EC. Moreover, the EC that was produced in fuel-rich zone of the flame might have been
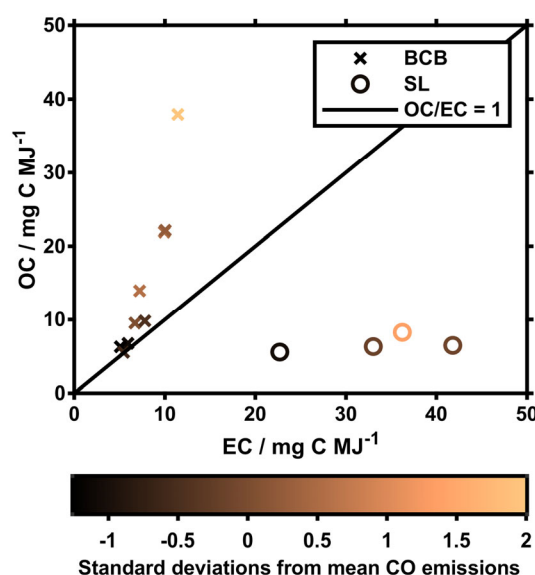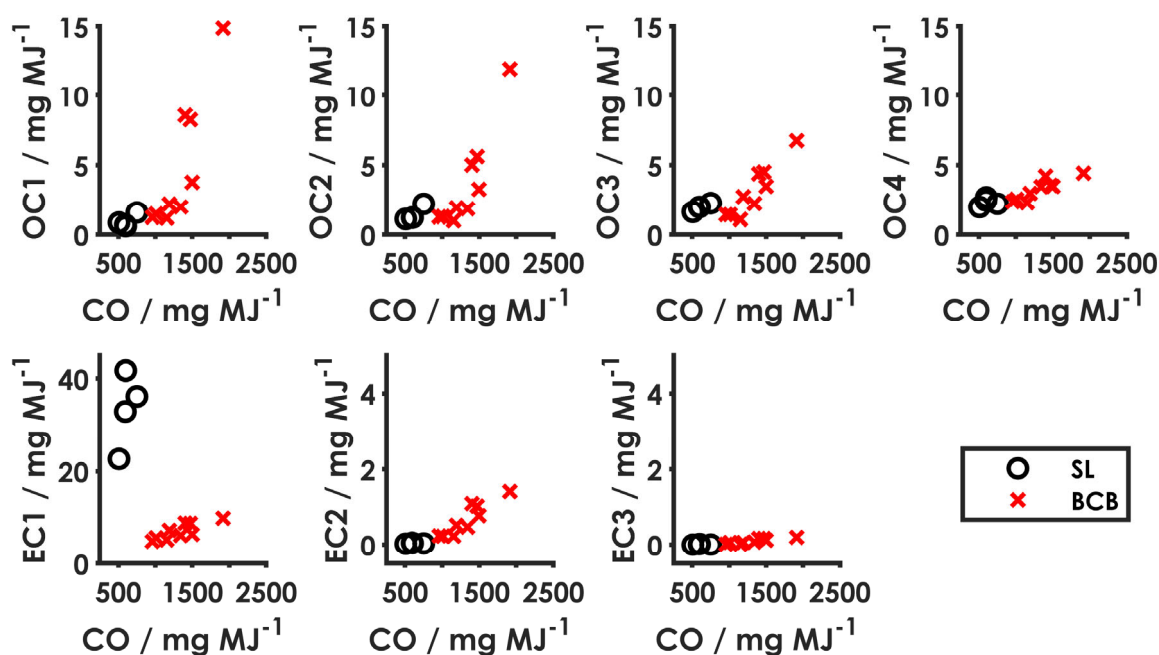

Figure 4-7 The impact of combustion quality on different volatility groups as indicated by individual organic and elemental carbon fractions, taken from Martens et al.[159].

more completely oxidized in the oxygen-rich zone of the flame was not quenched due to the flames not striking the inner casing of the stove.

Emissions of particle-bound organic constituents, that is, OC, seem to be primarily emitted during the ignition of a batch, which is in alignment with the results on VOCs.[169] Emissions from BCB burning, which is rich in OC, had pronounced emissions of particles during the ignition, whereas OC emissions from SL burning were comparable to the lowest observed levels of emissions from BCB burning. Flame dynamics might have also had an effect on the overall composition of OC that was emitted from the overall combustion process. The strong production of EC can only occur if constituents of the pyrolysis gas released by primary fuel pyrolysis underwent cracking reactions that lead to a noticeable production of EC precursors. Fewer production of EC and moreover the composition of VOCs[169] suggest that cracking reaction may have been less pronounced in BCB than in SL burning, and this was analyzed in more depth by means of the PI-ToF-MS and GC-MS.

4.1.5 De-functionalization of Aromatic Semi-Volatile Organic Compounds with Increasing Combustion Quality

Typically, semi-volatile organic compounds are targeted by methods relying on gas chromatography,[63,83,188] which was also used here.[189] However, the organic composition of combustion aerosols is highly complex and can span thousands of different compounds challenging even highly specific, state-of-the-art mass spectrometers with ultra-high resolving power[190] Atmospheric aerosols, being subject to photochemical oxidation, can be even more complex with tens of thousands of signals,[90] and their complexity alongside rather low levels, at least in ambient aerosols, demand more pragmatic analytical solution from scientific community. Nozière et al.[90] outlined various concepts and levels of identification in research on complex pollution sources, ranging from a description of macroscopic properties to the identification on a single-molecule level. Diab et al.[95] introduced a new approach of characterizing the particle-bound organics by coupling a thermal-optical carbon analyzer to PI-ToF-MS to gain information on the chemical composition of particle-bound organics on a semi-molecular level. This approach was used in conjunction with a REMPI-ToF-MS to gain information on semi-volatile compounds released from filter samples

Figure 4-8 Chemical signatures of semi-volatile organic emissions (A–C) and high molecular mass range (m/z 280–350) with characteristic fingerprint of high molecular-weight polycyclic aromatic hydrocarbons and aromatic biomarkers. The figure was adapted from Martens et al.[159].

during the fractions OC1 and OC2 (140 °C–280 °C) of the Improve_A thermal protocol. These fractions were analyzed combined due to the assumption that evolving compounds predominantly desorb from the filter and not decompose.[95]

Aromatic signatures from BCB burning (Figure 4-8 panel A and B) were generally more complex than those found in emissions from SL burning (Figure 4-8 panel C). Due to the specificity of [1+1] REMPI with 248 nm radiation on predominantly aromatic compounds, and by assuming that particle-bound organic
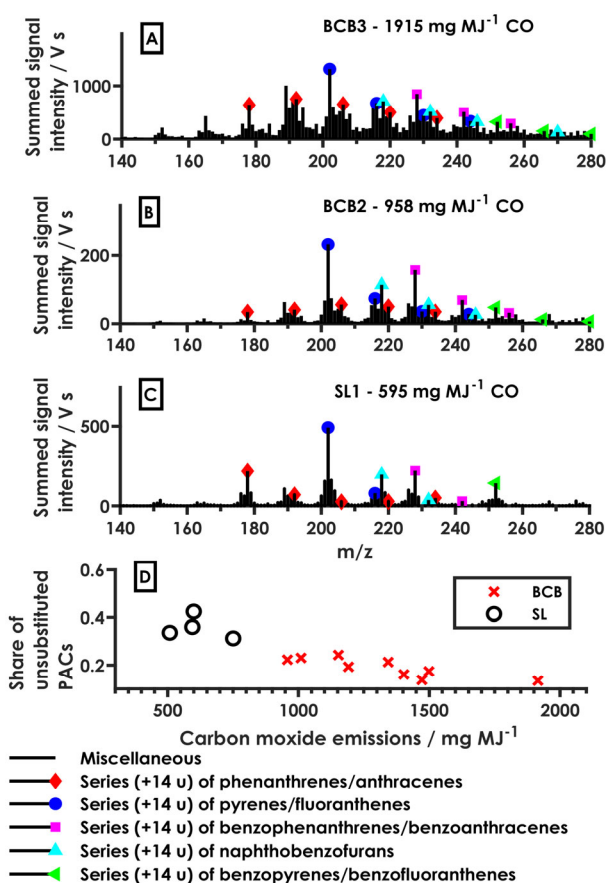
mainly consist of C, H, and O, which is common for combustion aerosols,[190] the prominent signals in each spectrum were interpreted to refer to parent PAHs (phenanthrene and anthracene: m/z 178; pyrene and fluoranthene: m/z 202; naphthobenzofurans: m/z 218; benzophenanthrenes and benzanthracenes: m/z 228; benzopyrenes and benzofluoranthenes: m/z 252), which are common species in combustion aerosols.[81,83,188,189,191] In emissions from BCB burning with low combustion quality, as indicated by CO emissions, signals referring to these compounds were intense, and so were the signals referring to their functionalized analogues, as indicated by their alkylation series (+14 u). In emissions from BCB burning with low CO emission, the overall signal intensity decreased substantially, which was expected since the amount of OC1 and OC2 also decreased. In emissions from SL burning, signals referring to these parent species were much more prominent, and signals referring to functionalized PAHs were less abundant (Figure 4-8 panel C). These parent ions (m/z 178, 202, 218, 228, 252) had a much larger contribution to the totals recorded signal intensity in emissions from SL burning than in emissions from BCB burning (Figure 4-8 panel D). For the latter, the contribution of these parent PAHs seemed to be related to the combustion quality, with emissions from BCB burning with low CO emissions having produced a higher share of these parent PAHs and emissions from BCB burning with high CO emissions having produced a lower share of these species. This can be interpreted as indication for a shift from petrogenic to pyrogenic emissions, with the functionalized molecules being species of petrogenic origin and the parent PAHs referring to pyrogenic emissions.

4.1.6 Low-Volatile Organic Compounds: A Transition of Aromatic Archipelagos to Condensed PAH-Islands with Increasing Combustion Quality?

Low-volatile compounds found in aerosols are generally difficult to analyze. Common approaches, such as liquid chromatography and high resolution MS, are generally feasible tools, however these techniques have also limitations. The scope of these methods is defined by the chosen extraction approach since the type of solvent biases the outcome of the analysis, as can be seen for crude oils in the work of Neumann et al.[192]. Moreover, some compounds that are practically insoluble in any common media, such as synthetic polymers, cannot be analyzed at all and thus require pyrolytic approaches for their characterization.[193] The carbon analyzer in conjunction with PI-ToF-MS offers a very large scope, covering semi-volatile compounds in OC1 and OC2 by evaporating compounds from filters as well as low-volatile compounds in OC3 and OC4 via analytical pyrolysis. While evaporation is thought to be the governing release mechanism in OC1 and OC 2, analytical pyrolysis at temperatures of 480°C and 580°C leads to the dissociation of chemical bonds ins low-volatile species causing the release of fragments with higher volatility, marked by shifting signals in the mass spectrum from comparatively high m/z to low ones.[95] The approach overcomes the issue of potential insoluble compounds not being analyzed at all and the sensitivity to the choice of the sample preparation procedure but has the drawback of not retaining molecular integrity. The scope of REMPI, which was used to provide insights into semi-volatile compounds is inappropriate for low-molecular weight compounds, a SPI-ToF-MS system was used to provide insights on analytical pyrolysis of low-volatile organic species in the carbon analyzer.

Emissions from BCB burning showed substantial variation in their chemical fingerprint upon analysis in the carbon analyzer. Low-quality burning of BCBs (Figure 4-10 panel A) led to emission of low-volatile compounds, which upon analytical pyrolysis in the analyzer released aliphatic and/or furanoic compounds (propene: m/z 42, butadiene m/z 56, etc.). Moreover, a complex fingerprint was observed in the range of m/z 90-200, which are signals that indicate a variety of functionalized single-ring aromatic species. Fragments of naphthalene (m/z 128) and phenanthrene/anthracene (m/z 178), as indicator for fused rings, were not prominent. High quality burning of BCBs (Figure 4-10 panel B) similarly emitted low-volatile compounds that were able to release aliphatic and/or furanoic compounds yet at a much lower level compared to the low-quality combustion sample. Chemical species in the m/z range of 90-200 mostly
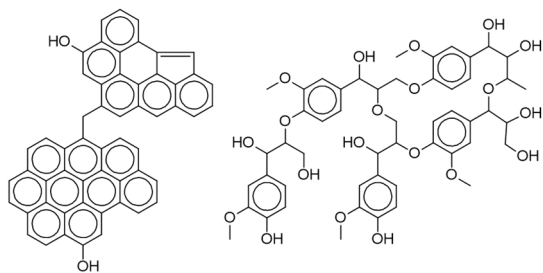
Figure 4-9 Example structures of island-type (left) and archipelago-type (right) low-volatile organic compounds.

disappeared, and instead their unsubstituted analogues, i.e., benzene and phenol, were more prominent in the spectrum. Signals referring to naphthalene (m/z 128) and phenanthrene/anthracene (m/z 178) were still not prominent. In emissions from SL burning with comparatively low combustion quality (Figure 4-10 panel C), signals that refer to aliphatic and furanoic compounds were even lower than in the high quality combustion of BCBs, and the substituted aromatic were almost entirely absent. Benzene (m/z 78) and phenol (m/z 94) became very prominent, and naphthalene (m/z 128) emerged in higher abundance. Emissions from SL burning with the lowest CO emissions, the latter three compounds made up almost the entirety of the spectrum, and aliphatic units and substituted aromatic are almost absent (Figure 4-10 panel D).

The results indicate that low-volatile organic compounds that have evolved upon burning SLs and BCBs may be differentiated into pyrogenic and petrogenic origin, as well. Emissions from SL burning, being characterized by large amounts of aromatic moieties and small amount of unsaturated aliphatics, point toward the pyrogenic origin. Emissions from BCB burning on the other hand had a higher share of moieties that retain fuel-specific motifs, i.e., substituted benzenes, phenols and catechols. Similar to the observation made on semi-volatile compounds, the degree of functionalization in emissions appeared to decrease with increasing combustion quality (Figure 4-10 panel E). By adapting concepts from other fields of research within the group of Prof. Zimmermann (Petroleomics), low-volatile organic compounds can either be described as island-type or archipelago-type (Figure 4-9), with the island-type asphaltenes containing larger PAH-like structures that are connected via rather short chain aliphatic bridges and the archipelago motif referring to rather small aromatic structures that are connected by longer aliphatic bridges.[192,194] The archipelago motif resembles the macromolecular structure of lignin or lignite, and in case of solid fuel combustion seems to be retained in emissions from BCB burning, indicated by the stronger presence of aliphatic moieties and the abundancy of substituted six-membered aromatic rings in the chemical fingerprint.
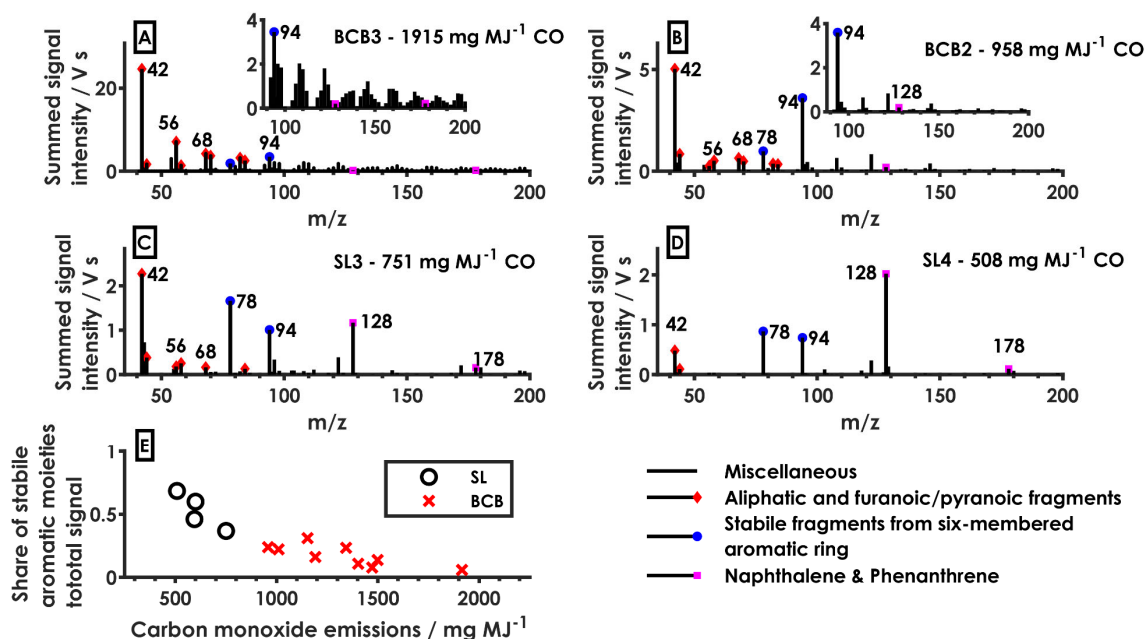

Figure 4-10 Signatures of low-volatile organics in emissions from brown coal briquettes and spruce logs at various combustion qualities, as indicated by CO emissions, taken from Martens et al.[159].

The island-type on the other hand seems to be dominating in emissions from SL burning, as indicated by the high share of unsubstituted aromatic units and low proportions of aliphatic units, which are likely olefins themselves.

4.2.   Toxic Effects of Particulate Matter Emitted by Solid Fuel Burning

4.2.1   Toxic Effects of Brown Coal

The central theme for the chemical analysis of carbonaceous emission emitted from solid fuel burning has been the classification of the chemical fingerprint as either petrogenic or pyrogenic. Both motifs appeared to be connected to the combustion quality, which was more obvious in emissions from BCB burning due to the higher variability in combustion quality observed in these experiments. The higher degree of graphitization in emissions from SL burning and the higher degree of functionalization in emissions from BCB burning may lead to different toxicological responses in humans and other organisms. For example, Kang et al.[195] have analyzed several unsubstituted and alkylated PAHs for their overall water solubility and partitioning coefficients in polydimethylsiloxane-water and liposome-water mixtures, with polydimethylsiloxane and liposome being proxies for biological membranes. They found that alkylated PAHs show both an elevated water solubility as well as elevated partitioning coefficients in polydimethylsiloxane-water and liposome-water mixtures in comparison to their unsubstituted parents, indicating a higher mobility of alkylated PAHs in cell fluids and other environmental media as well as diffusion through tissue. The elevated solubility of functionalized organics implies that chemical compounds of petrogenic origin may act over short time scales, whereas constituents of pyrogenic origin may act over longer time scales due to their slower accumulation cell fluids. This effect may further be enhanced by considering that compounds with pyrogenic origin (e.g., parent PAHs) are not toxic themselves due to their chemical inertness. Instead, the toxicity of these species is the results metabolic activity, with a common pathway being the enzymatic oxidation of PAHs to their diol epoxides. The metabolites are able to form adducts with nucleotides of deoxyribonucleic acid and damage the hereditary information stored in these biopolymers, affecting the metabolic function of cells.[196,197] Thus, apart from likely being more soluble in cell fluids, emissions from BCB burning likely require less or no activation via metabolic activity in order to reveal their toxic potency. Emission from SL burning on the other hand may take more time to be activated in addition to potentially slower dissolution in cell fluid, which implies a more latent effect. However, another aspect to consider is that the elevated functionalization makes functionalized compounds more available for clearance mechanisms of organisms, e.g., via glucuronyl transferases,[197] which would reduce their potency. Given the complexity of the interaction of chemical compounds in living organisms (uptake, metabolic activity, clearance, to name a few), it is difficult to make a verdict on the toxicity of emissions from solid fuel burning based on the chemical composition alone, which leaves a gap for toxicological research.

Results on the chemical composition, that is, concentration levels of a variety of VOCs as well results from thermal-optical carbon analysis on OC and EC fractions, were shared with collaborators from the University of Eastern Finland to substantiate findings on toxic responses from cells that were exposed to emissions from SL and BCB burning.[71] Toxic responses (cytotoxicity, inflammation, genotoxicity) were studied in a monoculture of the human alveolar cell line A549, which refer to diseased human epithelial cells affected by cancer, and a co-culture of A549 cells and THP-1 cells, with the latter being derived from an acute monocytic leukemia patient. Both the mono and co-culture have been exposed to diluted combustion aerosol using a commercial, automated exposure system (Vitrocell Systems GmbH, Germany). Due to significantly different particle size distribution (Figure 4.3), cells that were exposed to emissions from BCB burning received only half of the dose of PM in terms of mass when compared to the dose on cells, that were exposed to emissions from SLs. The targeted GC-MS analyses of particle-bound organics presented by Ihantola suggested that emissions from SLs were more toxic due higher emissions of parent, hydroxy

PAHs and other oxygen containing PAHs in emissions from SL burning. Differences in emissions of common, toxic inorganic constituents (e.g., Zn, Cd, and Cu) between both fuels were found to be rather small by Martens et al.[189]. Interestingly, despite being exposed to a higher dose of PM with higher concentrations of toxic PAHs, Ihantola et al.[71] have not found significant differences in toxic responses of cells exposed to emissions from SL and BCB burning. This emphasizes the need for results from untargeted methods, such as the PI-ToF-MS analyses from the carbon analyzer presented by Martens et al.[189], which are in contrast to the targeted analysis by GC-MS not inherently biased by the users choice of targets.

4.2.2 Toxic Effects from Open Biomass Burning

Emissions from solid fuel combustion in modern heating appliances as targeted by Martens es al.[169,189] and Ihantola et al.[71] is mainly a problem in Europe and North America. On a global scale, open biomass burning is a much more important form of solid fuel burning. [34] It refers to the uncontrolled burning of solid fuel, which is likely low in combustion quality, and intended burning of forests and grassland to provide new fertile land for agriculture, open burning of agricultural wastes in order to reduce waste management costs, and wildfires are three phenomena that can be categorized as open biomass burning.

In order to study effects from individual compound classes emitted from any form of solid fuel burning, particularly the effect of solubility of species, Pardo et al.[198] have pyrolyzed pine needles at 550 °C to produce
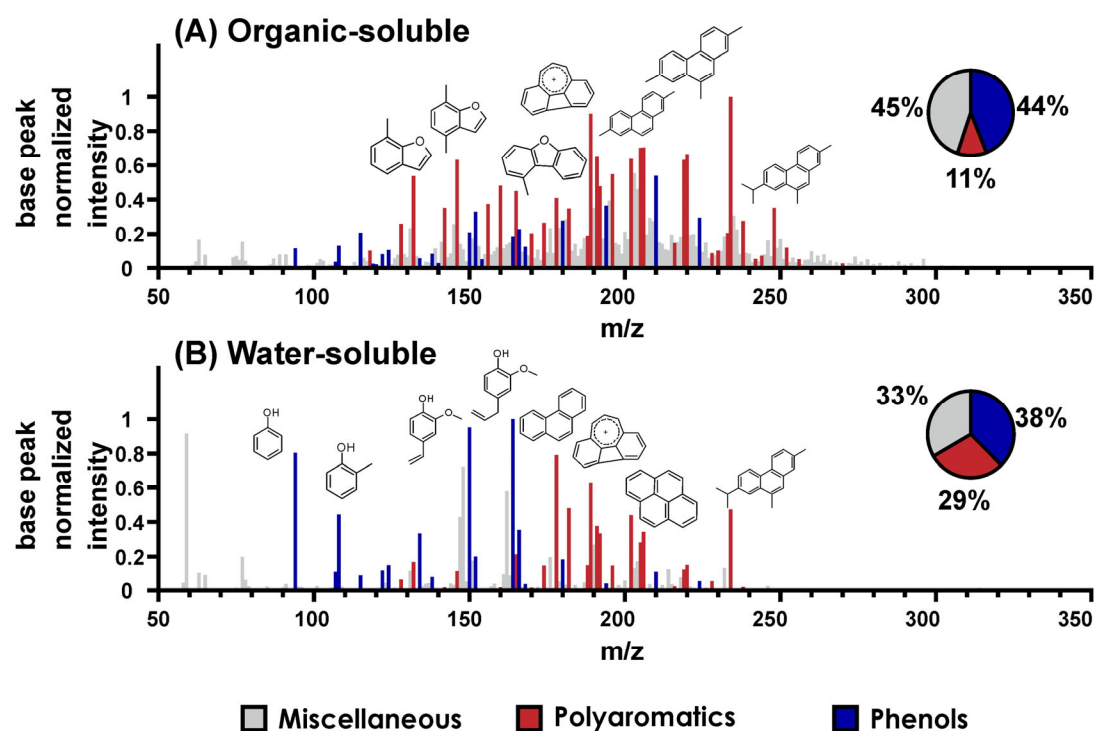
Figure 4-11 Composition of water-insoluble and water soluble tar fractions as revealed by thermal analysis in a carbon analyzer and REMPI-ToF-MS, adapted from Pardo et al.[172].

a large amount of tar that was collected with a water-cooled trap and freeze-dried to yield pure tar. Subsequently, a portion of the tar was re-dissolved in water and CH_2Cl_2-hexane to divide the tar into a water-soluble and organic-soluble fraction, and these extracts were tested for various toxic responses with two human epithelial cell lines, A549 and BEAS-2B, under submersed conditions.

Analysis of both extracts with REMPI-ToF-MS revealed signals that were tentatively assigned to various small phenols, that is, phenols, methoxy phenols and methyl phenols. These contributed relatively more to the total signal intensity in water-soluble than organic-soluble extracts likely due to their elevated water solubility, whereas the organic-soluble extracts comprised larger PAHs and oxygenated PAHs, particularly alkylated phenanthrenes and benzofurans.[198] Both sub-fractions of the tar decreased the cell viability *in vitro*, yet the flow cytometry revealed that these reactions occur at a different rate, with the organic-soluble

fractions taking more time to affect the cells. Toxic effects induced by the water-soluble fraction were associated with the production of reactive oxygen species that followed the exposure of cells to the water soluble tar. The organic-soluble fraction was found to lead to more direct effects of organs of the cell with the tar.

4.3. Toward Better Identification of Sources for Public Health Concerns

4.3.1 Challenges in the Differentiation of Coal and Biomass

Several substances were proposed to be biomarkers because they were thought to be either unique to a certain source, e.g., anhydrous sugars such as levoglucosan, manosan and galactosan are three compounds that were thought to be unique for biomass combustion phenomenon. Cellulose and hemicellulose, the precursors of these anhydrous sugars were reported to degrade in the early stages of coal metamorphosis, [108] but information on the presence of cellulose and hemicelluloses in Miocene lignites is accumulating.[199–203] Most studies that provide information of these anhydrous sugars in coal either analyze the unburned coal by pyrolytic analysis, e.g., pyrolysis GC-MS, or analyze the coal smoke from rather simple burning set-ups, for example, a crucible filled with 50 g portion of coal. The combustion quality of these set-ups may not accurately reflect the combustion quality of modern appliances, particularly those installed in Europe with high combustion quality. Thus, one part of this thesis was to investigate emissions of anhydrous sugars emitted from BCB burning in a modern combustion appliance and compare them to anhydrous sugar emissions in smoke samples from SL burning.[189]

Anhydrous sugars, that is, the sum of levoglucosan, manosan and galactosan, were found in comparable ranges of $5-380\ \mu g\ MJ^{-1}$ in emissions from SL burning and $29-580\ \mu g\ MJ^{-1}$ in emissions from BCB burning. This is also comparable to levels found in emissions from residential wood combustion with 53, 72, and $110\ \mu g\ MJ^{-1}$ from various wood types.[83] Nevertheless, it was possible to differentiate both fuels by their emissions galactosan and manosan, which were found to be emitted from SL combustion but not from BCB combustion. The results demonstrate that anhydrous sugars are not unique to biomass burning but can also be emitted from burning of low-maturity coals in state-of-the art combustion

Figure 4-12 High molecular weight fingerprint of emissions from spruce log (SL) and brown coal briquette (BCB) combustion in a residential heating appliance, taken from Martens et al.[159].

appliances at comparable levels. Yan et al.[203] have even found anhydrous sugars in smoke samples from burning very mature coals, such as semi-anthracite, in Chinese residential heating appliances. In their analysis however, emissions of anhydrous sugars by coal burning was outrivaled by burning of wood and crop waste by one to three orders of magnitude, whereas burning of the Lusatian Lignite was in the same order of magnitude to biomass combustion.
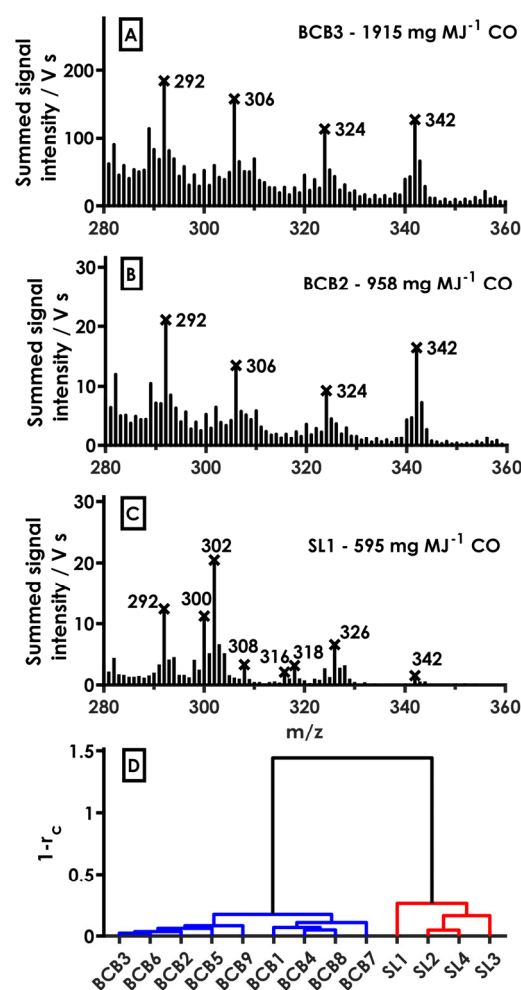
4.3.2 Resin Acids as Markers of Biomass and Coal

More promising than anhydrous sugars for source markers may be secondary plant constituents, specifically the resin acids, which can even be used to differentiate individual tree species and may therefore be much better markers.[204,205] In coal, these resins are fossilized,[81,206] which leads to chemical alteration of these structures, that is, saturation of double bonds and subsequently aromatization via a sequence of H addition and abstraction steps.[207] However, unaltered rests may still be present.[208] In the combined carbon analysis PI-ToF-MS approach, constituents cannot be resolved on a molecular basis, but approach may provide characteristic fingerprints of these species. From previous research, it is known that resins may occur in the higher m/z range, that is, m/z 280−400, starting in the OC2 fraction (280 °C) of the Improve_A protocol.[83] In order to also consider the possibility of some species forming due to the analytical pyrolysis occurring in the carbon analyzer, OC2 was combined with OC3 (480 °C) was also taken into account for the chemical fingerprint.

In emissions from BCB burning (Figure 4-12 A, B),[189] the prominent ions were attributed to a series of picene-like compounds, which are aromatic biomarkers that are known to be present in emissions from coal combustion, e.g., various C4-octahydropicenes (m/z 342), C3-tetrahydropicenes (m/z 324), C2-picenes (m/z 306), and C1-picene (m/z 292).[81] The difference in 18 u between these signals (342−324−306) may be explained by a loss of methane followed by a loss of H_2, leading to incremental increases in aromatization. In emissions from SL burning (Figure 4-12 C), the most abundant signals were m/z 300, 302, and 326, , which were attributed to larger PAH species, e.g., coronene and dibenzopyrenes, among others, which were also found in larger amounts in SL emissions in ID-TD-GC−MS analyses.[189] It seems likely that they could have formed in pyro synthesis as precursors of EC, with m/z 316, 318, and 342 possibly referring to the same species with an additional OH-group. These fingerprints can be used to clearly differentiate both fuels (Figure 4-12 D).

4.3.3 The nature of soot as an Indicator of Combustion Source

Different pollution source can already readily be differentiated by the thermal stability of the emitted soot. The main goal of this thesis was analyze solid fuel burning emissions, yet the work on other pollution sources is essential to better comprehend the bigger picture. For example, emissions from marine engine have been found as major pollution source, particularly in coastal areas,[209,210] research on marine engines is a major field of research of the group of Prof. Zimmermann,[74,211–215] Thus the work carried out in the study presented by Momenimovahed et al.[216] provided data to better put the data from solid fuel burning in residential heating appliance fueled with SLs and BCBs into perspective. Momenimovahed et al.[216] aimed to compare different commercially available instruments targeting BC and EC, yet the data can also be used to highlight differences in the combustion phenomena. The engine that was used is a single-cylinder research and development engine of the Institute of Piston Machines and Internal Combustion Engines at the University of Rostock, which has a displacement of 3.18 L and a rated power of 80 kW at 1500 revolutions, which was fueled with diesel fuel (DF), distillate marine oil grade A (DMA), and an intermediate fuel oil (IFO). The former two are examples of high grade distillate fuels with rather beneficial combustion properties, that is, low viscosity and low sulfur-content, whereas the IFO is rather low grade, much more viscous and has much higher sulfur content.

As already explained earlier, EC or BC are not unique substances with discrete properties but rather undefined substances. Based on the resistance of the soot toward oxidation at elevated temperatures, it is commonly classified as either low-refractory char-EC (EC1) or more refractory soot-EC (EC2+ EC3).[217] The temperature and pressure regimes under which combustion conditions may take place vary widely for different real-world sources. Solid fuel burning, occurring either in the open or in combustion appliances, proceeds regimes under atmospheric pressure and temperatures of up to 2000,[97] whereas engines compresses a combustible air-fuel mixture and either rely on the forced ignition via a sparking plug or auto

ignition of the mixture. The differences in these processes and the vastly different fuel properties led to characteristic ratios of char-EC and soot-EC. Residential wood combustion almost exclusively produced less refractory char-EC(Figure 4-13), whereas the combustion of the two high-grade fuels, DF and DMA, in the marine engine produced almost exclusively soot-EC. Previous research has found similar ratios for soot and char in biomass and coal combustion emitted from a variety of different appliance-fuel combinations commonly used in China with a share of char on total EC with 92% and 71% for coal and biomass burning, respectively.[218] The differences in the reactiveness could possibly be a result of the microstructure of EC, that is, the size of individual nanoparticles within the agglomerated, larger BC/EC particles.[219] Residential coal combustion and the combustion of IFO in the internal combustion engine both seem to not align with their respective analogues since they have produced mixtures of EC1 and EC2, indicating a transition between properties. Either way,

Figure 4-13 Ratios of char (EC1, oxidized at 580°C in the carbon analyzer) and soot (EC2 & EC3, oxidized at 740°C and 840°C in the carbon analyzer) from a 4-stroke, single cylinder marine engines fueled with diesel fuel (DF), distillate marine oil grade A (DMA), and an intermediate fuel oil (IFO), and residential solid fuel combustion with brown coal briquettes (BCBs) and spruce logs (SLs). The data was taken from experiments carried out by Momenimovahed et al.[192] and Martens et al.[159].

the occurrence of different microstructures in EC and BC from different combustion sources has already been proven useful in environmental studies aiming to impact of combustion sources on air, soil, and water.[220–222]
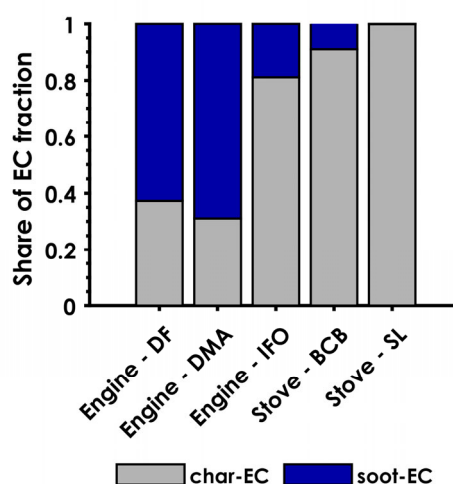
5.   Conclusion & Outlook

Aerosols from solid fuel burning are still a major contributor to regional air pollution in many parts of the world, such as developing countries in East Asia but also in developed countries in Central and Eastern Europe. Within this thesis, the major aim was to analyze physical properties and the chemical composition of emissions from solid fuel burning, with the focus being on solid fuel combustion in state-of-the-art heating appliances found in households of developed countries using common spruce logs and Lusatian brown coal briquettes as fuel.

Brown coal was found to be a notable emitter of ultrafine particles, that is, particles with diameters below 100 nm, that can deeply penetrate the lung. The bulk composition of emitted particles from burning brown coal were found to be comparatively rich in organic carbon, whereas wood combustion in modern heating appliances was comparatively rich in elemental carbon, implying that different the of organic pollutants were dominated by two different mechanisms. To gain further insights, emissions of organic aerosols of all volatility subgroups, that is, volatile to low-volatile organic compounds, were investigated relying on untargeted mass spectrometric approaches with a focus on photoionization methods. Across the entire volatility range of organic compounds, wood combustion was found to emit compounds that are low in oxygen and other hetero elements and predominantly consist of carbon and hydrogen with a high degree of aromaticity and graphitization, i.e., benzene and other small unsaturated hydrocarbon (propene, butene, etc.) as well as unsubstituted polycyclic aromatic hydrocarbons. Brown coal on the other hand was found to emit compounds that were richer in hetero elements and generally showed a higher degree of saturation. The varying composition was found to be associated to the changing combustion quality.

Moreover, the approach of thermal optical carbon analysis coupled to photoionization mass spectrometry was found to provide important insights into the nature of potential markers from solid fuel burning. Traditional markers of biomass burning, i.e., anhydrous sugars like levoglucosan, were found in comparable levels in emissions from both biomass and Lusatian brown coal, demonstrating that the use of these traditional markers is, at least to some degree, questionable and the need to find other potential markers. Coal origins from biomass and can still contain major constituents, such as cellulose. Analysis of filter samples in the carbon analyzer with photoionization revealed a rapid insight into emissions of resins and resin derivatives, and distinctive fingerprints of these secondary plant constituents may be used for source apportionment studies aiming to improve public health.

Lastly, the chemical evaluation of solid fuel burning emissions aided the investigation of toxic effects. Poorer burning conditions led to emissions that were enriched with organic species that were found to be more active in biological tissue. Toxic effects from wood and brown coal burning were found to be in the same order of magnitude, yet emissions from brown coal burning was found to be more potent as fewer particles were deposited in cells, which might be due to their enhanced solubility in aqueous media. The analysis of different solubility fraction of solid fuel burning aerosol helped providing insights into toxicological mechanisms exerted by compounds with different polarity and thus different uptake kinetics and processes. Water-soluble compounds were found to be passively taken up by cells, whereas the compounds that were categorized as organic-soluble has to be taken up by cells via an active transport, causing it to be slower. Organic-soluble constituents led to a direct cellular response to these toxins, whereas the exposure to water-soluble constituents was indirect by initially causing the production of reactive oxygen species, which subsequently cause cytotoxicity.

6. References

(1) Seinfeld, J. H.; Pandis, S. N. *Atmospheric Chemistry and Physics: From Air Pollution to Climate Change*, 3. Edition; John Wiley & Sons, 2016.

(2) DIN German Institute for Standardization. *Luftbeschaffenheit - Allgemeine Gesichtspunkte - Begriffe (ISO 4225:2020)*; Beuth Verlag GmbH, Berlin, 2020.

(3) Seigneur, C. *Air Pollution*, 1. Edition; Cambridge University Press, 2019.

(4) Després, V. R.; Huffman, J. A.; Burrows, S. M.; Hoose, C.; Safatov, A. S.; Buryak, G.; Fröhlich-Nowoisky, J.; Elbert, W.; Andreae, M. O.; Pöschl, U.; Jaenicke, R. Primary biological aerosol particles in the atmosphere: a review. *Tellus, Ser. B: Chem. Phys. Meteorol.* **2012**, *64* (1), 15598.

(5) Monks, P. S.; Granier, C.; Fuzzi, S.; Stohl, A.; Williams, M. L.; Akimoto, H.; Amann, M.; Baklanov, A.; Baltensperger, U.; Bey, I.; Blake, N.; Blake, R. S.; Carslaw, K.; Cooper, O. R.; Dentener, F.; Fowler, D.; Fragkou, E.; Frost, G. J.; Generoso, S.; Ginoux, P.; Grewe, V.; Guenther, A.; Hansson, H. C.; Henne, S.; Hjorth, J.; Hofzumahaus, A.; Huntrieser, H.; Isaksen, I.; Jenkin, M. E.; Kaiser, J.; Kanakidou, M.; Klimont, Z.; Kulmala, M.; Laj, P.; Lawrence, M. G.; Lee, J. D.; Liousse, C.; Maione, M.; McFiggans, G.; Metzger, A.; Mieville, A.; Moussiopoulos, N.; Orlando, J. J.; O'Dowd, C. D.; Palmer, P. I.; Parrish, D. D.; Petzold, A.; Platt, U.; Pöschl, U.; Prévôt, A.; Reeves, C. E.; Reimann, S.; Rudich, Y.; Sellegri, K.; Steinbrecher, R.; Simpson, D.; Brink, H. ten; Theloke, J.; van der Werf, G. R.; Vautard, R.; Vestreng, V.; Vlachokostas, C.; Glasow, R. von. Atmospheric composition change – global and regional air quality. *Atmos. Environ.* **2009**, *43* (33), 5268–5350.

(6) McDuffie, E. E.; Martin, R. V.; Spadaro, J. V.; Burnett, R.; Smith, S. J.; O'Rourke, P.; Hammer, M. S.; van Donkelaar, A.; Bindle, L.; Shah, V.; Jaeglé, L.; Luo, G.; Yu, F.; Adeniran, J. A.; Lin, J.; Brauer, M. Source sector and fuel contributions to ambient PM2.5 and attributable mortality across multiple spatial scales. *Nat Commun* **2021**, *12* (1).

(7) Atkinson, R. Atmospheric chemistry of VOCs and NOx. *Atmos. Environ.* **2000**, *34* (12-14), 2063–2101.

(8) Atkinson, R.; Arey, J. Atmospheric degradation of volatile organic compounds. *Chem. Rev.* **2003**, *103* (12), 4605–4638.

(9) Bianchi, F.; Kurtén, T.; Riva, M.; Mohr, C.; Rissanen, M. P.; Roldin, P.; Berndt, T.; Crounse, J. D.; Wennberg, P. O.; Mentel, T. F.; Wildt, J.; Junninen, H.; Jokinen, T.; Kulmala, M.; Worsnop, D. R.; Thornton, J. A.; Donahue, N.; Kjaergaard, H. G.; Ehn, M. Highly Oxygenated Organic Molecules (HOM) from Gas-Phase Autoxidation Involving Peroxy Radicals: A Key Contributor to Atmospheric Aerosol. *Chem. Rev.* **2019**, *119* (6), 3472–3509.

(10) Herrmann, H.; Schaefer, T.; Tilgner, A.; Styler, S. A.; Weller, C.; Teich, M.; Otto, T. Tropospheric aqueous-phase chemistry: kinetics, mechanisms, and its coupling to a changing gas phase. *Chem. Rev.* **2015**, *115* (10), 4259–4334.

(11) Herrmann, H. Kinetics of aqueous phase reactions relevant for atmospheric chemistry. *Chem. Rev.* **2003**, *103* (12), 4691–4716.

(12) Harris, E.; Sinha, B.; van Pinxteren, D.; Tilgner, A.; Fomba, K. W.; Schneider, J.; Roth, A.; Gnauk, T.; Fahlbusch, B.; Mertes, S.; Lee, T.; Collett, J.; Foley, S.; Borrmann, S.; Hoppe, P.; Herrmann, H. Enhanced role of transition metal ion catalysis during in-cloud oxidation of SO2. *Science* **2013**, *340* (6133), 727–730.

(13) George, C.; Ammann, M.; D'Anna, B.; Donaldson, D. J.; Nizkorodov, S. A. Heterogeneous photochemistry in the atmosphere. *Chem. Rev.* **2015**, *115* (10), 4218–4258. D

(14) Szopa, S.; Naik, V.; Adhikary, B.; Artaxo, P.; Berntsen, T.; Collins, W. D.; Fuzzi, S.; Gallardo, L.; Kiendler-Scharr, A.; Klimont, Z.; Liao, H.; Unger, N.; Zanis P. Short-lived Climate Forcers. In *Climate Change 2021 – The Physical Science Basis*; Change, I. P. o. C., Ed.; Cambridge University Press, 2021; pp 817–922.

(15) Lamarque, J.-F.; Bond, T. C.; Eyring, V.; Granier, C.; Heil, A.; Klimont, Z.; Lee, D.; Liousse, C.; Mieville, A.; Owen, B.; Schultz, M. G.; Shindell, D.; Smith, S. J.; Stehfest, E.; van Aardenne, J.; Cooper, O. R.; Kainuma, M.; Mahowald, N.; McConnell, J. R.; Naik, V.; Riahi, K.; van Vuuren, D. P. Historical (1850–2000) gridded anthropogenic and biomass burning emissions of reactive gases and aerosols: methodology and application. *Atmos. Chem. Phys.* **2010**, *10* (15), 7017–7039.

(16) IPCC. *Climate Change 2021: The Physical Science Basis. Contribution of Working Group I to the Sixth Assessment Report of the Intergovernmental Panel on Climate Change*; Cambridge University Press, 2021.

(17) Ravishankara, A. R.; Rudich, Y.; Wuebbles, D. J. Physical chemistry of climate metrics. *Chem. Rev.* **2015**, *115* (10), 3682–3703.

(18) Forster, P.; Storelvmo, T.; Armour, K.; Collins, W.; Dufresne, J.-L.; Frame, D.; Lunt, D. J.; Mauritsen, T.; Palmer, M. D.; Watanabe, M.; Wild, M.; Zhang, H. The Earth's Energy Budget, Climate Feedbacks and Climate Sensitivity. In *Climate Change 2021 – The Physical Science Basis*; Change, I. P. o. C., Ed.; Cambridge University Press, 2021; pp 923–1054.

(19) Wilkins, E. T. Air pollution aspects of the London fog of December 1952. *Q.J Royal Met. Soc.* **1954**, *80* (344), 267–271.

(20) Bell, M. L.; Davis, D. L. Reassessment of the lethal London fog of 1952: novel indicators of acute and chronic consequences of acute exposure to air pollution. *Environ. Health Perspect.* **2001**, *109 Suppl 3*, 389–394.

(21) Dockery, D. W.; Pope, C. A.; Xu, X.; Spengler, J. D.; Ware, J. H.; Fay, M. E.; Ferris, B. G.; Speizer, F. E. An association between air pollution and mortality in six U.S. cities. *N. Engl. J. Med* **1993**, *329* (24), 1753–1759.

(22) Beckerman, B. S.; Jerrett, M.; Serre, M.; Martin, R. V.; Lee, S.-J.; van Donkelaar, A.; Ross, Z.; Su, J.; Burnett, R. T. A hybrid approach to estimating national scale spatiotemporal variability of PM2.5 in the contiguous United States. *Environ. Sci. Technol.* **2013**, *47* (13), 7233–7241.

(23) Lipsett, M. J.; Ostro, B. D.; Reynolds, P.; Goldberg, D.; Hertz, A.; Jerrett, M.; Smith, D. F.; Garcia, C.; Chang, E. T.; Bernstein, L. Long-term exposure to air pollution and cardiorespiratory disease in the California teachers study cohort. *Am. J. Respir. Crit. Care Med.* **2011**, *184* (7), 828–835.

(24) Thurston, G. D.; Ahn, J.; Cromar, K. R.; Shao, Y.; Reynolds, H. R.; Jerrett, M.; Lim, C. C.; Shanley, R.; Park, Y.; Hayes, R. B. Ambient Particulate Matter Air Pollution Exposure and Mortality in the NIH-AARP Diet and Health Cohort. *Environ. Health Perspect.* **2016**, *124* (4), 484–490.

(25) Beelen, R.; Hoek, G.; Raaschou-Nielsen, O.; Stafoggia, M.; Andersen, Z. J.; Weinmayr, G.; Hoffmann, B.; Wolf, K.; Samoli, E.; Fischer, P. H.; Nieuwenhuijsen, M. J.; Xun, W. W.; Katsouyanni, K.; Dimakopoulou, K.; Marcon, A.; Vartiainen, E.; Lanki, T.; Yli-Tuomi, T.; Oftedal, B.; Schwarze, P. E.; Nafstad, P.; Faire, U. de; Pedersen, N. L.; Östenson, C.-G.; Fratiglioni, L.; Penell, J.; Korek, M.; Pershagen, G.; Eriksen, K. T.; Overvad, K.; Sørensen, M.; Eeftens, M.; Peeters, P. H.; Meliefste, K.; Wang, M.; Bueno-de-Mesquita, H. B.; Sugiri, D.; Krämer, U.; Heinrich, J.; Hoogh, K. de; Key, T.; Peters, A.; Hampel, R.; Concin, H.; Nagel, G.; Jaensch, A.; Ineichen, A.; Tsai, M.-Y.; Schaffner, E.; Probst-Hensch, N. M.; Schindler, C.; Ragettli, M. S.; Vilier, A.; Clavel-Chapelon, F.; Declercq, C.; Ricceri, F.; Sacerdote, C.; Galassi, C.; Migliore, E.; Ranzi, A.; Cesaroni, G.; Badaloni, C.; Forastiere, F.; Katsoulis, M.; Trichopoulou, A.; Keuken, M.; Jedynska, A.; Kooter, I. M.; Kukkonen, J.; Sokhi, R. S.; Vineis, P.; Brunekreef, B. Natural-cause mortality and long-term exposure to particle components: an analysis of 19 European cohorts within the multi-center ESCAPE project. *Environ. Health Perspect.* **2015**, *123* (6), 525–533.

(26) Bentayeb, M.; Wagner, V.; Stempfelet, M.; Zins, M.; Goldberg, M.; Pascal, M.; Larrieu, S.; Beaudeau, P.; Cassadou, S.; Eilstein, D.; Filleul, L.; Le Tertre, A.; Medina, S.; Pascal, L.; Prouvost, H.; Quénel, P.; Zeghnoun, A.; Lefranc, A. Association between long-term exposure to air pollution and mortality in France: A 25-year follow-up study. *Environ. Int.* **2015**, *85*, 5–14.

(27) Stafoggia, M.; Cesaroni, G.; Peters, A.; Andersen, Z. J.; Badaloni, C.; Beelen, R.; Caracciolo, B.; Cyrys, J.; Faire, U. de; Hoogh, K. de; Eriksen, K. T.; Fratiglioni, L.; Galassi, C.; Gigante, B.; Havulinna, A. S.; Hennig, F.; Hilding, A.; Hoek, G.; Hoffmann, B.; Houthuijs, D.; Korek, M.; Lanki, T.; Leander, K.; Magnusson, P. K.; Meisinger, C.; Migliore, E.; Overvad, K.; Ostenson, C.-G.; Pedersen, N. L.; Pekkanen, J.; Penell, J.; Pershagen, G.; Pundt, N.; Pyko, A.; Raaschou-Nielsen, O.; Ranzi, A.; Ricceri, F.; Sacerdote, C.; Swart, W. J. R.; Turunen, A. W.; Vineis, P.; Weimar, C.; Weinmayr, G.; Wolf, K.; Brunekreef, B.; Forastiere, F. Long-term exposure to ambient air pollution and incidence of cerebrovascular events: results from 11 European cohorts within the ESCAPE project. *Environ. Health Perspect.* **2014**, *122* (9), 919–925.

(28) Shi, L.; Zanobetti, A.; Kloog, I.; Coull, B. A.; Koutrakis, P.; Melly, S. J.; Schwartz, J. D. Low-Concentration PM2.5 and Mortality: Estimating Acute and Chronic Effects in a Population-Based Study. *Environ. Health Perspect.* **2016**, *124* (1), 46–52.

(29) Wong, C. M.; Lai, H. K.; Tsang, H.; Thach, T. Q.; Thomas, G. N.; Lam, K. B. H.; Chan, K. P.; Yang, L.; Lau, A. K. H.; Ayres, J. G.; Lee, S. Y.; Chan, W. M.; Hedley, A. J.; Lam, T. H. Satellite-Based Estimates of Long-Term Exposure to Fine Particles and Association with Mortality in Elderly Hong Kong Residents. *Environ. Health Perspect.* **2015**, *123* (11), 1167–1172.

(30) Murray, C. J.; Lopez, A. D. Global mortality, disability, and the contribution of risk factors: Global Burden of Disease Study. *Lancet* **1997**, *349* (9063), 1436–1442.

(31) Apte, J. S.; Marshall, J. D.; Cohen, A. J.; Brauer, M. Addressing Global Mortality from Ambient PM2.5. *Environ. Sci. Technol.* **2015**, *49* (13), 8057–8066.

(32) Burnett, R.; Chen, H.; Szyszkowicz, M.; Fann, N.; Hubbell, B.; Pope, C. A.; Apte, J. S.; Brauer, M.; Cohen, A.; Weichenthal, S.; Coggins, J.; Di, Q.; Brunekreef, B.; Frostad, J.; Lim, S. S.; Kan, H.; Walker, K. D.; Thurston, G. D.; Hayes, R. B.; Lim, C. C.; Turner, M. C.; Jerrett, M.; Krewski, D.; Gapstur, S. M.; Diver, W. R.; Ostro, B.; Goldberg, D.; Crouse, D. L.; Martin, R. V.; Peters, P.; Pinault, L.; Tjepkema, M.; van Donkelaar, A.; Villeneuve, P. J.; Miller, A. B.; Yin, P.; Zhou, M.; Wang, L.; Janssen, N. A. H.; Marra, M.; Atkinson, R. W.; Tsang, H.; Quoc Thach, T.; Cannon, J. B.; Allen, R. T.; Hart, J. E.; Laden, F.; Cesaroni, G.; Forastiere, F.; Weinmayr, G.; Jaensch, A.; Nagel, G.; Concin, H.; Spadaro, J. V. Global estimates of mortality associated with long-term exposure to outdoor fine particulate matter. *Proc. Natl. Acad. Sci. U. S. A.* **2018**, *115* (38), 9592–9597.

(33) Global burden of 369 diseases and injuries in 204 countries and territories, 1990-2019: a systematic analysis for the Global Burden of Disease Study 2019. *Lancet* **2020**, *396* (10258), 1204–1222.

(34) Cohen, A. J.; Brauer, M.; Burnett, R.; Anderson, H. R.; Frostad, J.; Estep, K.; Balakrishnan, K.; Brunekreef, B.; Dandona, L.; Dandona, R.; Feigin, V.; Freedman, G.; Hubbell, B.; Jobling, A.; Kan, H.; Knibbs, L.; Liu, Y.; Martin, R.; Morawska, L.; Pope, C. A.; Shin, H.; Straif, K.; Shaddick, G.; Thomas, M.; van Dingenen, R.; van Donkelaar, A.; Vos, T.; Murray, C. J. L.; Forouzanfar, M. H. Estimates and 25-year trends of the global burden of disease attributable to ambient air pollution: an analysis of data from the Global Burden of Diseases Study 2015. *Lancet* **2017**, *389* (10082), 1907–1918.

(35) Global Burden of Disease Collaborative Network. *Global Burden of Disease Study 2019 (GBD 2019) Results.*, Seattle, United States of America, 2020. https://vizhub.healthdata.org/gbd-results/.

(36) Silva, R. A.; Adelman, Z.; Fry, M. M.; West, J. J. The Impact of Individual Anthropogenic Emissions Sectors on the Global Burden of Human Mortality due to Ambient Air Pollution. *Environ. Health Perspect.* **2016**, *124* (11), 1776–1784.

(37) Junninen, H.; Mønster, J.; Rey, M.; Cancelinha, J.; Douglas, K.; Duane, M.; Forcina, V.; Müller, A.; Lagler, F.; Marelli, L.; Borowiak, A.; Niedzialek, J.; Paradiz, B.; Mira-Salama, D.; Jimenez, J.; Hansen, U.; Astorga, C.; Stanczyk, K.; Viana, M.; Querol, X.; Duvall, R. M.; Norris, G. A.; Tsakovski, S.; Wåhlin, P.; Horák, J.; Larsen, B. R. Quantifying the impact of residential heating on the urban air quality in a typical European coal combustion region. *Environ. Sci. Technol.* **2009**, *43* (20), 7964–7970.

(38) Leoni, C.; Pokorná, P.; Hovorka, J.; Masiol, M.; Topinka, J.; Zhao, Y.; Křůmal, K.; Cliff, S.; Mikuška, P.; Hopke, P. K. Source apportionment of aerosol particles at a European air pollution hot spot using particle number size distributions and chemical composition. *Environ. Pollut.* **2018**, *234*, 145–154.

(39) Pokorná, P.; Hovorka, J.; Klán, M.; Hopke, P. K. Source apportionment of size resolved particulate matter at a European air pollution hot spot. *Sci. Total Environ.* **2015**, *502*, 172–183.

(40) Pokorná, P.; Hovorka, J.; Hopke, P. K. Elemental composition and source identification of very fine aerosol particles in a European air pollution hot-spot. *Atmos. Pollut. Res.* **2016**, *7* (4), 671–679.

(41) Tobler, A. K.; Skiba, A.; Canonaco, F.; Močnik, G.; Rai, P.; Chen, G.; Bartyzel, J.; Zimnoch, M.; Styszko, K.; Nęcki, J.; Furger, M.; Różański, K.; Baltensperger, U.; Slowik, J. G.; Prevot, A. S. H. Characterization of non-refractory (NR) PM_1 and source apportionment of organic aerosol in Kraków, Poland. *Atmos. Chem. Phys.* **2021**, *21* (19), 14893–14906.

(42) Vossler, T.; Černikovský, L.; Novák, J.; Williams, R. Source apportionment with uncertainty estimates of fine particulate matter in Ostrava, Czech Republic using Positive Matrix Factorization. *Atmos. Pollut. Res.* **2016**, *7* (3), 503–512.

(43) Hinds, W. C.; Zhu, Y. *Aerosol Technology:Properties, Behavior, and Measurement of Airborne Particles*, 3. Edition; Wiley, 2022.

(44) Heyder, J. Deposition of inhaled particles in the human respiratory tract and consequences for regional targeting in respiratory drug delivery. *Proc. Am. Thorac. Soc.* **2004**, *1* (4), 315–320.

(45) Schwarz, M.; Schneider, A.; Cyrys, J.; Bastian, S.; Breitner, S.; Peters, A. Impact of ultrafine particles and total particle number concentration on five cause-specific hospital admission endpoints in three German cities. *Environ. Int.* **2023**, *178*, 108032.

(46) Peters, A.; Wichmann, H. E.; Tuch, T.; Heinrich, J.; Heyder, J. Respiratory effects are associated with the number of ultrafine particles. *Am. J. Respir. Crit. Care Med.* **1997**, *155* (4), 1376–1383.

(47) Pieters, N.; Koppen, G.; van Poppel, M.; Prins, S. de; Cox, B.; Dons, E.; Nelen, V.; Panis, L. I.; Plusquin, M.; Schoeters, G.; Nawrot, T. S. Blood Pressure and Same-Day Exposure to Air Pollution at School: Associations with Nano-Sized to Coarse PM in Children. *Environ. Health Perspect.* **2015**, *123* (7), 737–742.

(48) Baldauf, R. W.; Devlin, R. B.; Gehr, P.; Giannelli, R.; Hassett-Sipple, B.; Jung, H.; Martini, G.; McDonald, J.; Sacks, J. D.; Walker, K. Ultrafine Particle Metrics and Research Considerations: Review of the 2015 UFP Workshop. *Int. J. Environ. Res. Public Health* **2016**, *13* (11), 1054.

(49) Schmid, O.; Stoeger, T. Surface area is the biologically most effective dose metric for acute nanoparticle toxicity in the lung. *J. Aerosol Sci.* **2016**, *99*, 133–143.

(50) Murphy, F. A.; Schinwald, A.; Poland, C. A.; Donaldson, K. The mechanism of pleural inflammation by long carbon nanotubes: interaction of long fibres with macrophages stimulates them to amplify pro-inflammatory responses in mesothelial cells. *Part. Fibre Toxicol.* **2012**, *9*, 8.

(51) Poland, C. A.; Duffin, R.; Kinloch, I.; Maynard, A.; Wallace, W. A. H.; Seaton, A.; Stone, V.; Brown, S.; Macnee, W.; Donaldson, K. Carbon nanotubes introduced into the abdominal cavity of mice show asbestos-like pathogenicity in a pilot study. *Nat. Nanotechnol.* **2008**, *3* (7), 423–428.

(52) *Directive 2008/50/EC of the European Parliament and of the Council of 21 May 2008 on ambient air quality and cleaner air for Europe.*

(53) Putaud, J.-P.; Raes, F.; van Dingenen, R.; Brüggemann, E.; Facchini, M.-C.; Decesari, S.; Fuzzi, S.; Gehrig, R.; Hüglin, C.; Laj, P.; Lorbeer, G.; Maenhaut, W.; Mihalopoulos, N.; Müller, K.; Querol, X.; Rodriguez, S.; Schneider, J.; Spindler, G.; Brink, H. ten; Tørseth, K.; Wiedensohler, A. A European aerosol phenomenology—2: chemical characteristics of particulate matter at kerbside, urban, rural and background sites in Europe. *Atmos. Environ.* **2004**, *38* (16), 2579–2595.

(54) Huntzicker, J. J.; Johnson, R. L.; Shah, J. J.; Cary, R. A. Analysis of Organic and Elemental Carbon in Ambient Aerosols by a Thermal-Optical Method. In *Particulate Carbon*; Wolff, G. T., Klimisch, R. L., Eds.; Springer US, 1982; pp 79–88.

(55) Chow, J. C.; Watson, J. G.; Pritchett, L. C.; Pierson, W. R.; Frazier, C. A.; Purcell, R. G. The dri thermal/optical reflectance carbon analysis system: description, evaluation and applications in U.S. Air quality studies. *Atmos. Environ.* **1993**, *27* (8), 1185–1201. DOI: 10.1016/0960-1686(93)90245-T.

(56) Pöschl, U.; Shiraiwa, M. Multiphase chemistry at the atmosphere-biosphere interface influencing climate and public health in the anthropocene. *Chem. Rev.* **2015**, *115* (10), 4440–4475.

(57) Andreae, M. O.; Ramanathan, V. Climate change. Climate's dark forcings. *Science* **2013**, *340* (6130), 280–281.

(58) van Donkelaar, A.; Martin, R. V.; Brauer, M.; Boys, B. L. Use of satellite observations for long-term exposure assessment of global concentrations of fine particulate matter. *Environ. Health Perspect.* **2015**, *123* (2), 135–143.

(59) van Donkelaar, A.; Martin, R. V.; Brauer, M.; Kahn, R.; Levy, R.; Verduzco, C.; Villeneuve, P. J. Global estimates of ambient fine particulate matter concentrations from satellite-based aerosol optical depth: development and application. *Environ. Health Perspect.* **2010**, *118* (6), 847–855.

(60) Janssen, N. A. H.; Hoek, G.; Simic-Lawson, M.; Fischer, P.; van Bree, L.; Brink, H. ten; Keuken, M.; Atkinson, R. W.; Anderson, H. R.; Brunekreef, B.; Cassee, F. R. Black carbon as an additional indicator of the adverse health effects of airborne particles compared with PM10 and PM2.5. *Environ. Health Perspect.* **2011**, *119* (12), 1691–1699.

(61) Shiraiwa, M.; Ueda, K.; Pozzer, A.; Lammel, G.; Kampf, C. J.; Fushimi, A.; Enami, S.; Arangio, A. M.; Fröhlich-Nowoisky, J.; Fujitani, Y.; Furuyama, A.; Lakey, P. S. J.; Lelieveld, J.; Lucas, K.; Morino, Y.; Pöschl, U.; Takahama, S.; Takami, A.; Tong, H.; Weber, B.; Yoshino, A.; Sato, K. Aerosol Health Effects from Molecular to Global Scales. *Environ. Sci. Technol.* **2017**, *51* (23), 13545–13567.

(62) Schnelle-Kreis, J.; Sklorz, M.; Orasche, J.; Stölzel, M.; Peters, A.; Zimmermann, R. Semi volatile organic compounds in ambient PM2.5. Seasonal trends and daily resolved source contributions. *Environ. Sci. Technol.* **2007**, *41* (11), 3821–3828.

(63) Orasche, J.; Schnelle-Kreis, J.; Schön, C.; Hartmann, H.; Ruppert, H.; Arteaga-Salas, J. M.; Zimmermann, R. Comparison of Emissions from Wood Combustion. Part 2: Impact of Combustion Conditions on Emission Factors and Characteristics of Particle-Bound Organic Species and Polycyclic Aromatic Hydrocarbon (PAH)-Related Toxicological Potential. *Energy Fuels* **2013**, *27* (3), 1482–1491.

(64) Offer, S.; Hartner, E.; Di Bucchianico, S.; Bisig, C.; Bauer, S.; Pantzke, J.; Zimmermann, E. J.; Cao, X.; Binder, S.; Kuhn, E.; Huber, A.; Jeong, S.; Käfer, U.; Martens, P.; Mesceriakovas, A.; Bendl, J.; Brejcha, R.; Buchholz, A.; Gat, D.; Hohaus, T.; Rastak, N.; Jakobi, G.; Kalberer, M.; Kanashova, T.; Hu, Y.; Ogris, C.; Marsico, A.; Theis, F.; Pardo, M.; Gröger, T.; Oeder, S.; Orasche, J.; Paul, A.; Ziehm, T.; Zhang, Z.-H.; Adam, T.; Sippula, O.; Sklorz, M.; Schnelle-Kreis, J.; Czech, H.; Kiendler-Scharr, A.; Rudich, Y.; Zimmermann, R. Effect of Atmospheric Aging on Soot Particle Toxicity in Lung Cell Models at the Air-Liquid Interface: Differential Toxicological Impacts of Biogenic and Anthropogenic Secondary Organic Aerosols (SOAs). *Environ. Health Perspect.* **2022**, *130* (2), 27003.

(65) Burnett, R. T.; Pope, C. A.; Ezzati, M.; Olives, C.; Lim, S. S.; Mehta, S.; Shin, H. H.; Singh, G.; Hubbell, B.; Brauer, M.; Anderson, H. R.; Smith, K. R.; Balmes, J. R.; Bruce, N. G.; Kan, H.; Laden, F.; Prüss-Ustün, A.; Turner, M. C.; Gapstur, S. M.; Diver, W. R.; Cohen, A. An integrated risk function for

estimating the global burden of disease attributable to ambient fine particulate matter exposure. *Environ. Health Perspect.* **2014**, *122* (4), 397–403.

(66) Brauer, M.; Amann, M.; Burnett, R. T.; Cohen, A.; Dentener, F.; Ezzati, M.; Henderson, S. B.; Krzyzanowski, M.; Martin, R. V.; van Dingenen, R.; van Donkelaar, A.; Thurston, G. D. Exposure assessment for estimation of the global burden of disease attributable to outdoor air pollution. *Environ. Sci. Technol.* **2012**, *46* (2), 652–660.

(67) Park, M.; Joo, H. S.; Lee, K.; Jang, M.; Kim, S. D.; Kim, I.; Borlaza, L. J. S.; Lim, H.; Shin, H.; Chung, K. H.; Choi, Y.-H.; Park, S. G.; Bae, M.-S.; Lee, J.; Song, H.; Park, K. Differential toxicities of fine particulate matters from various sources. *Sci. Rep.* **2018**, *8* (1), 17007.

(68) Di Wu; Zheng, H.; Li, Q.; Jin, L.; Lyu, R.; Ding, X.; Huo, Y.; Zhao, B.; Jiang, J.; Chen, J.; Li, X.; Wang, S. Toxic potency-adjusted control of air pollution for solid fuel combustion. *Nat Energy* **2022**, *7* (2), 194–202.

(69) Kasurinen, S.; Jalava, P. I.; Tapanainen, M.; Uski, O.; Happo, M. S.; Mäki-Paakkanen, J.; Lamberg, H.; Koponen, H.; Nuutinen, I.; Kortelainen, M.; Jokiniemi, J.; Hirvonen, M.-R. Toxicological effects of particulate emissions – A comparison of oil and wood fuels in small- and medium-scale heating systems. *Atmos. Environ.* **2015**, *103*, 321–330.

(70) Kanashova, T.; Sippula, O.; Oeder, S.; Streibel, T.; Passig, Johannes, Czech, Hendryk; Kaoma, T.; Sapcariu, S. C.; Dilger, M.; Paur, H.-R.; Schlager, C.; Mülhopt, S.; Weiss Carsten; Schmidt-Weber, C.; Traidl-Hofmann, C.; Michalke, B.; Krebs, T.; Karg, E.; Jakobi, G.; Scholtes, S.; Schnelle-Kreis, J.; Sklorz, M.; Orasche, J.; Müller, L.; Reda, A.; Rüger, C.; Neumann, A.; Abbaszade, G.; Radischat, C.; Hiller, K.; Grigonyte, J.; Kortelainen, M.; Kuuspalo, K.; Lamberg, H.; Leskinen, J.; Nuutinen, I.; Torvela, T.; Tissari, J.; Jalava, P.; Kasurinen, S.; Uski, O.; Hirvonen, M.-R.; Buters, Jeroen, Dittmar, Gunnar; Jokiniemi, J.; Zimmermann, R. Emissions from a modern log wood masonry heater and wood pellet boiler: Composition and biological impact on air-liquid interface exposed human lung cancer cells. *J Mol Clin Med* **2018**, *1* (1).

(71) Ihantola, T.; Hirvonen, M.-R.; Ihalainen, M.; Hakkarainen, H.; Sippula, O.; Tissari, J.; Bauer, S.; Di Bucchianico, S.; Rastak, N.; Hartikainen, A.; Leskinen, J.; Yli-Pirilä, P.; Martikainen, M.-V.; Miettinen, M.; Suhonen, H.; Rönkkö, T. J.; Kortelainen, M.; Lamberg, H.; Czech, H.; Martens, P.; Orasche, J.; Michalke, B.; Yildirim, A. Ö.; Jokiniemi, J.; Zimmermann, R.; Jalava, P. I. Genotoxic and inflammatory effects of spruce and brown coal briquettes combustion aerosols on lung cells at the air-liquid interface. *Sci. Total Environ.* **2022**, *806* (1), 150489.

(72) Ihantola, T.; Di Bucchianico, S.; Happo, M.; Ihalainen, M.; Uski, O.; Bauer, S.; Kuuspalo, K.; Sippula, O.; Tissari, J.; Oeder, S.; Hartikainen, A.; Rönkkö, T. J.; Martikainen, M.-V.; Huttunen, K.; Vartiainen, P.; Suhonen, H.; Kortelainen, M.; Lamberg, H.; Leskinen, A.; Sklorz, M.; Michalke, B.; Dilger, M.; Weiss, C.; Dittmar, G.; Beckers, J.; Irmler, M.; Buters, J.; Candeias, J.; Czech, H.; Yli-Pirilä, P.; Abbaszade, G.; Jakobi, G.; Orasche, J.; Schnelle-Kreis, J.; Kanashova, T.; Karg, E.; Streibel, T.; Passig, J.; Hakkarainen, H.; Jokiniemi, J.; Zimmermann, R.; Hirvonen, M.-R.; Jalava, P. I. Influence of wood species on toxicity of log-wood stove combustion aerosols: a parallel animal and air-liquid interface cell exposure study on spruce and pine smoke. *Part. Fibre Toxicol.* **2020**, *17* (1), 27.

(73) Kasurinen, S.; Jalava, P. I.; Happo, M. S.; Sippula, O.; Uski, O.; Koponen, H.; Orasche, J.; Zimmermann, R.; Jokiniemi, J.; Hirvonen, M.-R. Particulate emissions from the combustion of birch, beech, and spruce logs cause different cytotoxic responses in A549 cells. *Environ. Toxicol.* **2017**, *32* (5), 1487–1499.

(74) Oeder, S.; Kanashova, T.; Sippula, O.; Sapcariu, S. C.; Streibel, T.; Arteaga-Salas, J. M.; Passig, J.; Dilger, M.; Paur, H.-R.; Schlager, C.; Mülhopt, S.; Diabaté, S.; Weiss, C.; Stengel, B.; Rabe, R.; Harndorf, H.; Torvela, T.; Jokiniemi, J. K.; Hirvonen, M.-R.; Schmidt-Weber, C.; Traidl-Hoffmann, C.; BéruBé, K. A.; Wlodarczyk, A. J.; Prytherch, Z.; Michalke, B.; Krebs, T.; Prévôt, A. S. H.; Kelbg, M.; Tiggesbäumker, J.; Karg, E.; Jakobi, G.; Scholtes, S.; Schnelle-Kreis, J.; Lintelmann, J.; Matuschek, G.; Sklorz, M.; Klingbeil, S.; Orasche, J.; Richthammer, P.; Müller, L.; Elsasser, M.; Reda, A.; Gröger, T.; Weggler, B.; Schwemer, T.; Czech, H.; Rüger, C. P.; Abbaszade, G.; Radischat, C.; Hiller, K.; Buters, J. T. M.; Dittmar, G.; Zimmermann, R. Particulate matter from both heavy fuel oil and diesel fuel shipping emissions show strong biological effects on human lung cells at realistic and comparable in vitro exposure conditions. *PloS one* **2015**, *10* (6), e0126536.

(75) Hopke, P. K.; Dai, Q.; Li, L.; Feng, Y. Global review of recent source apportionments for airborne particulate matter. *Sci. Total Environ.* **2020**, *740*, 140091.

(76) Hopke, P. K. An introduction to receptor modeling. *Chemometrics and Intelligent Laboratory Systems* **1991**, *10* (1-2), 21–43.

(77) Watson, J. G.; Robinson, N. F.; Chow, J. C.; Henry, R. C.; Kim, B. M.; Pace, T. G.; Meyer, E. L.; Nguyen, Q. The USEPA/DRI chemical mass balance receptor model, CMB 7.0. *Environ. Softw.* **1990**, *5* (1), 38–49.

(78) Watson, J. G.; Chow, J. C. Receptor Models and Measurements for Identifying and Quantifying Air Pollution Sources. In *Introduction to Environmental Forensics*; Elsevier, 2015; pp 677–706.

(79) Simoneit, B. R. Biomass burning — a review of organic tracers for smoke from incomplete combustion. *Appl. Geochem.* **2002**, *17* (3), 129–162.

(80) Fine, P. M.; Cass, G. R.; Simoneit, B. R. T. Chemical characterzation of fine particle emissions from the fireplace combustion of woods grown in the Southern United States. *Environ. Sci. Technol.* **2002**, *36* (7), 1442–1451.

(81) Oros, D. R.; Simoneit, B. Identification and emission rates of molecular tracers in coal smoke particulate matter. *Fuel* **2000**, *79* (5), 515–536.

(82) Bi, X.; Simoneit, B. R.; Sheng, G.; Fu, J. Characterization of molecular markers in smoke from residential coal combustion in China. *Fuel* **2008**, *87* (1), 112–119.

(83) Czech, H.; Miersch, T.; Orasche, J.; Abbaszade, G.; Sippula, O.; Tissari, J.; Michalke, B.; Schnelle-Kreis, J.; Streibel, T.; Jokiniemi, J.; Zimmermann, R. Chemical composition and speciation of particulate organic matter from modern residential small-scale wood combustion appliances. *Sci. Total Environ.* **2018**, *612*, 636–648.

(84) Cai, T.; Schauer, J. J.; Huang, W.; Fang, D.; Shang, J.; Wang, Y.; Zhang, Y. Sensitivity of source apportionment results to mobile source profiles. *Environ. Pollut.* **2016**, *219*, 821–828.

(85) Sheesley, R. J.; Schauer, J. J.; Zheng, M.; Wang, B. Sensitivity of molecular marker-based CMB models to biomass burning source profiles. *Atmos. Environ.* **2007**, *41* (39), 9050–9063.

(86) Paatero, P.; Tapper, U. Positive matrix factorization: A non-negative factor model with optimal utilization of error estimates of data values. *Environmetrics* **1994**, *5* (2), 111–126.

(87) Paatero, P. Least squares formulation of robust non-negative factor analysis. *Chemom. Intell. Lab. Syst.* **1997**, *37* (1), 23–35.

(88) Lin, C.; Ceburnis, D.; Hellebust, S.; Buckley, P.; Wenger, J.; Canonaco, F.; Prévôt, A. S. H.; Huang, R.-J.; O'Dowd, C.; Ovadnevaite, J. Characterization of Primary Organic Aerosol from Domestic Wood, Peat, and Coal Burning in Ireland. *Environ. Sci. Technol.* **2017**, *51* (18), 10624–10632.

(89) Rivas, I.; Beddows, D. C. S.; Amato, F.; Green, D. C.; Järvi, L.; Hueglin, C.; Reche, C.; Timonen, H.; Fuller, G. W.; Niemi, J. V.; Pérez, N.; Aurela, M.; Hopke, P. K.; Alastuey, A.; Kulmala, M.; Harrison, R. M.; Querol, X.; Kelly, F. J. Source apportionment of particle number size distribution in urban background and traffic stations in four European cities. *Environ. Int.* **2020**, *135*, 105345.

(90) Nozière, B.; Kalberer, M.; Claeys, M.; Allan, J.; D'Anna, B.; Decesari, S.; Finessi, E.; Glasius, M.; Grgić, I.; Hamilton, J. F.; Hoffmann, T.; Iinuma, Y.; Jaoui, M.; Kahnt, A.; Kampf, C. J.; Kourtchev, I.; Maenhaut, W.; Marsden, N.; Saarikoski, S.; Schnelle-Kreis, J.; Surratt, J. D.; Szidat, S.; Szmigielski, R.; Wisthaler, A. The molecular identification of organic compounds in the atmosphere: state of the art and challenges. *Chem. Rev.* **2015**, *115* (10), 3919–3983.

(91) Jayne, J. T.; Leard, D. C.; Zhang, X.; Davidovits, P.; Smith, K. A.; Kolb, C. E.; Worsnop, D. R. Development of an Aerosol Mass Spectrometer for Size and Composition Analysis of Submicron Particles. *Aerosol Sci. Technol.* **2000**, *33* (1-2), 49–70.

(92) DeCarlo, P. F.; Kimmel, J. R.; Trimborn, A.; Northway, M. J.; Jayne, J. T.; Aiken, A. C.; Gonin, M.; Fuhrer, K.; Horvath, T.; Docherty, K. S.; Worsnop, D. R.; Jimenez, J. L. Field-deployable, high-resolution, time-of-flight aerosol mass spectrometer. *Analytical chemistry* **2006**, *78* (24), 8281–8289.

(93) Prather, K. A.; Nordmeyer, T.; Salt, K. Real-time characterization of individual aerosol particles using time-of-flight mass spectrometry. *Anal. Chem.* **1994**, *66* (9), 1403–1407.

(94) Passig, J.; Schade, J.; Oster, M.; Fuchs, M.; Ehlert, S.; Jäger, C.; Sklorz, M.; Zimmermann, R. Aerosol Mass Spectrometer for Simultaneous Detection of Polyaromatic Hydrocarbons and Inorganic Components from Individual Particles. *Anal. Chem.* **2017**, *89* (12), 6341–6345.

(95) Diab, J.; Streibel, T.; Cavalli, F.; Lee, S. C.; Saathoff, H.; Mamakos, A.; Chow, J. C.; Chen, L.-W. A.; Watson, J. G.; Sippula, O.; Zimmermann, R. Hyphenation of a EC / OC thermal–optical carbon analyzer to photo-ionization time-of-flight mass spectrometry: an off-line aerosol mass spectrometric approach for characterization of primary and secondary particulate matter. *Atmos. Meas. Tech.* **2015**, *8* (8), 3337–3353.

(96) Rein, G. Smouldering Fires and Natural Fuels. In *Fire Phenomena and the Earth System.An Interdisciplinary Guide to Fire Science,* 1. Edition; Belcher, C. M., Ed.; John Wiley & Sons, 2013; pp 15–33. DOI: 10.1002/9781118529539.ch2.

(97) Rangwala, A. S.; Raghavan, V. *Mechanism of Fires:Chemistry and Physical Aspects*, 1. Edition; Springer International Publishing, 2022.

(98) Rogaume, T. Thermal decomposition and pyrolysis of solid fuels: Objectives, challenges and modelling. *Fire Saf. J.* **2019**, *106*, 177–188.

(99) Beyler, C. Flammability Limits of Premixed and Diffusion Flames. In *SFPE Handbook of Fire Protection Engineering,* 5. Edition; Hurley, M. J., Gottuk, D., Hall, J. R., Harada, K., Kuligowski, E., Puchovsky, M., Torero, J., Watts, J. M., Wieczorek, C., Eds.; Springer New York, 2016; pp 529–553.

(100) Rein, G. Smoldering Combustion. In *SFPE Handbook of Fire Protection Engineering,* 5. Edition; Hurley, M. J., Gottuk, D., Hall, J. R., Harada, K., Kuligowski, E., Puchovsky, M., Torero, J., Watts, J. M., Wieczorek, C., Eds.; Springer New York, 2016; pp 581–603.

(101) Torero, J. Flaming Ignition of Solid Fuels. In *SFPE Handbook of Fire Protection Engineering,* 5. Edition; Hurley, M. J., Gottuk, D., Hall, J. R., Harada, K., Kuligowski, E., Puchovsky, M., Torero, J., Watts, J. M., Wieczorek, C., Eds.; Springer New York, 2016; pp 633–661.

(102) Lautenberger, C. Gpyro3D: A Three Dimensional Generalized Pyrolysis Model. *Fire Saf. Sci.* **2014**, *11*, 193–207.

(103) Heß, D. *Pflanzenphysiologie*, 11. Edition; Ulmer, 2008.

(104) Cseke, L. J. *Natural products from plants*, 2. Edition; CRC Press, 2006.

(105) Wink, M. Introduction: Biochemistry, Physiology and Ecological Functions of Secondary Metabolites. In *Annual Plant Reviews Volume 40:Biochemistry of Plant Secondary Metabolism*; Wink, M., Ed.; Wiley-Blackwell, 2010; pp 1–19.

(106) More, A.; Elder, T.; Jiang, Z. A review of lignin hydrogen peroxide oxidation chemistry with emphasis on aromatic aldehydes and acids. *Holzforschung* **2021**, *75* (9), 806–823.

(107) Meschede, M.; Murawski, H.; Meyer, W. *Geologisches Wörterbuch*, 13. Auflage; Springer Spektrum, 2022.

(108) O'Keefe, J. M.; Bechtel, A.; Christanis, K.; Dai, S.; DiMichele, W. A.; Eble, C. F.; Esterle, J. S.; Mastalerz, M.; Raymond, A. L.; Valentim, B. V.; Wagner, N. J.; Ward, C. R.; Hower, J. C. On the fundamental difference between coal rank and coal type. *Int. J. Coal Geol.* **2013**, *118*, 58–87.

(109) Collard, F.-X.; Blin, J. A review on pyrolysis of biomass constituents: Mechanisms and composition of the products obtained from the conversion of cellulose, hemicelluloses and lignin. *Renewable Sustainable Energy Rev.* **2014**, *38*, 594–608.

(110) Bhaskaran, K.; Roth, P. The shock tube as wave reactor for kinetic studies and material systems. *Prog. Energy Combust. Sci.* **2002**, *28* (2), 151–192.

(111) Cassady, S. J.; Choudhary, R.; Pinkowski, N. H.; Shao, J.; Davidson, D. F.; Hanson, R. K. The thermal decomposition of ethane. *Fuel* **2020**, *268*, 117409.

(112) Utsav, K. C.; Mohamed, B.; Aamir, F. Simultaneous measurements of acetylene and soot during the pyrolysis of ethylene and benzene in a shock tube. *Prog. Energy Combust. Sci.* **2017**, *36* (1), 833–840.

(113) Hidaka, Y. Shock-tube and modeling study of methane pyrolysis and oxidation. *Combust. Flame* **1999**, *118* (3), 340–358.

(114) Matsukawa, Y.; Ono, K.; Dewa, K.; Watanabe, A.; Saito, Y.; Matsushita, Y.; Aoki, H.; Era, K.; Aoki, T.; Yamaguchi, T. Reaction pathway for nascent soot in ethylene pyrolysis. *Comb. Flame* **2016**, *167*, 248–258. DOI: 10.1016/j.combustflame.2016.02.008.

(115) Sun, W.; Hamadi, A.; Abid, S.; Chaumeix, N.; Comandini, A. Influences of propylene/propyne addition on toluene pyrolysis in a single-pulse shock tube. *Comb. Flame* **2022**, *236*, 111799.

(116) Sun, W.; Hamadi, A.; Abid, S.; Chaumeix, N.; Comandini, A. A comparative kinetic study of C8–C10 linear alkylbenzenes pyrolysis in a single-pulse shock tube. *Comb. Flame* **2020**, *221*, 136–149.

(117) Wennberg, P. O.; Bates, K. H.; Crounse, J. D.; Dodson, L. G.; McVay, R. C.; Mertens, L. A.; Nguyen, T. B.; Praske, E.; Schwantes, R. H.; Smarte, M. D.; St Clair, J. M.; Teng, A. P.; Zhang, X.; Seinfeld, J. H. Gas-Phase Reactions of Isoprene and Its Major Oxidation Products. *Chem. Rev.* **2018**, *118* (7), 3337–3390.

(118) Mitra, T.; Chu, C.; Naseri, A.; Thomson, M. J. Polycyclic aromatic hydrocarbon formation in a flame of the alkylated aromatic trimethylbenzene compared to those of the alkane dodecane. *Combust. Flame* **2021**, *223*, 495–510.

(119) Shu, B.; Herzler, J.; Peukert, S.; Fikri, M.; Schulz, C. A Shock Tube and Modeling Study about Anisole Pyrolysis Using Time-Resolved CO Absorption Measurements. *Int. J. Chem. Kinet.* **2017**, *49* (9), 656–667.

(120) Scheer, A. M.; Mukarakate, C.; Robichaud, D. J.; Ellison, G. B.; Nimlos, M. R. Radical chemistry in the thermal decomposition of anisole and deuterated anisoles: an investigation of aromatic growth. *J. Phys. Chem. A* **2010**, *114* (34), 9043–9056.

(121) Laskin, A.; Lifshitz, A. Thermal decomposition of indene. Experimental results and kinetic modeling. *Symp. (Int.) Combust., [Proc.]* **1998**, *27* (1), 313–320.

(122) Lifshitz, A.; Tamburu, C.; Suslensky, A.; Dubnikova, F. Decomposition, Isomerization, and Ring Expansion in 2-Methylindene: Single-pulse Shock Tube and Modeling Study. *J. Phys. Chem. A* **2004**, *108* (16), 3430–3438.

(123) Qiu, L.; Cheng, X.; Wang, X.; Li, Z.; Li, Y.; Wang, Z.; Wu, H. Development of a Reduced n-Decane/α-Methylnaphthalene/Polycyclic Aromatic Hydrocarbon Mechanism and Its Application for Combustion and Soot Prediction. *Energy Fuels* **2016**, *30* (12), 10875–10885.

(124) Leininger, J.-P.; Lorant, F.; Minot, C.; Behar, F. Mechanisms of 1-Methylnaphthalene Pyrolysis in a Batch Reactor. *Energy Fuels* **2006**, *20* (6), 2518–2530.

(125) Weber, I.; Friese, P.; Olzmann, M. H-Atom-Forming Reaction Pathways in the Pyrolysis of Furan, 2-Methylfuran, and 2,5-Dimethylfuran: A Shock-Tube and Modeling Study. *J. Phys. Chem. A* **2018**, *122* (32), 6500–6508.

(126) Alexandrino, K.; Baena, C.; Millera, Á.; Bilbao, R.; Alzueta, M. U. 2-methylfuran pyrolysis: Gas-phase modelling and soot formation. *Combust. Flame* **2018**, *188*, 376–387.

(127) Sikes, T.; Banyon, C.; Schwind, R. A.; Lynch, P. T.; Comandini, A.; Sivaramakrishnan, R.; Tranter, R. S. Initiation reactions in the high temperature decomposition of styrene. *Phys. Chem. Chem. Phys.* **2021**, *23* (34), 18432–18448.

(128) Sun, J.; Zhi, G.; Hitzenberger, R.; Chen, Y.; Tian, C.; Zhang, Y.; Feng, Y.; Cheng, M.; Zhang, Y.; Cai, J.; Chen, F.; Qiu, Y.; Jiang, Z.; Li, J.; Zhang, G.; Mo, Y. Emission factors and light absorption properties of brown carbon from household coal combustion in China. *Atmos. Chem. Phys.* **2017**, *17* (7), 4769–4780.

(129) Reizer, E.; Viskolcz, B.; Fiser, B. Formation and growth mechanisms of polycyclic aromatic hydrocarbons: A mini-review. *Chemosphere* **2022**, *291* (Pt 1), 132793.

(130) Frenklach, M. Reaction mechanism of soot formation in flames. *Phys. Chem. Chem. Phys.* **2002**, *4* (11), 2028–2037.

(131) Richter, H.; Howard, J. Formation of polycyclic aromatic hydrocarbons and their growth to soot—a review of chemical reaction pathways. *Progress in Energy and Combustion Science* **2000**, *26* (4-6), 565–608.

(132) Frenklach, M.; Clary, D. W.; Gardiner, W. C.; Stein, S. E. Detailed kinetic modeling of soot formation in shock-tube pyrolysis of acetylene. *Symp. (Int.) Combust., [Proc.]* **1985**, *20* (1), 887–901.

(133) Shukla, B.; Miyoshi, A.; Koshi, M. Role of methyl radicals in the growth of PAHs. *Journal of the American Society for Mass Spectrometry* **2010**, *21* (4), 534–544.

(134) Shukla, B.; Susa, A.; Miyoshi, A.; Koshi, M. Role of phenyl radicals in the growth of polycyclic aromatic hydrocarbons. *The journal of physical chemistry. A* **2008**, *112* (11), 2362–2369.

(135) Shukla, B.; Koshi, M. A novel route for PAH growth in HACA based mechanisms. *Combustion and Flame* **2012**, *159* (12), 3589–3596.

(136) Wang, H. Formation of nascent soot and other condensed-phase materials in flames. *Proceedings of the Combustion Institute* **2011**, *33* (1), 41–67.

(137) Frenklach, M.; Wang, H. Detailed modeling of soot particle nucleation and growth. *Symposium (International) on Combustion* **1991**, *23* (1), 1559–1566.

(138) Singh, J.; Patterson, R. I.; Kraft, M.; Wang, H. Numerical simulation and sensitivity analysis of detailed soot particle size distribution in laminar premixed ethylene flames. *Comb. Flame* **2006**, *145* (1-2), 117–127.

(139) Johansson, K. O.; Head-Gordon, M. P.; Schrader, P. E.; Wilson, K. R.; Michelsen, H. A. Resonance-stabilized hydrocarbon-radical chain reactions may explain soot inception and growth. *Science* **2018**, *361* (6406), 997–1000.

(140) *Commission Regulation (EU) 2015/1185 of 24 April 2015 implementing Directive 2009/125/EC of the European Parliament and of the Council with regard to ecodesign requirements for solid fuel local space heaters*, 2015.

(141) Křůmal, K.; Mikuška, P.; Horák, J.; Hopan, F.; Krpec, K. Comparison of emissions of gaseous and particulate pollutants from the combustion of biomass and coal in modern and old-type boilers used for residential heating in the Czech Republic, Central Europe. *Chemosphere* **2019**, *229*, 51–59.

(142) Krpec, K.; Horák, J.; Laciok, V.; Hopan, F.; Kubesa, P.; Lamberg, H.; Jokiniemi, J.; Tomšejová, Š. Impact of Boiler Type, Heat Output, and Combusted Fuel on Emission Factors for Gaseous and Particulate Pollutants. *Energy Fuels* **2016**, *30* (10), 8448–8456.

(143) Šyc, M.; Horák, J.; Hopan, F.; Krpec, K.; Tomšej, T.; Ocelka, T.; Pekárek, V. Effect of Fuels and Domestic Heating Appliance Types on Emission Factors of Selected Organic Pollutants. *Environ. Sci. Technol.* **2011**, *45* (21), 9427–9434.

(144) Horak, J.; Kubonova, L.; Krpec, K.; Hopan, F.; Kubesa, P.; Motyka, O.; Laciok, V.; Dej, M.; Ochodek, T.; Placha, D. PAH emissions from old and new types of domestic hot water boilers. *Environ. Pollut.* **2017**, *225*, 31–39.

(145) Shen, G.; Tao, S.; Wei, S.; Zhang, Y.; Wang, R.; Wang, B.; Li, W.; Shen, H.; Huang, Y.; Yang, Y.; Wang, W.; Wang, X.; Simonich, S. L. M. Retene emission from residential solid fuels in China and evaluation of retene as a unique marker for soft wood combustion. *Environ. Sci. Technol.* **2012**, *46* (8), 4666–4672.

(146) Shen, G.; Tao, S.; Chen, Y.; Zhang, Y.; Wei, S.; Xue, M.; Wang, B.; Wang, R.; Lu, Y.; Li, W.; Shen, H.; Huang, Y.; Chen, H. Emission characteristics for polycyclic aromatic hydrocarbons from solid fuels burned in domestic stoves in rural China. *Environ. Sci. Technol.* **2013**, *47* (24), 14485–14494.

(147) Shen, G.; Chen, Y.; Xue, C.; Lin, N.; Huang, Y.; Shen, H.; Wang, Y.; Li, T.; Zhang, Y.; Su, S.; Huangfu, Y.; Zhang, W.; Chen, X.; Liu, G.; Liu, W.; Wang, X.; Wong, M.-H.; Tao, S. Pollutant emissions from improved coal- and wood-fuelled cookstoves in rural households. *Environ. Sci. Technol.* **2015**, *49* (11), 6590–6598.

(148) Shen, G.; Yang, Y.; Wang, W.; Tao, S.; Zhu, C.; Min, Y.; Xue, M.; Ding, J.; Wang, B.; Wang, R.; Shen, H.; Li, W.; Wang, X.; Russell, A. G. Emission factors of particulate matter and elemental carbon for crop residues and coals burned in typical household stoves in China. *Environ. Sci. Technol.* **2010**, *44* (18), 7157–7162.

(149) Shen, H.; Luo, Z.; Xiong, R.; Liu, X.; Zhang, L.; Li, Y.; Du, W.; Chen, Y.; Cheng, H.; Shen, G.; Tao, S. A critical review of pollutant emission factors from fuel combustion in home stoves. *Environment international* **2021**, *157*, 106841.

(150) Tsai, S. M.; Zhang, J. J.; Smith, K. R.; Ma, Y.; Rasmussen, R. A.; Khalil, M. A. K. Characterization of non-methane hydrocarbons emitted from various cookstoves used in China. *Environ. Sci. Technol.* **2003**, *37* (13), 2869–2877.

(151) Wang, Q.; Geng, C.; Lu, S.; Chen, W.; Shao, M. Emission factors of gaseous carbonaceous species from residential combustion of coal and crop residue briquettes. *Front. Environ. Sci. Eng.* **2013**, *7* (1), 66–76.

(152) Wang, X.; Cotter, E.; Iyer, K. N.; Fang, J.; Williams, B. J.; Biswas, P. Relationship between pyrolysis products and organic aerosols formed during coal combustion. *Proc. Combust. Inst.* **2015**, *35* (2), 2347–2354.

(153) Wang, Y.; Xu, Y.; Chen, Y.; Tian, C.; Feng, Y.; Chen, T.; Li, J.; Zhang, G. Influence of different types of coals and stoves on the emissions of parent and oxygenated PAHs from residential coal combustion in China. *Environ. Pollut.* **2016**, *212*, 1–8.

(154) Zhang, J.; Smith, K.; Ma, Y.; Ye, S.; Jiang, F.; Qi, W.; Liu, P.; Khalil, M.; Rasmussen, R.; Thorneloe, S. Greenhouse gases and other airborne pollutants from household stoves in China: a database for emission factors. *Atmos. Environ.* **2000**, *34* (26), 4537–4549.

(155) Czech, H.; Sippula, O.; Kortelainen, M.; Tissari, J.; Radischat, C.; Passig, J.; Streibel, T.; Jokiniemi, J.; Zimmermann, R. On-line analysis of organic emissions from residential wood combustion with single-photon ionisation time-of-flight mass spectrometry (SPI-TOFMS). *Fuel* **2016**, *177*, 334–342.

(156) Griffiths, P. R.; Haseth, James A. de Haseth. *Fourier TransformInfrared Spectrometry*, 2. Edition; John Wiley & Sons, 2006.

(157) Gross, J. H. *Mass spectrometry:A textbook*, 3. Edition; Springer, 2017.

(158) Eichler, H. J.; Eichler, J.; Lux, O., Eds. *Lasers*; Springer Series in Optical Sciences; Springer International Publishing, 2018.

(159) Butcher, D. J. Vacuum Ultraviolet Radiation for Single-Photoionization Mass Spectrometry: A Review. *Microchem. J.* **1999**, *62* (3), 354–362.

(160) Boyd, R. *Nonlinear optics*, 3. Edition; Academic Press, 2008.

(161) Boesl, U. Laser mass spectrometry for environmental and industrial chemical trace analysis. *J. Mass Spectrom.* **2000**, *35* (3), 289–304.

(162) Boesl, U.; Weinkauf, R.; Weickhardt, C.; Schlag, E. W. Laser ion sources for time-of-flight mass spectrometry. *Int. J. Mass Spectrom. Ion Processes* **1994**, *131*, 87–124.

(163) Guilhaus, M. Special feature: Tutorial. Principles and instrumentation in time-of-flight mass spectrometry. Physical and instrumental concepts. *J. Mass Spectrom.* **1995**, *30* (11), 1519–1532. DOI: 10.1002/jms.1190301102.

(164) Wiley, W. C.; McLaren, I. H. Time-of-Flight Mass Spectrometer with Improved Resolution. *Rev. Sci. Instrum.* **1955**, *26* (12), 1150–1157.

(165) Mamyrin, B. A. Laser assisted reflectron time-of-flight mass spectrometry. *Int. J. Mass Spectrom. Ion Processes* **1994**, *131*, 1–19.

(166) Ladislas Wiza, J. Microchannel plate detectors. *Nucl. Instrum. Methods* **1979**, *162* (1-3), 587–601.

(167) VDI Association of German Engeneers. *Measurement of particles in ambient air:Determination of the particle number concentration and number size distribution of aerosols*; Beuth Verlag GmbH, Düsseldorf, 2012.

(168) Nuutinen, K.; Jokiniemi, J.; Sippula, O.; Lamberg, H.; Sutinen, J.; Horttanainen, P.; Tissari, J. Effect of air staging on fine particle, dust and gaseous emissions from masonry heaters. *Biomass Bioenergy* **2014**, *67*, 167–178.

(169) Martens, P.; Czech, H.; Tissari, J.; Ihalainen, M.; Suhonen, H.; Sklorz, M.; Jokiniemi, J.; Sippula, O.; Zimmermann, R. Emissions of Gases and Volatile Organic Compounds from Residential Heating: A Comparison of Brown Coal Briquettes and Logwood Combustion. *Energy Fuels* **2021**, *35* (17), 14010–14022.

(170) Lamberg, H.; Nuutinen, K.; Tissari, J.; Ruusunen, J.; Yli-Pirilä, P.; Sippula, O.; Tapanainen, M.; Jalava, P.; Makkonen, U.; Teinilä, K.; Saarnio, K.; Hillamo, R.; Hirvonen, M.-R.; Jokiniemi, J. Physicochemical characterization of fine particles from small-scale wood combustion. *Atmos. Environ.* **2011**, *45* (40), 7635–7643.

(171) Kistler, M.; Schmidl, C.; Padouvas, E.; Giebl, H.; Lohninger, J.; Ellinger, R.; Bauer, H.; Puxbaum, H. Odor, gaseous and PM10 emissions from small scale combustion of wood types indigenous to Central Europe. *Atmos. Environ.* **2012**, *51* (C), 86–93.

(172) Liu, C.; Zhang, C.; Mu, Y.; Liu, J.; Zhang, Y. Emission of volatile organic compounds from domestic coal stove with the actual alternation of flaming and smoldering combustion processes. *Environ. Pollut.* **2017**, *221*, 385–391.

(173) Elsasser, M.; Busch, C.; Orasche, J.; Schön, C.; Hartmann, H.; Schnelle-Kreis, J.; Zimmermann, R. Dynamic Changes of the Aerosol Composition and Concentration during Different Burning Phases of Wood Combustion. *Energy Fuels* **2013**, *27* (8), 4959–4968.

(174) Vassilev, S. V.; Vassileva, C. G.; Vassilev, V. S. Advantages and disadvantages of composition and properties of biomass in comparison with coal: An overview. *Fuel* **2015**, *158*, 330–350.

(175) Friebel, J.; Köpsel, R. The fate of nitrogen during pyrolysis of German low rank coals — a parameter study. *Fuel* **1999**, *78* (8), 923–932.

(176) He, K.; Shen, Z.; Zhang, B.; Sun, J.; Zou, H.; Zhou, M.; Zhang, Z.; Xu, H.; Ho, S. S. H.; Cao, J. Emission profiles of volatile organic compounds from various geological maturity coal and its clean coal briquetting in China. *Atmos. Res.* **2022**, *274*, 106200.

(177) Klein, F.; Pieber, S. M.; Ni, H.; Stefenelli, G.; Bertrand, A.; Kilic, D.; Pospisilova, V.; Temime-Roussel, B.; Marchand, N.; El Haddad, I.; Slowik, J. G.; Baltensperger, U.; Cao, J.; Huang, R.-J.; Prévôt, A. S. H. Characterization of Gas-Phase Organics Using Proton Transfer Reaction Time-of-Flight Mass Spectrometry: Residential Coal Combustion. *Environ. Sci. Technol.* **2018** (5), 2612–2617.

(178) Khatami, R.; Levendis, Y. A. An overview of coal rank influence on ignition and combustion phenomena at the particle level. *Comb. Flame* **2016**, *164*, 22–34.

(179) Song, Y.; Tahmasebi, A.; Yu, J. Co-pyrolysis of pine sawdust and lignite in a thermogravimetric analyzer and a fixed-bed reactor. *Bioresour. Technol.* **2014**, *174*, 204–211.

(180) McDonald, J. D.; Zielinska, B.; Fujita, E. M.; Sagebiel, J. C.; Chow, J. C.; Watson, J. G. Fine Particle and Gaseous Emission Rates from Residential Wood Combustion. *Environ. Sci. Technol.* **2000**, *34* (11), 2080–2091.

(181) Adam, T.; Zimmermann, R. Determination of single photon ionization cross sections for quantitative analysis of complex organic mixtures. *Anal. Bioanal. Chem.* **2007**, *389* (6), 1941–1951.

(182) Chen, Y.; Zhi, G.; Feng, Y.; Liu, D.; Zhang, G.; Li, J.; Sheng, G.; Fu, J. Measurements of black and organic carbon emission factors for household coal combustion in China: implication for emission reduction. *Environ. Sci. Technol.* **2009**, *43* (24), 9495–9500.

(183) Chen, Y.; Sheng, G.; Bi, X.; Feng, Y.; Mai, B.; Fu, J. Emission factors for carbonaceous particles and polycyclic aromatic hydrocarbons from residential coal combustion in China. *Environ. Sci. Technol.* **2005**, *39* (6), 1861–1867.

(184) Zhi, G.; Chen, Y.; Feng, Y.; Xiong, S.; Li, J.; Zhang, G.; Sheng, G.; Fu, J. Emission characteristics of carbonaceous particles from various residential coal-stoves in China. *Environ. Sci. Technol.* **2008**, *42* (9), 3310–3315.

(185) Zhang, Y.; Schauer, J. J.; Zhang, Y.; Zeng, L.; Wei, Y.; Liu, Y.; Shao, M. Characteristics of particulate carbon emissions from real-world Chinese coal combustion. *Environ. Sci. Technol.* **2008**, *42* (14), 5068–5073.

(186) Miersch, T.; Czech, H.; Hartikainen, A.; Ihalainen, M.; Orasche, J.; Abbaszade, G.; Tissari, J.; Streibel, T.; Jokiniemi, J.; Sippula, O.; Zimmermann, R. Impact of photochemical ageing on Polycyclic Aromatic Hydrocarbons (PAH) and oxygenated PAH (Oxy-PAH/OH-PAH) in logwood stove emissions. *Sci. Total Environ.* **2019**, *686*, 382–392.

(187) Schmidl, C.; Luisser, M.; Padouvas, E.; Lasselsberger, L.; Rzaca, M.; Ramirez-Santa Cruz, C.; Handler, M.; Peng, G.; Bauer, H.; Puxbaum, H. Particulate and gaseous emissions from manually and automatically fired small scale combustion systems. *Atmos. Environ.* **2011**, *45* (39), 7443–7454.

(188) Orasche, J.; Seidel, T.; Hartmann, H.; Schnelle-Kreis, J.; Chow, J. C.; Ruppert, H.; Zimmermann, R. Comparison of Emissions from Wood Combustion. Part 1: Emission Factors and Characteristics from Different Small-Scale Residential Heating Appliances Considering Particulate Matter and Polycyclic Aromatic Hydrocarbon (PAH)-Related Toxicological Potential of Particle-Bound Organic Species. *Energy Fuels* **2012**, *26* (11), 6695–6704.

(189) Martens, P.; Czech, H.; Orasche, J.; Abbaszade, G.; Sklorz, M.; Michalke, B.; Tissari, J.; Bizjak, T.; Ihalainen, M.; Suhonen, H.; Yli-Pirilä, P.; Jokiniemi, J.; Sippula, O.; Zimmermann, R. Brown Coal and Logwood Combustion in a Modern Heating Appliance: The Impact of Combustion Quality and Fuel on Organic Aerosol Composition. *Environ. Sci. Technol.* **2023**, *57* (14), 5532–5543.

(190) Rüger, C. P.; Le Maître, J.; Riches, E.; Palmer, M.; Orasche, J.; Sippula, O.; Jokiniemi, J.; Afonso, C.; Giusti, P.; Zimmermann, R. Cyclic Ion Mobility Spectrometry Coupled to High-Resolution Time-of-Flight Mass Spectrometry Equipped with Atmospheric Solid Analysis Probe for the Molecular Characterization of Combustion Particulate Matter. *J. Am. Soc. Mass Spectrom.* **2021**, *32* (1), 206–217.

(191) Schauer, J. J.; Kleeman, M. J.; Cass, G. R.; Simoneit, B. R. Measurement of emissions from air pollution sources. 3. C1-C29 organic compounds from fireplace combustion of wood. *Environ. Sci. Technol.* **2001**, *35* (9), 1716–1728.

(192) Neumann, A.; Chacón-Patiño, M. L.; Rodgers, R. P.; Rüger, C. P.; Zimmermann, R. Investigation of Island/Single-Core- and Archipelago/Multicore-Enriched Asphaltenes and Their Solubility Fractions by Thermal Analysis Coupled with High-Resolution Fourier Transform Ion Cyclotron Resonance Mass Spectrometry. *Energy Fuels* **2021**, *35* (5), 3808–3824.

(193) Friederici, L.; Schneider, E.; Burnens, G.; Streibel, T.; Giusti, P.; Rüger, C. P.; Zimmermann, R. Comprehensive Chemical Description of Pyrolysis Chars from Low-Density Polyethylene by Thermal Analysis Hyphenated to Different Mass Spectrometric Approaches. *Energy Fuels* **2021**, *35* (22), 18185–18193.

(194) Chacón-Patiño, M. L.; Rowland, S. M.; Rodgers, R. P. Advances in Asphaltene Petroleomics. Part 1: Asphaltenes Are Composed of Abundant Island and Archipelago Structural Motifs. *Energy Fuels* **2017**, *31* (12), 13509–13518.

(195) Kang, H.-J.; Lee, S.-Y.; Kwon, J.-H. Physico-chemical properties and toxicity of alkylated polycyclic aromatic hydrocarbons. *J. Hazard. Mater.* **2016**, *312*, 200–207.

(196) Fu, C.; Li, Y.; Xi, H.; Niu, Z.; Chen, N.; Wang, R.; Yan, Y.; Gan, X.; Wang, M.; Zhang, W.; Zhang, Y.; Lv, P. Benzo(a)pyrene and cardiovascular diseases: An overview of pre-clinical studies focused on the underlying molecular mechanism. *Front. Nutr.* **2022**, *9*, 978475.

(197) Moorthy, B.; Chu, C.; Carlin, D. J. Polycyclic aromatic hydrocarbons: from metabolism to lung cancer. *Toxicol. Sci.* **2015**, *145* (1), 5–15.

(198) Pardo, M.; Li, C.; Fang, Z.; Levin-Zaidman, S.; Dezorella, N.; Czech, H.; Martens, P.; Käfer, U.; Gröger, T.; Rüger, C. P.; Friederici, L.; Zimmermann, R.; Rudich, Y. Toxicity of Water- and Organic-Soluble Wood Tar Fractions from Biomass Burning in Lung Epithelial Cells. *Chem. Res. Toxicol.* **2021**, *34* (6), 1588–1603.

(199) Rybicki, M.; Marynowski, L.; Simoneit, B. R. T. Composition of organic compounds from low-temperature burning of lignite and their application as tracers in ambient air. *Chemosphere* **2020**, *249*, 126087.

(200) Marynowski, L.; Bucha, M.; Lempart-Drozd, M.; Stępień, M.; Kondratowicz, M.; Smolarek-Lach, J.; Rybicki, M.; Goryl, M.; Brocks, J.; Simoneit, B. R. Preservation of hemicellulose remnants in sedimentary organic matter. *Geochim. Cosmochim. Acta* **2021**, *310*, 32–46.

(201) Fabbri, D.; Torri, C.; Simoneit, B. R.; Marynowski, L.; Rushdi, A. I.; Fabiańska, M. J. Levoglucosan and other cellulose and lignin markers in emissions from burning of Miocene lignites. *Atmos. Environ.* **2009**, *43* (14), 2286–2295.

(202) Fabbri, D.; Marynowski, L.; Fabiańska, M. J.; Zatoń, M.; Simoneit, B. R. T. Levoglucosan and other cellulose markers in pyrolysates of Miocene lignites: geochemical and environmental implications. *Environ. Sci. Technol.* **2008**, *42* (8), 2957–2963.

(203) Yan, C.; Zheng, M.; Sullivan, A. P.; Shen, G.; Chen, Y.; Wang, S.; Zhao, B.; Cai, S.; Desyaterik, Y.; Li, X.; Zhou, T.; Gustafsson, Ö.; Collett, J. L. Residential Coal Combustion as a Source of Levoglucosan in China. *Environ. Sci. Technol.* **2018**, *52* (3), 1665–1674.

(204) Fine, P. M.; Cass, G. R.; Simoneit, B. R. Chemical characterization of fine particle emissions from fireplace combustion of woods grown in the northeastern United States. *Environ. Sci. Technol.* **2001**, *35* (13), 2665–2675.

(205) Fine, P. M.; Cass, G. R.; Simoneit, B. R. T. Organic compounds in biomass smoke from residential wood combustion: Emissions characterization at a continental scale. *J. Geophys. Res* **2002**, *107* (D21), ICC 11-1-ICC 11-9.

(206) Havelcová, M.; Sýkorová, I.; Mach, K.; Dvořák, Z. Organic Geochemistry of Fossil Resins from the Czech Republic. *Procedia Earth Planet. Sci.* **2014**, *10*, 303–312.

(207) Frenkel, M.; Heller-Kallai, L. Aromatization of limonene—a geochemical model. *Org. Geochem.* **1977**, *1* (1), 3–5.

(208) Otto, A.; Simoneit, B. R. T.; Wilde, V. Terpenoids as chemosystematic markers in selected fossil and extant species of pine (Pinus, Pinaceae). *Bot. J. Linn. Soc.* **2007**, *154* (1), 129–140.

(209) Kuittinen, N.; Jalkanen, J.-P.; Alanen, J.; Ntziachristos, L.; Hannuniemi, H.; Johansson, L.; Karjalainen, P.; Saukko, E.; Isotalo, M.; Aakko-Saksa, P.; Lehtoranta, K.; Keskinen, J.; Simonen, P.; Saarikoski, S.; Asmi, E.; Laurila, T.; Hillamo, R.; Mylläri, F.; Lihavainen, H.; Timonen, H.; Rönkkö, T. Shipping Remains a Globally Significant Source of Anthropogenic PN Emissions Even after 2020 Sulfur Regulation. *Environ. Sci. Technol.* **2021**, *55* (1), 129–138.

(210) Ausmeel, S.; Eriksson, A.; Ahlberg, E.; Sporre, M. K.; Spanne, M.; Kristensson, A. Ship plumes in the Baltic Sea Sulfur Emission Control Area: chemical characterization and contribution to coastal aerosol concentrations. *Atmos. Chem. Phys.* **2020**, *20* (15), 9135–9151.

(211) Anders, L.; Schade, J.; Rosewig, E. I.; Kröger-Badge, T.; Irsig, R.; Jeong, S.; Bendl, J.; Saraji-Bozorgzad, M. R.; Huang, J.-H.; Zhang, F.-Y.; Wang, C. C.; Adam, T.; Sklorz, M.; Etzien, U.; Buchholz, B.; Czech, H.; Streibel, T.; Passig, J.; Zimmermann, R. Detection of ship emissions from distillate fuel operation via single-particle profiling of polycyclic aromatic hydrocarbons. *Environ. Sci.: Atmos.* **2023**, *3* (8), 1134–1144.

(212) Rosewig, E. I.; Schade, J.; Passig, J.; Osterholz, H.; Irsig, R.; Smok, D.; Gawlitta, N.; Schnelle-Kreis, J.; Hovorka, J.; Schulz-Bull, D.; Zimmermann, R.; Adam, T. W. Remote Detection of Different Marine Fuels in Exhaust Plumes by Onboard Measurements in the Baltic Sea Using Single-Particle Mass Spectrometry. *Atmosphere* **2023**, *14* (5), 849.

(213) Jeong, S.; Bendl, J.; Saraji-Bozorgzad, M.; Käfer, U.; Etzien, U.; Schade, J.; Bauer, M.; Jakobi, G.; Orasche, J.; Fisch, K.; Cwierz, P. P.; Rüger, C. P.; Czech, H.; Karg, E.; Heyen, G.; Krausnick, M.; Geissler, A.; Geipel, C.; Streibel, T.; Schnelle-Kreis, J.; Sklorz, M.; Schulz-Bull, D. E.; Buchholz, B.; Adam, T.; Zimmermann, R. Aerosol emissions from a marine diesel engine running on different fuels and effects of exhaust gas cleaning measures. *Environ. Pollut.* **2023**, *316* (1), 120526.

(214) Sippula, O.; Stengel, B.; Sklorz, M.; Streibel, T.; Rabe, R.; Orasche, J.; Lintelmann, J.; Michalke, B.; Abbaszade, G.; Radischat, C.; Gröger, T.; Schnelle-Kreis, J.; Harndorf, H.; Zimmermann, R. Particle emissions from a marine engine: chemical composition and aromatic emission profiles under various operating conditions. *Environ. Sci. Technol.* **2014**, *48* (19), 11721–11729.

(215) Streibel, T.; Schnelle-Kreis, J.; Czech, H.; Harndorf, H.; Jakobi, G.; Jokiniemi, J.; Karg, E.; Lintelmann, J.; Matuschek, G.; Michalke, B.; Müller, L.; Orasche, J.; Passig, J.; Radischat, C.; Rabe, R.; Reda, A.; Rüger, C.; Schwemer, T.; Sippula, O.; Stengel, B.; Sklorz, M.; Torvela, T.; Weggler, B.; Zimmermann, R. Aerosol emissions of a ship diesel engine operated with diesel fuel or heavy fuel oil. *Environ. Sci. Pollut. Res.* **2017**, *24* (12), 10976–10991.

(216) Momenimovahed, A.; Gagné, S.; Martens, P.; Jakobi, G.; Czech, H.; Wichmann, V.; Buchholz, B.; Zimmermann, R.; Behrends, B.; Thomson, K. A. Comparison of black carbon measurement techniques for marine engine emissions using three marine fuel types. *Aerosol Sci. Technol.* **2022**, *56* (1), 46–62.

(217) Han, Y.; Cao, J.; Chow, J. C.; Watson, J. G.; An, Z.; Jin, Z.; Fung, K.; Liu, S. Evaluation of the thermal/optical reflectance method for discrimination between char- and soot-EC. *Chemosphere* **2007**, *69* (4), 569–574.

(218) Zhang, L.; Luo, Z.; Xiong, R.; Liu, X.; Li, Y.; Du, W.; Chen, Y.; Pan, B.; Cheng, H.; Shen, G.; Tao, S. Mass Absorption Efficiency of Black Carbon from Residential Solid Fuel Combustion and Its Association with Carbonaceous Fractions. *Environ. Sci. Technol.* **2021**, *55* (15), 10662–10671.

(219) Müller, J.-O.; Su, D. S.; Jentoft, R. E.; Kröhnert, J.; Jentoft, F. C.; Schlögl, R. Morphology-controlled reactivity of carbonaceous materials towards oxidation. *Catal. Today* **2005**, *102-103*, 259–265.

(220) Xie, F.; Guo, L.; Wang, Z.; Tian, Y.; Yue, C.; Zhou, X.; Wang, W.; Xin, J.; Lü, C. Geochemical characteristics and socioeconomic associations of carbonaceous aerosols in coal-fueled cities with significant seasonal pollution pattern. *Environ. Int.* **2023**, *179*, 108179.

(221) Han, Y. M.; Bandowe, B. A. M.; Wei, C.; Cao, J. J.; Wilcke, W.; Wang, G. H.; Ni, H. Y.; Jin, Z. D.; An, Z. S.; Yan, B. Z. Stronger association of polycyclic aromatic hydrocarbons with soot than with char in soils and sediments. *Chemosphere* **2015**, *119*, 1335–1345.

(222) Han, Y. M.; Cao, J. J.; Lee, S. C.; Ho, K. F.; An, Z. S. Different characteristics of char and soot in the atmosphere and their ratio as an indicator for source identification in Xi'an, China. *Atmos. Chem. Phys.* **2010**, *10* (2), 595–607.

7.   List of Figures

8.   List of Tables

9.   Abbreviations

BC .... *Black Carbon*
DMA...*Differential Mobility Analyzer*
EC .... *Elemental Carbon*
EI .... *Electron Ionization*
FTIR ....*Fourier-Transform Infrared*
GC.. *Gas Chromatography*
HACA .... *Hydrogen Abstraction C2-Absorbtion Mechanisms*
HICE.. *Helmholtz Virtual Institute of Complex Molecular Systems in Environmental Health*
IE .... *Ionization Energy*
IR*Infrared Spectroscopy*
MCP..*Micro Channel Plate*
MS .... *Mass Spectrometry*
Nd:YAG ....*Nd3+-Doped Yttrium Aluminum Garnet Crystal*
NOx.. *Nitrogen Oxides*
OC .... *Organic Carbon*
PAH...*Polycyclic Aromatic Hydrocarbon*
PI*Photoionization*
PM...*Particulate Matter*
PM10... *Particulate Matter with a Diameter below 10 μm*
PM2.5 .... *Particulate Matter with a Diameter below 2.5 μm*
REMPI .... *Resonance Enhanced Multi-Photon Ionization*
SPI..*Single-Photon Ionization*
ToF ....*Time-of-Flight*
VOC ....*Volatile Organic Compound*

10. Curriculum Vitae

Personal Information   **Contact Details**

Date of Birth   24.08.1995   Address   Soester Straße 17, 18057 Rostock

Place of Birth   Waren (Müritz)   E-Mail   patrick.martens@uni-rostock.de

Nationality   German

Education

10/2019-present   PhD candidate,
                     Chair of Analytical Chemistry at University of Rostock
                     Group of Prof. Dr. Zimmermann

10/2017-09/2019   Master of Science, Chemistry,
                     University of Rostock, Final Grade 1.3

10/2014-09/2017   Bachelor of Science, Chemistry,
                     University of Rostock, Final Grade 2.3

Working Experience

04/2020-present   Scientific Staff,
                     Chair of Analytical Chemistry at University of Rostock
                     Group of Prof. Dr. Zimmermann

10/2019-03/2020   Scientific Assistant,
                     Chair of Analytical Chemistry at University of Rostock
                     Group of Prof. Dr. Zimmermann

11/2018-01/2019   Scientific Assistant,
                     Chair of Analytical Chemistry at University of Rostock
                     Group of Prof. Dr. Zimmermann

11/2017-12/2017   Student Assistant,
                     Chair of Analytical Chemistry at University of Rostock
                     Group of Prof. Dr. Zimmermann

Rostock,   18.09.2023
                                             _____
                                             Patrick Martens

11.   Declaration of Independence

Erklärung gemäß §4 Absatz 1 Buchstaben g und h der Promotionsordnung der Mathematisch-Naturwissenschaftlichen Fakultät der Universität Rostock

Name: Patrick Martens   **Matrikelnummer:**   214202723
Anschrift: Soester Straße 17

Ich habe die Dissertation mit dem Titel Thema

Toward Understanding the Chemical Composition of Carbonaceous Aerosols Emitted by Solid Fuel Burning

an der Mathematisch-Naturwissenschaftlichen Fakultät der Universität Rostock angefertigt. Dabei wurde ich von Herrn Prof. Dr. Ralf Zimmermann betreut.

Ich gebe folgende Erklärung ab:

(1)   Die Gelegenheit zum vorliegenden Promotionsvorhaben ist mir nicht kommerziell vermittelt worden. Insbesondere habe ich keine Organisation eingeschaltet, die gegen Entgelt Betreuerinnen/Betreuer für die Anfertigung von Dissertationen sucht oder die mir obliegenden Pflichten hinsichtlich der Prüfungsleistungen für mich ganz oder teilweise erledigt.

(2)   Ich versichere hiermit an Eides statt, dass ich die vorliegende Arbeit selbstständig angefertigt und ohne fremde Hilfe verfasst habe. Dazu habe ich keine außer den von mir angegebenen Hilfsmitteln und Quellen verwendet und die den benutzten Werken inhaltlich und wörtlich entnommenen Stellen habe ich als solche kenntlich gemacht

Rostock,   18.09.2023   _____

12. Contribution of to Peer-Reviewed Publications

1	**Title**	Emissions of Gases and Volatile Organic Compounds from Residential Heating: A Comparison of Brown Coal Briquettes and Logwood Combustion
	Authors	Patrick Martens, Hendryk Czech, Jarkko Tissari, Mika Ihalainen, Heikki Suhonen, Martin Sklorz, Jorma Jokiniemi, Olli Sippula, and Ralf Zimmermann
	Journal information	*Energy Fuels* **2021**, 56 (1), 14010–14022
	Contribution	Patrick Martens processed and evaluated data, wrote the manuscript, and defended the work within the peer-review process.
2	**Title**	Brown Coal and Logwood Combustion in a Modern Heating Appliance: The Impact of Combustion Quality and Fuel on Organic Aerosol Composition
	Authors	Patrick Martens, Hendryk Czech, Jürgen Orasche, Gülcin Abbaszade, Martin Sklorz, Bernhard Michalke, Jarkko Tissari, Tine Bizjak, Mika Ihalainen, Heikki Suhonen, Pasi Yli-Pirilä, Jorma Jokiniemi, Olli Sippula, and Ralf Zimmermann
	Journal information	*Environ. Sci. Technol.* **2023**, 57 (14), 5532–5543
	Contribution	Patrick Martens carried out the thermal-optical carbon analysis with photoionization mass spectrometry, compiled and evaluated data from all other instruments, wrote the manuscript, and defended the work within the peer-review process.
3	**Title**	Genotoxic and inflammatory effects of spruce and brown coal briquettes combustion aerosols on lung cells at the air-liquid interface
	Authors	Tuukka Ihantola, Maija-Riitta Hirvonen, Mika Ihalainen, Henri Hakkarainen, Olli Sippula, Jarkko Tissari, Stefanie Bauer, Sebastiano Di Bucchianico, Narges Rastak, Anni Hartikainen, Jani Leskinen; Pasi Yli-Pirilä; Maria-Viola Martikainen, Mirella Miettinen, Heikki Suhonen, Teemu J. Rönkkö, Miika Kortelainen, Heikki Lamberg, Hendryk Czech, Patrick Martens, Jürgen Orasche, Bernhard Michalke; Ali Önder Yildirim; Jorma Jokiniemi, Ralf Zimmermann, and Pasi I. Jalava,
	Journal information	*Sci. Total Environ.* **2022**, 806 (1), 150489
	Contribution	Patrick Martens carried out the carbon analysis, compiled on-line data from a photoionization mass spectrometer, and reviewed and edited the manuscript.

4	Title	Comparison of black carbon measurement techniques for marine engine emissions using three marine fuel types
	Authors	Ali Momenimovahed, Stéphanie Gagné, Patrick Martens, Gert Jakobi, Hendryk Czech; Volker Wichmann, Bert Buchholz, Ralf Zimmermann, Brigitte Behrends, and Kevin A. Thomson
	Journal information	*Aerosol Sci. Technol.*, **2022**, 56 (1), 46–62
	Contribution	Patrick Martens carried out the carbon analysis, contributed to the interpretation of data, and reviewed and edited the manuscript.
5	Title	Toxicity of Water- And Organic-Soluble Wood Tar Fractions from Biomass Burning in Lung Epithelial Cells
	Authors	Michal Pardo, Chunlin Li, Zheng Fang, Smadar Levin-Zaidman, Nili Dezorella, Hendryk Czech; Patrick Martens, Uwe Käfer, Thomas Gröger, Christopher P. Rüger, Lukas Friederici, Ralf Zimmermann, and Yinon Rudich
	Journal information	*Chem. Res. Toxicol.* **2021**, 34 (6), 1588–1603
	Contribution	Patrick Martens carried out the analysis of tar balls with photoionization mass spectrometry, and he reviewed and approved the manuscript.
6	Title	Effect of Atmospheric Aging on Soot Particle Toxicity in Lung Cell Models at the Air-Liquid Interface: Differential Toxicological Impacts of Biogenic and Anthropogenic Secondary Organic Aerosols (SOAs)
	Authors	Svenja Offer, Elena Hartner, Sebastiano Di Bucchianico, Christoph Bisig, Stefanie Bauer, Jana Pantzke; Elias J. Zimmermann, Xin Cao, Stefanie Binder, Evelyn Kuhn, Anja Huber; Seongho Jeong, Uwe Käfer, Patrick Martens, Arunas Mesceriakovas, Jan Bendl, Ramona Brechja, Angela Buchholz, Daniella Gat, Thorsten Hohaus, Narges Rastak, Gert Jakobi, Markus Kalberer, Tamara Kanashova, Yue Hu, Christoph Ogris, Annalisa Marsico, Fabian Theis, Michal Pardo, Thomas Gröger, Sebastian Oeder, Jürgen Orasche, Andreas Paul, Till Ziehm, Zhi-Hui Zhang, Thomas Adam, Olli Sippula Martin Sklorz, Jürgen Schnelle-Kreis; Hendryk Czech, Astrid Kiendler-Scharr, Yinon Rudich, and Ralf Zimmermann
	Journal information	*Environ. Health Perspect.* **2022**, *130* (2), 27003
	Contribution	Patrick Martens designed and performed the experiments.